T.C
YEDITEPE UNIVERSITY
INSTITUTE OF HEALTH SCIENCES
DEPARTMENT OF HISTOLOGY AND EMBRYOLOGY

DETERMINATION OF THE RELATIONSHIP BETWEEN c-ABL TYROSINE KINASE AND YAP IN RESPONSE TO DNA DAMAGE IN MOUSE GRANULOSA CELLS

MASTER THESIS

NİLSU TALAŞ

İstanbul-2021

T.C
YEDITEPE UNIVERSITY
INSTITUTE OF HEALTH SCIENCES
DEPARTMENT OF HISTOLOGY AND EMBRYOLOGY

DETERMINATION OF THE RELATIONSHIP BETWEEN c-ABL TYROSINE KINASE AND YAP IN RESPONSE TO DNA DAMAGE IN MOUSE GRANULOSA CELLS

MASTER THESIS

NİLSU TALAŞ

SUPERVISOR
Assoc.Prof. Aylin YABA UÇAR

İstanbul-2021

THESIS APPROVAL FORM

Institute : Yeditepe University Institute of Health Sciences

Programme : Histology and Embryology

Title of the Thesis : Determination of relationship between c-Abl ytrosine kinase and YAP in response to DNA damage in mouse granulosa cells

Owner of the Thesis : Nilsu TALAŞ

Examination Date : 08.11.2021

This study have approved as a Master Thesis in regard to content and quality by the Jury.

	Title, Name-Surname (Institution)
Chair of the Jury:	Assoc. Prof. Aylin YABA UÇAR Yeditepe University
Supervisor:	Assoc. Prof Aylin YABA UÇAR Yeditepe University
Member/Examiner:	Assist. Prof. Alev CUMBUL Yeditepe University
Member/Examiner:	Assist. Prof. Murat BAŞAR Biruni University

APPROVAL

This thesis has been deemed by the jury in accordance with the relevant articles of Yeditepe University Graduate Education and Examinations Regulation and has been approved by Administrative Board of Institute with decision dated ..... and numbered .....

Prof. Dr. Bayram YILMAZ
Director of Institute of Health Sciences

DECLARATION

I hereby declare that this thesis is my own work and that, to the best of my knowledge and belief, it contains no material previously published or written by another person nor material which has been accepted for the award of any other degree except where due acknowledgment has been made in the text.

Date
18.11.2021

Nilsu TALAŞ

ACKNOWLEDGEMENT

I exceptionally would like to thank my counsel Assoc. Prof. Aylin Yaba UÇAR who has encouraged me and has been very helpful to me in my laboratory experiments. I am also appreciative for the checks and corrections she has made about my thesis. I am grateful to Assoc. Prof. Aylin Yaba UÇAR for her psychological support and friendliness also. Working with Assoc. Prof. Aylin Yaba UÇAR has been a privilege for me; I think she has contributed greatly to my academic point of view.

I have taken pleasure in working with Ecem Yıldırım, Tuğçe Önel and Gizem Bora while doing my experiments; I give them endless thanks for their understanding and encouragement. I am also appreciative for their interest and help in conducting the thesis experiments.

I was deeply affected with the help of my close friends Selinay Şenkal, Miray Şenkal, Derya Garip and Serra Şener really thank them for the close interest and supportive approache they showed me throughout my studies. Also, I would like to thank my biggest supporter Ekrem Erem for his endless psychological support and love.

And the last thanks are for my mom Hale Talaş, my father Tuncay Talaş and my sister Necmiye Talaş; the work they spent on me and the patience they showed can never be paid. I am also grateful to them for their unconditional, real love and endless interest.

TABLE OF CONTENTS

LIST OF FIGURES

LIST OF SYMBOLS AND ABBREVIATIONS

ATM	Ataxia- telangiectasia- mutated gene
BMP-15	Bone morphogenetic protein
c-Abl	Abelson murine leukemia viral oncogene
COC	Cumulus-oocyte complex
CycE	Cyclin E
DDIT4	DNA damage inducible transcript 4 gene
DNA-PKs	DNA protein kinases
DNA	Deoxyribonucleic acid
DSB	Double strand break
Fat4	Protocadherin fat4
FGF	Fibroblastic growth factor
FSH	Follicle-stimulating hormone
GCs	Granulosa cells
GDF-9	Growth differentiation factor
GnRH	Gonadotropin releasing hormone
H_2O_2	Hydrogen peroxide
IR	Ionizing radiation
Kibra	Kidney and brain expressed protein
LATS1/2	Large tumor suppressor kinase ½
LH	Luteinizing hormone
MOB1A/B	MOB kinase activator 1A/1B
MST1	Macrophage-stimulating 1 gene
NCOA6	Nuclear receptor coactivator 6
NDR	Nuclear Dbf2 associated kinase family
NES	Nuclear export signals
Nf2	Neurofibromatosis type II, neurofibromin 2
NHEJ	Non-homologous end joining repair
NLSs	Nuclear localization signals
NuRD	Nucleosome remodeling and deacetylase complex

ODPFs	Oocyte derived paracrine factors
OOX	Oocytectomy
Rb	Retinoblastoma protein
Sav	Salvador
SCF-E3	Skp, Cullin, F-box containing E3 ubiquitin ligase complex
SH2	Src homology 2
SH3	Src homology 3
STAT	Signal transducer and activator of transcription
STK3	Serine/threonine-protein kinase 3
STK4	Serine/threonine-protein kinase 4
TAOK1/2/3	Serine/threonine-protein kinase TAO1/2/3
TAZ	Tafazzin (WWTR1)
TEAD	TEA domain family member
TGF-β	Transforming growth factor family
TZPs	Transzonal projections
UV	Ultraviolet radiation
VGLL4	Vestigial-like protein 4
Wts	Warts
YAP	Yes-associated protein
Yki	Transcriptional coactivator yorkie

ABSTRACT

Talaş, N. (2021). Determination of the Relationship Between c-Abl Tyrosine Kinase and YAP in Response to DNA Damage in Mouse Granulosa Cells. Yeditepe University, Institute of Health Science, Department of Histology and Embryology, MSc thesis, İstanbul

Granulosa cells are the crucial type of cell in the ovarian tissue. These cells provide the physical support and microenvironment necessary for the development and maturation of oocyte. Granulosa cell proliferation and function are very curicial for a healthy follicle development, maturation, ovulation and atresia. Yes-associated protein (YAP) translocates to the nucleus and becomes activated when Hippo pathway is inactivated. c-Abl is a tyrosine kinase which can be activated by DNA damage and functioning in apoptosis, stress response and adhesion. It has been known that under the DNA damage, c-Abl alters the oncogenic function of YAP to tumor supressor. In this thesis study, by performing double immunofluorescence staining and immunoblotting assay, we aimed to exert the changes in the expression of c-Abl and YAP in response to 2.5μM, 5μM, 10μM, 20μM, 50μM hydrogen peroxide (H_2O_2) concentrations and 100μM, 200μM and 400μM hydrogen peroxide (H_2O_2) concentrations in mouse GCs. According to the results, it was obvious that the nuclear expression of c-Abl decreased in 5μM, 10μM, 20μM, 50μM H_2O_2 concentrations. Similarly, nuclear localization of c-Abl decreased in 100μM, 200μM and 400μM H_2O_2 treated GCs in compare with positive control which meant that cytoplasmic c-Abl could be activated in response to increasing H_2O_2 concentrations. According to the results, this cytoplasmic c-Abl activity caused to preserved nuclear YAP and increased p73 protein expression in normal GCs. Our findings indicated that to the fill the gap between oxidative stress and c-Abl/YAP activation-dependent GCs proliferation, migration and apoptosis, the determination of signaling relation between c-Abl and YAP is very important.

Key words: Granulosa cell (GC), Yes-associated protein (YAP), Abelson tyrosine kinase (c-Abl), Hydrogen peroxide (H_2O_2)

ÖZET

Talaş, N. (2021). Fare Granüloza Hücrelerinde DNA Hasarına Karşı Yanıtta c-Abl Tirozin Kinaz ile YAP Arasındaki İlişkinin Belirlenmesi. Yeditepe Üniversitesi, Sağlık Bilimleri Enstitüsü, Histoloji ve Embriyoloji Anabilim Dalı, Yüksek Lisans Tezi, İstanbul.

Granüloza hücreleri, ovaryumda oositin olgunlaşması için gerekli olan fiziksel desteği ve mikro ortamı sağlayan birincil hücre tipidir. Granüloza hücre proliferasyonu, sağlıklı bir folikülün gelişimi, olgunlaşması, ovulasyonu ve atrezi mekanizması için çok önemlidir. Yes ile ilişkili protein (YAP), Hippo sinyal yolağı inaktif hale geldiğinde çekirdeğe yerleşerek aktif hale gelmektedir. Abelson tirozin kinaz (c-Abl) ise DNA hasarı ile aktive edilebilen ve apoptoz, stres yanıtı ve adhezyon gibi hücresel olaylarda işlev gören bir tirozin kinaz türü olarak bilinmektedir. DNA hasarı altında, c-Abl'in YAP'ın onkojenik fonksiyonunu tümör baskılayıcı fonksiyona değiştirdiği bilinmektedir. Bu tez çalışmasında fare granüloza hücrelerinde 2.5μM,5μM,10μM,20μM ve 50μM hidrojen peroksit (H_2O_2) konsantrasyonlarına ve 100μM, 200μM, 400μM hidrojen peroksit konsantrasyonlarına yanıt olarak c-Abl ve YAP ekspresyonundaki değişiklikleri çift immunofloresan boyama yöntemi ve western blot yöntemi ile ortaya koymayı amaçladık. Elde edilen sonuçlar doğrultusunda, c-Abl'in nükleer ekspresyonunun 5μM, 10μM, 20μM, 50μM şeklinde artan hidrojen peroksit ile muamele edilen granüloza hücrelerinde kontrole kıyasla azaldığı ortaya çıktı. Benzer şekilde c-Abl'in nükleer ekspresyonu, artan hidrojen peroksit konsantrasyonlarına yanıt olarak sitoplazmik c-Abl'in aktive edilebileceği anlamına gelen pozitif kontrol ile karşılaştırıldğında 100 μM, 200 μM ve 400 μM hidrojen peroksit ile muamele edilmiş granüloza hücrelerinde de azalmıştır. Sonuçlara göre bu sitoplazmik c-Abl aktivitesi, normal granüloza hücrelerinde nükleer YAP seviyesinin korunmasına ve p73 ekspresyonunun artmasına neden olmuştur. Bulgularımız, oksidatif stres ile c-Abl/YAP aktivasyonuna bağlı granüloza hücrelerinin çoğalması, göçü ve apoptozu arasındaki boşluğu doldurabilmek için c-Abl ve YAP arasındaki sinyal ilişkisinin belirlenmesinin oldukça önemli olduğunu göstermiştir.

Anahtar kelimeler: Granulosa cell (GC), Yes-associated protein (YAP), Abelson tyrosine kinase (c-Abl), Hydrogen peroxide (H_2O_2)

1.INTRODUCTION AND PURPOSE

Hippo signalling pathway has important roles such as regulating proliferation of cells, differentiation and survival of cells. Additionally, it has been obvious that Hippo pathway functions in regulation of organ size and embryonic development (1). The proteins of Hippo signalling pathway are present in ovary and also they are expressed in ovary. Moreover, these proteins are involved in ovarian functions (2,3).

In Hippo signalling pathway, there are many negative regulators act in the kinase cascade. Kinase cascade phosphorylates and inactivate downstream effectors and trascription co-activators. These regulators are; Yes-associated protein (YAP1) and Tafazzin (TAZ) also known as WWTRT (2). When kinases of Hippo signalling pathway are activated, (MST1/2) causes to kinase cascade consisting of phosphorylation and activation of kinases LATS1 and LATS2. In this way, YAP1 and TAZ are phosphorylated and inactivated. When YAP1 and TAZ proteins are phosphorylated, they are maintained in the cytoplasm. Also, they are inhibited from act as transcriptional coactivators. If the Hippo signalling pathway is inhibited, YAP1 and TAZ are in unphosphorylated form and located in the nucleus. In the nucleus, they start to activate genes which are associated with proliferation and survival. According to the studies, when the some members of Hippo signalling pathway are absent, some defects occur in the ovary. For instance; follicle development decreases, loss of germ cells take place and follicular tumors can be seen in LATS1 deficient mice (4,5).

Addition to this, when DNA damage occurs, pro-apoptotic genes are activated by the YAP with the aid of p73. This situation is supported by the c-Abl (Abelson murine leukemia viral oncogene). c-Abl leads to phosphorylation of YAP at the Y357 residue (6). So, YAP effector activity is turned on and off by Hippo signalling pathway. Additionally, activity of YAP is switched to opposing manner by DNA damage response (7).

Granulosa cells are known as somatic members of follicles. These cells create contact with the oocytes and in this way growth and maturation of oocytes are supported by granulosa cells. Granulosa cells promote the follicle growth and they respond to

stimulus from neighboring cells. Also, they promote the secretion of sex hormones which are important for reproduction (8).

In the follicles which are progressed, proliferation of granulosa cells rapidly maintains and this lead to support follicle growth (9). It has been obvious that it is unknown that the mechanism underlying the regulation of GC proliferation even though rapid progression has been made in the regulation of follicle development.

Although YAP possess important role in GC proliferation and c-Abl transforms the YAP function from oncogenic to tumor suppressor, the correlation between the YAP and c-Abl in ovarian granulosa cells is still unknown. In order to clarify this obscurity, we suggest that DNA-damage stimulate c-Abl activation may lead to switch in the function of YAP from pro-proliferative form to pro-apoptotic form in mouse ovarian GCs. Thus, we aimed to exert the changes in the expressions of YAP and p73 after DNA damage induces c-Abl activation in vitro mouse ovarian GCs.

2.LITERATURE REVIEW

2.1. Structure of Ovary

Ovaries are gonads known as the most functional unit of the female reproductive system. These gonads are mainly involved in the creation of oocytes and releasing of steroid hormones required for fertilization and embryonic development. Size of each ovary is about 2-3.5cm in length. Ovaries resemble to an almond in the context of size. Ovaries are clouded white and consist of dense fibrous tissue (10).

The gonads are present in the pelvic cavity. Ovaries are connected laterally to the pelvic wall with suspensory ligaments. Medially, they are attached to the uterus by ovarian ligaments. As additional support, the ovaries are connected from the anterior to the back of the broad ligament with the aid of mesovarium (11).

Blood, lymphatic vessels and nerves enter the ovary through the hilus. The ovarian artery branches from the abdominal aorta. This artery passes through the suspensory ligament. Then, it enters into ovary through the mesoovarium of the broad ligament. Ovarian veins progress along the mesovarium and suspensory ligament. These veins combine with the inferior vena cava on the right and the renal vein on the left (12).

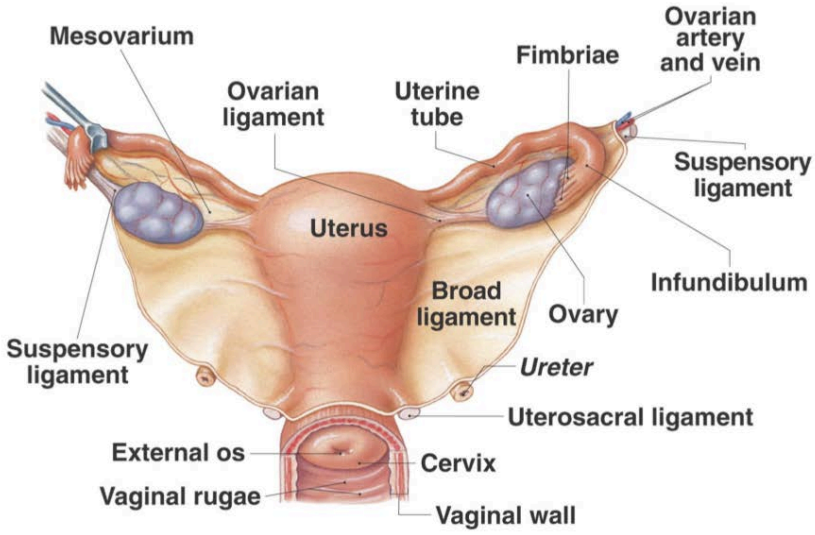

Figure 2.1.1. Structures of female reproductive system (13).

2.2. Histology of Ovary

Ovary includes two main parts which are cortex and medulla. Stroma which refers to the major part of ovary establishes the cortex. While the cortex including oocytes at diverse stages of development forms the outer part of the ovary, the medulla containing stromal cells, blood vessels and nerves forms the interior part of the ovary.

Each developing oocyte is encompassed by cells which leads to support. When oocyte and cells leading to support come together, they called as an ovarian follicle. For the development of oocytes, the ovarian follicles which are in the stroma of cortex provide a microenvironment. The diameter of the ovarian follicle indicates the stage of the developing oocyte. The stroma surrounding the follicles includes smooth muscle fibers. The boundary between the medulla and the cortex is not exactly distinguished.

The surface of the ovary is covered with an epithelium called the germinal epithelium. Type of this epithelium is a simple cuboidal or simple squamous epithelium. The mesovarium is surrounded by mesothelium, and the germinal epithelium is continuous with this mesothelium. Previously, germ cells were thought to originate from the germinal epithelium during embryonic development. But today, it is known that primordial germ cells are of extragonadal origin. These cells migrate from the embryonic

yolk sac to the cortex of the embryonic gonad. In this way, these cells begin to differentiate. Between the germinal epithelium and the cortex, there is a structure with a tight connective tissue layer. This structure is called tunica albuginea which gives the whitish color to the ovary (14).

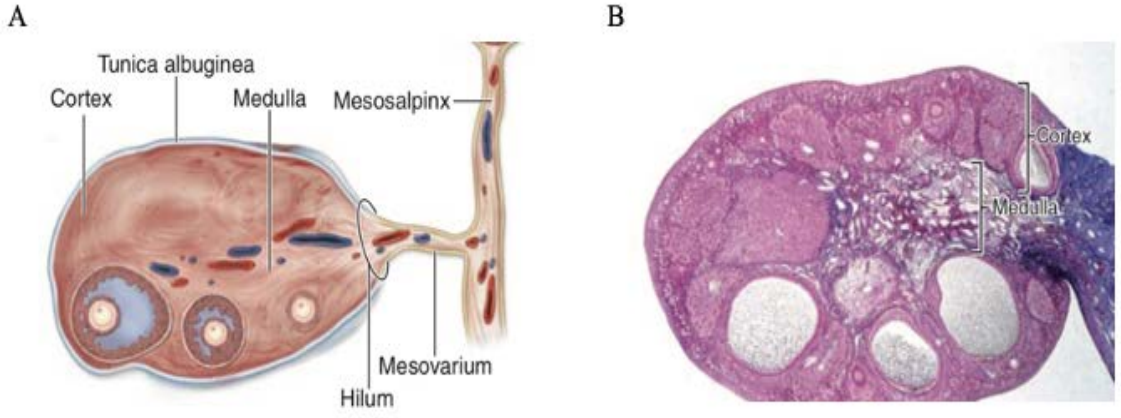

Figure 2.2.1. A sectioned ovary. Representative lateral view of ovary **(A)** Stained image of ovary section **(B)** (15).

2.3. Ovarian Cycle, Uterine Cycle and Their Hormonal Control

Menstrual cycle includes three different phases. These are the follicular stage, the ovulatory stage and the luteal stage. In the follicular stage, a mature or graafian follicle develops from the primordial follicle (16). There are three basic type of ovarian follicles according to histological development stages. These types of ovarian follicles are primordial follicles, developing follicles and mature (graafian) follicles (16).

During follicular development; primordial follicle, primary follicle, secondary follicle and mature (graafian) follicle stages are seen. Gonadotropin stimulation is not effective in the early stage of primordial follicle development phase. At this stage, there is primary oocyte arrested in the prophase 1 stage. Also, primary oocytes are enclosed with the pre-granulosa cells which are flattened and single layer (17). As the primordial follicle turns into a growing follicle, oocytes continue to grow and primary follicles start

to develop. Pre-granulosa cells surrounding oocyte become cubic granulosa cells at this follicular stage (18). As granulosa cells become cuboidal, some changes take place in the oocyte and granulosa cells. Zona pellucida occurs between oocyte and granulosa cells. Because of the ocuurence of zona pellucida, contact between oocyte and granulosa cells is maintained with the aid of transzonal processes. (TZPs) (19). When granulosa cells proliferate and develop, multilayered structure occurs. In the around of this multilayered structure, there are layers of cells that are callled theca cells. At this stage, follicles are called as secondary follicles. As the proliferation of granulosa cells continues, the diameter of the follicle grows and a fluid-filled cavity begins to form between the granulosa cells. The fluid continues to accumulate, and then the cavities merge to form the gap, called the antrum. The follicle is now called as preovulatory or antral follicle that includes secondary oocyte. At this stage, there are two types of cells that are the cumulus granulosa cells and mural granulosa cells. Oocytes are enclosed by cumulus granulosa cells and the inner part of follicle wall is formed by mural granulosa cells (20). In the connection of cumulus cells and oocyte, gap junctions have an important role. One of these gap junction members is connexin 37 protein. In addition, in the interaction between cumulus layers and mural layers, connexin 43 that is another gap junction protein plays an important role (21). In addition to follicular growth, the size of oocytes developes. When female animals pass to the stage of puberty, resuming meiosis I of grown oocytes is induced by the gonadotropic surge. In this way, these oocytes get ready to pass metaphase II phase. Then, oocytes are ready to be ovulated (22).

In the folliculogenesis process, the release of FSH and LH from the anterior pituitary begins to act with the effect of the GnRH (Gonadotropin releasing hormone) released from the hypothalamus. FSH secreted by the pituitary stimulates the maturation of a large number of primordial follicles. FSH is the main hormone that affects follicle development in 8-10 days of ovarian cycle. FSH stimulates the proliferation of granulosa cells and theca cells. These cells then produce estrogens and produced estrogen is secreted into the follicle lumen. As estrogen production increases in the dominant follicle, releasing of FSH is inhibited by a negative feedback loop. Estrogen continues to accumulate in the follicle lumen. As it approaches the end of the follicular phase, estrogen and FSH stimulate the synthesis of LH receptor in follicular cells. Progesterone

production starts to increase before ovulation under the influence of LH. Ovulation occurs 10-12 hours after the sudden rise in LH. In the ovulation, secondary oocyte is released by graafian follicle. When an ovarian follicle releases a secondary oocyte during the ovulation phase, the opened follicle closes and forms the structure which is called as corpus luteum. The corpus luteum is responsible for the production of progesteron that induces the uterus to further thicken while preparing for implantation of a fertilized oocyte. During this luteinization phase, the cells of granulosa and theca interna layers are called as granulosa luteal and theca luteal cells. Estrogen and progesterone are secreted from the corpus luetum. If fertilization takes place, production of progesterone continues. If fertilization does not occur, the corpus luteum regresses and levels of FSH and LH decrease. Ovarial cycle and hormonal changes cause the uterine cycle to occur in the uterus. Uterine cycle and ovarial cycle take place simultaneously. Uterine cycle consists of three phases. These are proliferation, secretory and menstrual phase. With the effect of estrogen, the thickness of the endometrium begins to increase in the proliferation phase. In the secretory phase, the endometrial glands begin to secrete and the vessels lengthen. In the menstrual phase, if fertilization does not occur, the corpus luteum regresses. With the effect of this regression, hormone levels decrease and the developing functional layer of the endometrium undergoes necrosis (14).

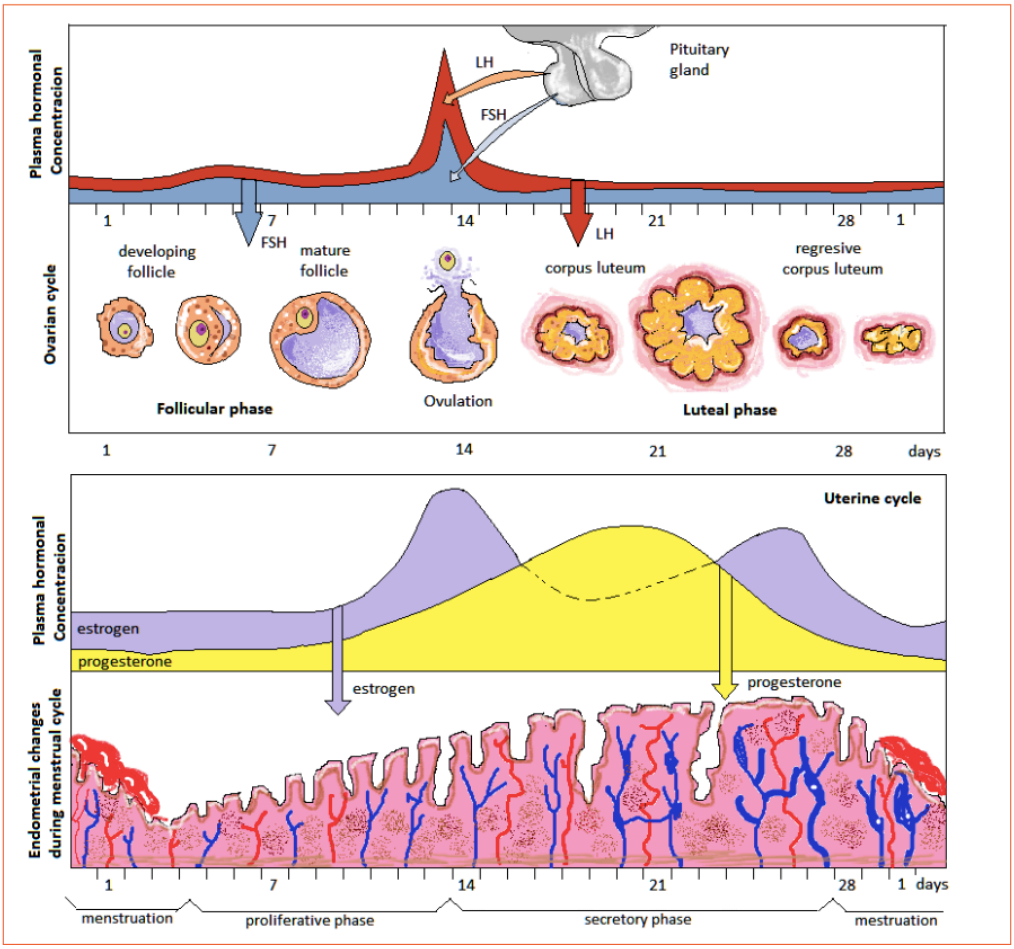

Figure 2.3.1. Hormonal changes in ovarian and uterine cycle (23).

2.4. Interactions Between Oocytes and Granulosa Cells

According to the accomplished researches, while follicular growth continuining, expression of germ cell role can be cell-autonomous. In addition to this, expression of germ cell can be dependent on differentiation of GCs (24). Additionally, differentiation of granulosa cells and growth of follicles can be modulated and affected by oocyte (24). It has been thought that oocytes have an inactive role in the ovary although in the absence of oocytes any follicles cannot formed (25). In point of fact, proliferation of granulosa cells is induced by oocytes. In addition to this, expression of LH receptor mRNA in granulosa cells is supressed by oocytes (26).

Previous studies have been showed that there are direct interactions between oocytes and GCs. In one of these previous studies, the existence of gap junctions between GCs and oocytes have been showed (27). With the aid of gap junctions, regulation of oocytes is supported by GCs. Some molecules that are necessary for regulation of oocytes such as metabolic precursors and nutrients are provided by granulosa cells. Also, molecular signals are provided by granulosa cells for the regulation of oocytes (28). Thus, before oocyte derived growth factors were discovered, it was a consideration that growth of oocytes was managed by in one direction. According to this consideration, oocytes were supported by surrounding granulosa cells in the aspect of nutrients. Additionally, proliferation of granulosa cells was regulated by FSH (28). GCs provide support to the oocytes. In addition to this, there are some factors that facilitate the bidirectional communication between oocytes and GCs. These factors are known as oocyte-derived growth factors which are growth differentiation factor (GDF-9) and bone morphogenetic protein 15 (BMP15) (29).

2.4.1. Transzonal Projections between Oocytes and Granulosa Cells

With the aid of adherens and gap junctions, granulosa cells and oocytes are linked in a primordial follicle. Mainly, N-cadherin is expressed by granulosa cells and E-cadherin is expressed by oocytes (30).

Additionally, during in the growth of oocytes, extracellular coat which is called as zona pellucida is produced by oocyte (31,32). Initially, zona pellucida is in the form of small aggregates. Subsequently, these small aggregates combine together. In this way, they produce an envelope structure around the oocyte. This envelope leads to oocyte disjoins from the granulosa cells.

Transzonal projections (TZPs) which are cytoplasmic filaments lead to occurence of contact between the oocyte and GCs. The size of these filaments can be 1 μm in diameter. Additionally, these structures are originated from the granulosa cells. Also, they extend to oocytes (33).

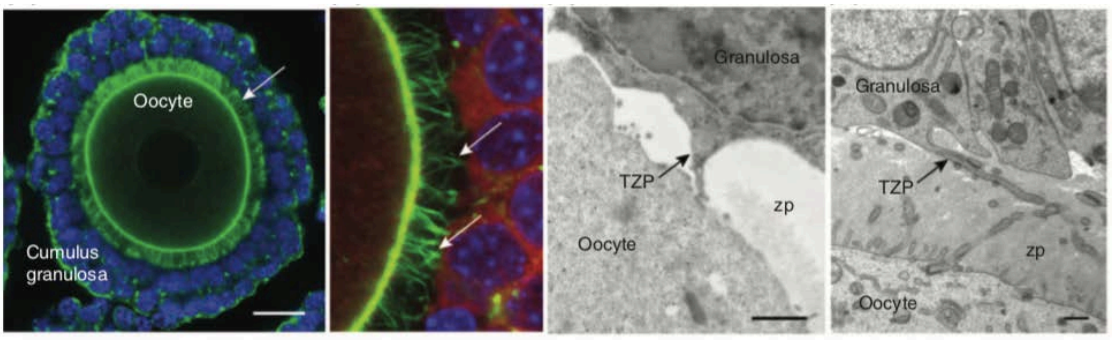

Figure 2.4.1.1. Transzonal projections (TZPs). TZPs are showed by arrows (33).

Transzonal projections diffuse into the oocyte membranes' involvings. Because of these properties, region of membrane contact between oocyte and GCs increases. Additionally, bidirectional communication between oocyte and GCs enhance too. It has been unknown that the source of transzonal projections. It has been mentioned about there are two different mechanisms related with the origin of TZPs. Before the zona pellucida accumulates around the oocyte, these structures may indicate the regions of connection which present between granulosa cells and oocytes (32). One of these models related with the how TZPs occur is that 'stretching' mechanism. According to this mechanism, zona pellucida become accumulated and then it leads to granulosa cells to away from oocytes. Therefore, at the region of connection, two cells persist attached. Subsequently, zona pellucida continues to become thick and this leading to cytoplasmic finger elongation. In this way, transzonal projections (TZPs) are generated. In addition to this, transzonal projections may occur after zona pellucida has been accumulated. 'Pushing' is another mechanism that is related with the how TZPs occur. This mechanism supports the idea that the granulosa cells elaborate transzonal projections (TZPs) and these structures mature towards to the oocytes (33).

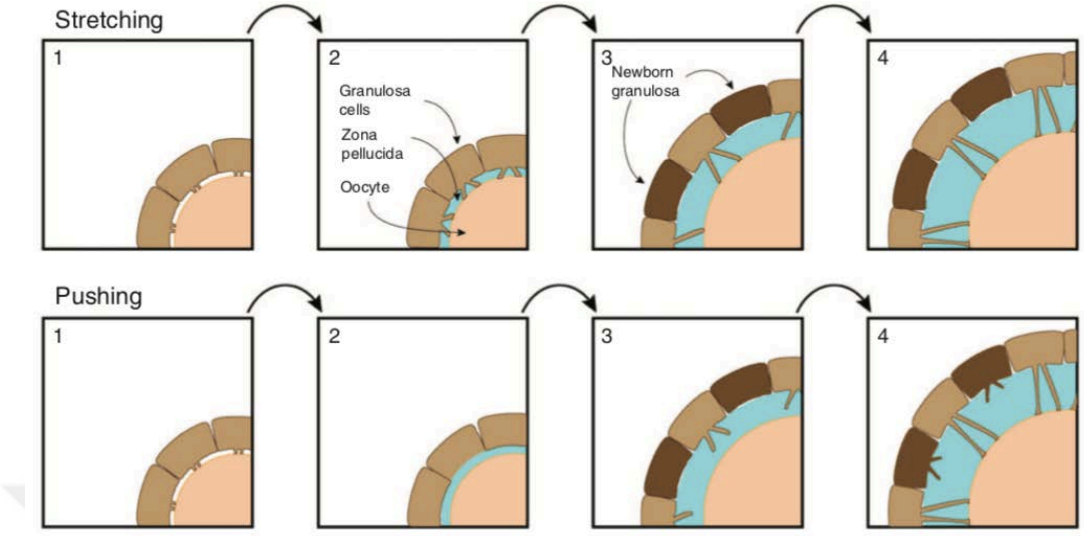

Figure 2.4.1.2. Two mechanisms that indicates how TZPs may occur. Upper panel shows ‘streching’ mechanism while lower panel shows ‘pushing’ mechanism (33).

2.4.2. Signal Transferring from Oocytes to Granulosa Cells

It has been known that oocytes acquire signals coming from surrounding cells. Additionally, oocytes also send signals which have important roles in the differentiation of somatic part of follicle. This information has been intimated many years ago with the aid of conducting an observation related with the granulosa cells and oocytes. According to this observation, in the absence of oocyte, granulosa cells become luteinized. Normally, luteinization occurs only after ovulation (34).

It has been known that oocyte sends signals to the granulosa cells with the aid of gap junctions. However, these signals have not been identified yet. Also, oocytes secrete factors and these factors modulate the differentiation of granulosa cells (35).

There are some growth factors such as growth differentiation factor (GDF9) and bone morphogenic factor (BMP15) which are known as members of transforming growth factor (TGF-β) family. According to the some immunohistochemical studies, GDF9 and BMP15 are originated by the oocyte (36). While oocyte is growing, mRNA levels of GDF9 and BMP15 start to increase. Also, in primary follicle stage and following stages of folliculogenesis, protein of GDF9 is present. Before the ovulation phase takes place, BMP15 is not produced in huge amounts. The reason of this situation is that KITL-

mediated inhibiton of production (37). According to some studies, there are GDF9 and BMP15 expression in granulosa cells also (38).

Mice not having GDF9 are infertile and anovulatory. When GDF9 is deficient in female mice, proliferation of granulosa cells is interrupted. Also, more than one cell layer surrounding oocyte cannot be generated by granulosa cells in the absence of GDF9. The reason of this proliferative defect of granulosa cells is that increasing creation of inhibin in GDF9 -/- females (39). It has been also known that when GDF9 deficiency present in GCs, they fail to interact with the oocytes.

Paracrine factors which are oocyte-derived (ODPFs) have effects on the GCs. Because of these effects, oocyte also support the development of itself. Glucose is metabolized by the granulosa cells to produce pyruvate. Then, this pyruvate is transferred to the oocyte. In the oocytectomy (OOX) procedure in which oocytes are removed from the cumulus-oocyte complex (COC), since the oocytes are removed, amounts of mRNAs that encodes enzymes having roles in glycolytic pathway decrease. Additionally, glycolysis rate in the remaining-cumulus cells decreases too (40). When OOX shells are incubated with grown oocytes, decreased mRNA levels and glycolytic activity are rescued. In the BMP15-/-; GDP9+/- mice, mRNA levels and glycolytic activity also decreased in the cumulus granulosa cells. When OOX shells are incubated with BMP15 and fibroblastic growth factor (FGF), mRNA levels and glycolytic activity are rescued. Therefore, granulosa cells are stimulated by oocyte-derived paracrine factors and they produce pyruvate which is transferred to oocyte. Likewise, the amount of mRNAs that encodes enzymes for synthesis of cholesterol decreased in the granulosa cells in BMP15−/−; GDF9+/− mice and in the OOX shells of wild-type mice. Also, synthesis of cholesterol is impaired. When the OOX shells are incubated with grown oocytes, decreased mRNA levels and impaired cholesterol synthesis are rescued partially (41). So, factors that are created and secreted by the oocytes induce the GCs. In this way, molecular nutrients are produced by GCs and these nutrients are in turn support to the oocyte (41).

2.5. Overview of Hippo Signaling Pathway

The pathway which was associated with tissue growth and has been firstly recognized two decades ago in Drosophila melanogaster is called as Hippo signalling

pathway. Especially in recent years, it has become a signal pathway that has been started to be studied in detail in mammals except Drosophila melanogaster (42).

The Hippo signal pathway contains a kinase cascade, transcription coactivators and DNA binding members within the core. However, studies over time have shown that the Hippo signalling pathway has more than 30 components and the signal pathway has become complicated. Intrinsic cell mechanisms such as cell to cell contact, cell polarization and actin cytoskeleton play a role in the regulation of this pathway. In addition, signals such as cellular energy status, mechanical stress and G-protein bound receptors are also effective in regulation of this pathway (42).

There are main functions of the Hippo signalling pathway that play role in limiting tissue growth in adults and modulating cell proliferation, differentiation and migration in growing organs. In addition to these functions, abnormal cell growth and neoplasia occur as a result of a defect in the Hippo signalling pathway (42).

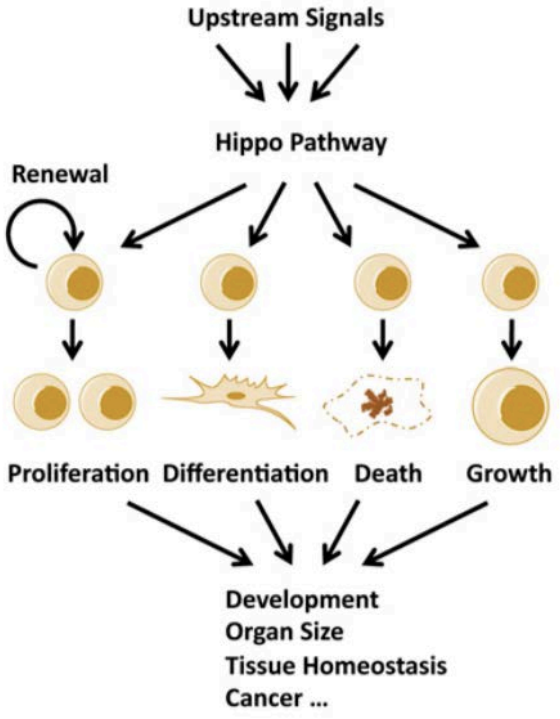

Figure 2.5.1. Effects of Hippo pathway in cell biology. Cell proliferation, differentiation, growth and death are regulated by Hippo signalling pathway (43).

2.5.1. Core Components of Hippo Signalling Pathway in Mammalians

In mammals, the core of the Hippo pathway is a kinase cascade. In this kinase cascade, large tumor supressor 1/2 (LATS 1/2: Homolog of Drosophila Wts) is phosphorylated and activated by mammalian Ste20-like kinases 1/2 (MST1/2). The activities of YAP and transcriptional coactivator with PDZ-binding motif (TAZ) are restricted by the physiological output of this cascade. When YAP and TAZ are activated, they translocate into the nucleus to bind the TEAD (TEA domain family member) transcription factor. In this way, expression of genes that are responsible in survival is stimulated (42). TAO kinases (TAOK1/2/3) can initiate the Hippo kinase cascade. The activation loop of MST1/2 is phosphorylated by these kinases. In this way, activation of MST1/2 takes place (44,45). In addition, phosphorylation of activation loop can be accomplished by autophosphorylation of MST1/2 (46). Consistent with this, dimerization of MST1/2 enhances the activation loop phosphorylation (47). Because of this reason, activation of MST1/2 can be started by dimerization without aid of upstream kinases. When MST1/2 is activated, two scaffold proteins are phosphorylated. These proteins are SAV1 and MOB1A/B (48). In the recruitment and phosphorylation of LATS1/2 at their hydrophobic motifs, these proteins assist MST1/2. T1079 is hydrophobic motif for LATS1 and T1041 is hydrophobic motif for LATS2 (49,50). NF2/Merlin is another critical player in this action. It can interact with LATS1/2 and in this way, phosphorylation of LATS1/2 by the MST1/2-SAV1 complex is facilitated (50). LATS1/2 is autophosphorylated and activated respectively. Then, YAP and TAZ are phosphorylated and inactivated (51).

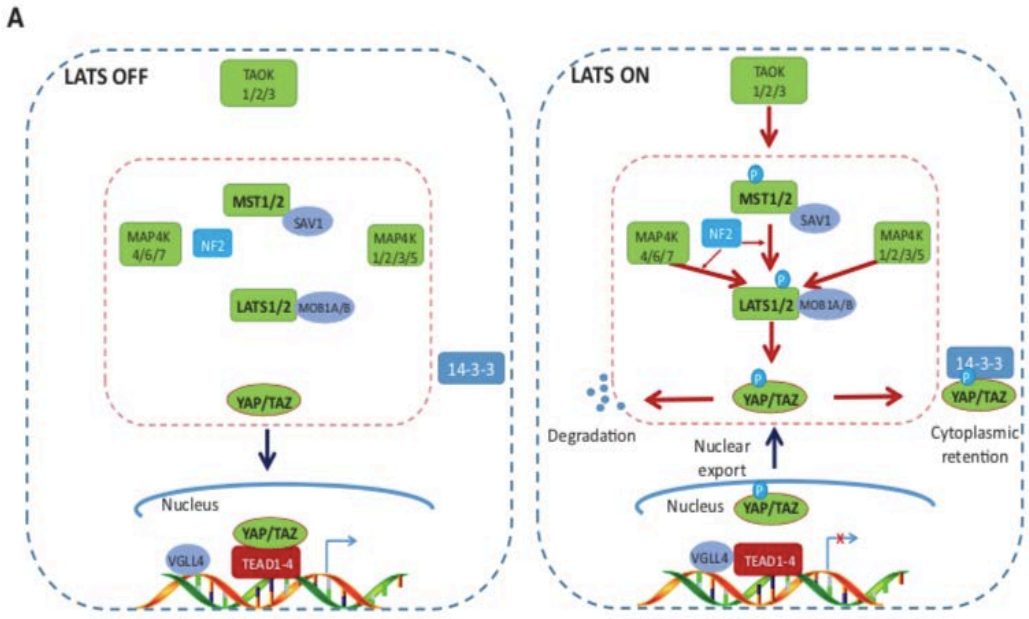

Fig 2.5.1.1. Hippo pathway in mammalians (42).

In addition to these, there are two groups of MAP4Ks (mitogen activated protein kinase kinase kinase kinase). First one is the MAP4K1/2/3/5 which is a homolog of Drosophila [Hppy] and second one is the MAP4K4/6/7 which is a homolog of Drosophila [Msn]. LATS1/2 is also phosphorylated at their hydrophobic motifs by these two groups. In this way, activation of LATS1/2 takes place. It is known that in the regulation of Hippo pathway under certain conditions, MAP4Ks play more recognizable role than MST (42). There are LATS-activating signals which are contact inhibiton, energy stress, F-actin diassembly and serum deprivation. In response to these signals, both MST1/2 and MAP4Ks must be deleted in order to eliminate the YAP phosphorylation (42). Thus, both MST1/2 and MAP4Ks have important roles in the regulation of LATS1/2 (52). When YAP and TAZ are phosphorylated, they connect with 14-3-3. In this way, cytoplasmic segregation of YAP/TAZ takes place (53). Moreover, phosphorylation of YAP/TAZ by casein kinase and recruitment of the SCF-E3 (Skp, Cullin, F-box including E3 ubiquitin ligase complex) ubiquitin ligase are promoted by LATS-mediated phosphorylation. As a result of this, degradation of YAP/TAZ occurs (54). Also, autophagy cause YAP to degrade (55). YAP and TAZ do not posses DNA-binding domains. When YAP and TAZ

located into nucleus, gene expression is regulated by interaction between YAP/TAZ and TEAD1-4. Also, TEAD1-4 connects to VGLL4 (vestigial-like protein 4) in the nucleus. Thus, it serve as transcriptional repressor in the nucleus. When YAP/TAZ interacts with TEAD1-4, VGLL4 segregate from TEAD1-4. In this way, TEAD-induced transcription of genes is activated for supporting tissue growth and inhibiting apoptosis (56). When MST1/2, SAV1, MOB1A/B, NF2 is deleted or LATS1/2 or YAP are overexpressed, TEAD target gene expression is upregulated in mouse models. In addition to this, expansion of progenitor cells increases and growth of tissues continues. Because of all these events, critical roles of these genes in Hippo pathway is supported (57).

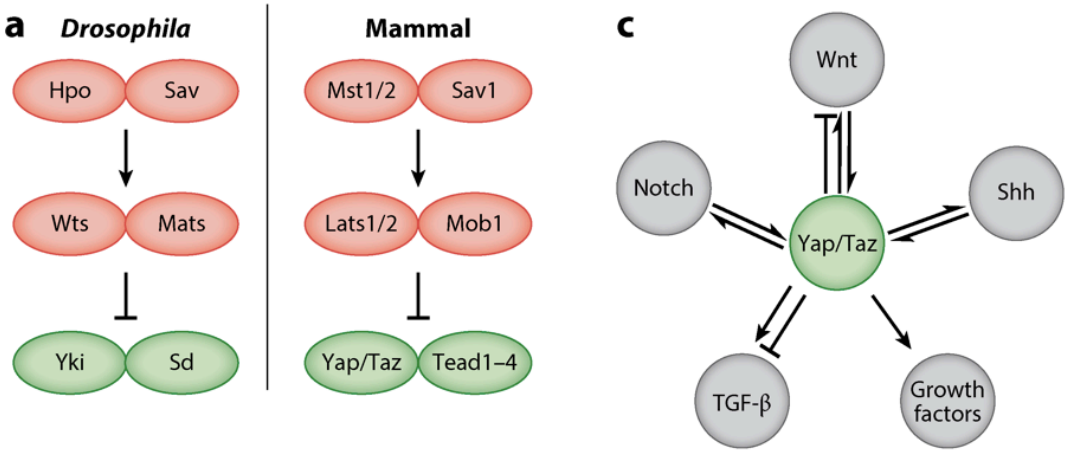

Fig 2.5.1.2. Core members of Hippo Signalling Pathway**.** A. Comparision of Hippo pathway core members between Drosophila and Mammalians. C. Interactions between Hippo and another signalling pathway (58).

2.5.2. Upstream Regulation of Hippo Signaling Pathway

There are homologs in the genome of mammalians. These homologs are present for upstream regulators in the Hippo signalling pathway. These homologs are; Kibra, Ex, Mer (NF2/Mer), Ft (Fat4/Fat-j), Ds (Dchs1 and Dchs2), Fj (Fjx1), Lft (Lix1 and Lix1-like) and Crb (Crb1, Crb2 and Crb3) (59).

NF2 / Mer is among the mammalian genes that correspond to Drosophila and have been included as Hippo signal pathway upstream regulators. This gene is the most intensively studied gene (60). Mer / NF2 was first discovered about twenty years ago. In general, this gene has been identified as a tumor suppressor. When mutation occurs in this tumor suppressor gene, Neurofibromatosis 2 occurs. Neurofibromatosis 2 is an autosomal dominant disease and it is identified by the growth of benign schwannomas NF2/Mer has been observed as connected to Ras, Rac, STAT or PI3K signaling. In addition, NF2 / Mer has been shown to be linked to different effector pathways and cellular functions. The degradation of membrane receptors such as EGFR or the inhibition of E3 ubiquitin ligase $CRL4^{DCAF1}$ in the nucleus can be defined as some of these pathways and functions (61). In addition, NF2 plays an important role in contact inhibition mediated by cell surface receptors or tight junctions. When Nf2 becomes inactive, it causes hepatocellular carcinoma and bile duct tumors (62). Also, when mutation takes place in the Mst1/2 and Sav1 components, similar double tumor phenotypes occurs (63). The loss of YAP leads to the loss of hepatocytes and bile epithelial cells. However, when YAP is deleted as heterozygous, it does not lead to a phenotypic finding alone. In line with these findings, genetic evidence was provided for NF2/Mer to be physiologically located in the upstream step of the Hippo signalling pathway (62).

Lats1/2 phosphorylation and YAP activity in mammalian cell cultures are stimulated and inhibited, respectively, by over-expressed human homologs of some elements of the Drosophila Kibra-Ex-Mer complex contacting with each other physically or with constituents of the Hippo signalling pathway (53).

Only Fat4 is the Drosophila Ft homologue among the other four mammalian atypical cadherins with similar cytoplasmic tail. Fat4 posses vital roles in controlling inner orientation of hair cell and elongation of neural tube. In addition, any mutations in Fat4 leads to occurence of cystic kidney disorder that is described by reduction of orientated cell division (64).

2.5.3. Mechanisms Activating Hippo Kinase Cascade

LATS1/2 pertain to the NDR (nuclear Dbf2 associated) kinase family. NDR1 and NDR2 are another members of NDR family. In several new studies of the Hippo

signalling pathway, NDR1/2 is placed in the network of Hippo pathway (65). NDR1/2 can function as a YAP kinase. In this way, it inhibits YAP-induced tumorigenesis in the intestinal epithelium (66). NDR1/2 and LATS1/2 exhibit similar phosphorylation motifs. However, in many conditions involving the deletion of LATS1/2, phosphorylation of YAP disappears and the nuclear localization of YAP occurs. Therefore, the exact role of NDR1/2 has not been identified in the regulation of the Hippo pathway (66). There are some requirements for the activation of NDR family kinases. One of these are phosphorylation of hydrophobic regulatory site. Another one is that conserved Ser/Thr residue should be phosphorylated in the loop of activation.

Some upstream Ste20-like kinases conduct the phosphorylation of hydrophobic motif. One of these kinases are MST1/2 which is for LATS1/2 and NDR1/2. Another one is MST3 for NDR1/2 (67). Some researches in recent years have shown that LATS1/2 is phosphorylated by MAP4Ks. Phosphorylation takes place in the hydrophobic motif region. MAP4Ks is a member of the Ste20 family (67). LATS autophosphorylation is promoted when Ste20-like kinase phosphorylates hydrophobic motif. Thus, kinase activity increases (68). NDR family kinases have common features. One of them is the interaction between MOB proteins and the N-terminal regulatory domain of kinases. However, LATS1/2 and NDR1/2 use different subgroups of MOB proteins. MOB1A/B which is a member of MOB protein family is correlated with both LATS1/2 and NDR1/2. MOB2 which is an another member of the MOB protein family, intercedes inhibitory connection with NDR1/2. However, MOB2 does not interact with LATS1/2 (69,70). New studies support new molecular perceptions into the role of MOB1 in phosphorylation of LATS1/2. These studies also give new insights into the activation of MST1/2. Autophosphorylation occurs between MST2's own binding kinase domain and the SARA domain. Because of this autophosphorylation, a phosphor retention motif is formed that can also include MOB1. When the structure of the MOB1-phosphoMST2 complex is examined, it is obvious that MOB1 is attached to phosphorylated MST2. With this binding, MOB1 is rescued from its unique autoinhibitory configuration. Thus, MOB1 becomes accessible to LATS1. LATS1 is then bound to the MOB1-phosphoMST2 complex. In this way, the MST2-MOB1-LATS1 triple complex is formed. Thus, phosphorylation is increased by MST2 in the N-terminal tail of MOB1. Also,

phosphorylation increases in the hydrophobic motif (T1079) of LATS1. When MST2 phosphorylates T1079 in LATS1, it directly contributes to LATS1 activation. Separation of phosphorylated LATS1 and MOB1 from MST2 is triggered by phosphorylation of MOB1. Mechanism of LATS1/2 activation by MST1/2 is elucidated by these studies. Also, crucial function of MOB is elucidated by studies in this process (42).

2.6. Transcriptional programs of YAP/TAZ and their functional end product

In recent years, much more purified transgenic mouse models have been created with tissue specific deletion and induced over-expression. Thanks to these mouse model studies, the physiological contribution of the Hippo signal pathway members to growth of tissue, differentiation of cell, competition of cell and malignant transformation has been more extensively characterized (71). The Hippo signalling pathway has different functions. Inactivation of YAP and TAZ is one of these functions in differentiated cells to protect the silence of cell (72). When the tissue is damaged, the Hippo pathway is suppressed. Accordingly, YAP and TAZ trigger the self-renewal of the progenitor cells and stimulate tissue repair. When an injury occurs in cells cultured in an in vitro environment, YAP is activated. Nuclear YAP supports wound healing by directing cell migration and proliferation (53). TEAD1-4 is often necessary for YAP and TAZ to function. YAP and TAZ cannot be directly linked to DNA. Therefore, they perform as transcriptional coactivators of TEAD1-4. In addition, YAP and TAZ also have interactions with different transcription factors (73). TEAD activates many genes transcriptionally (74). The components of the SWI / SNF chromatin remodeling complex are recruited by YAP and TAZ. In addition, the NCOA6 histone methyl transferase complex can be recruited by YAP and TAZ. Thus, transcriptional activity of TEAD is stimulated (75). The complex of YAP/TAZ – TEAD can perform as transcriptional corepressor. For target genes, it recruits the NuRD histone deacetylate complex. Some of these target genes are DDIT4 and Trail (76) or ΔNp63 (**77**). In order to exert the character of YAP/TAZ as transcriptional repressor, further researches are required. In addition, gene expression is either stimulated or repressed by nuclear YAP/TAZ.

2.7. Yes-associated protein (YAP) Signalling in Ovary

Proteins which are present in Hippo signalling pathway are expressed in ovarian tissue. These proteins also involved in functions of ovary (78). Studies conducted previously showed that if members of Hippo pathway are deleted, many defects in ovary is observed. These defects are reduced follicular development, loss of germ cells, follicular cysts and decreased fertility (4,5). To be able to provide growth of follicle and maturation of oocyte, proliferation of granulosa cells occurs rapidly in growing follicle (9). Nowadays, mechanism which underlies the regulation of GC proliferation and differentiation is not clear yet. According to previous studies in Drosophila, Hippo pathway has a role in development of ovary (79,80). Additionally, according to many another studies, Hippo-YAP pathway functioning in the regulation of mammalian ovarian function. Studies conducted in Hsueh laboratory showed that if YAP1 is activated with the aid of physical fragmentation of ovary, follicle growth is promoted. Also, if any chemical treatments are used to activate YAP1, growth of follicle is promoted too (81,82). According to an another study, to be able to regulate proliferation and differentiation of GCs, YAP1 connects with many other signalling pathways. Additionally, it was suggested that activation of YAP1 is crucial for cell function of granulosa (83).

2.8. Structure, Localization and Function of c-Abl

The type of non-receptor tyrosine kinase which is a 140 kDa is called as c-Abl. It is a proto-oncoprotein and it belongs to Src family of tyrosine kinases. It was discovered as homolog of an oncogene which is called as v-Abl previously. This is the Abelson murine leukemia virus's oncogene. The phosphate group of ATP is transferred to a tyrosine residue of a protein by this tyrosine kinase. Nowadays, it has been cloned with using of human, mouse, nematode and Drosophila (84). In various cellular processes, c-Abl performs some vital roles. Cell death, differentiation, stress response, apoptosis and cell adhesion are some of these processes. In addition, transforming variants of c-Abl participate in tumorigenesis and play role in many crucial cellular processes. In order to be able to investigate the function of c-Abl, downstream targets of it should be identified. With the aid of this approach, many candidates that are members of DNA repair machinery can be identified (84).

In animal cells, c-Abl is expressed in whole site of cell. It can localize in either nucleus or cytoplasm. In various sites, it performs different roles. c-Abl exerts nuclear localization in fibroblasts. Unlike this, it localizes into cytoplasm in neurons and haematopoietic cells. In addition, all the Abl strains which are transforming show cytoplasmic localization. Both nuclear localization signals (NLSs) and nuclear export signals (NES) control the subcellular position of c-Abl (84).

c-Abl posseses some of functional domains. These domains share common properties such as the myristoylation site. Another common feature is having tyrosine kinase domain with substrate specificity and having Src homology 2 (SH2) and SH3. These are both regulate activity of c-Abl with the aid of discriminating interactions between proteins (84).

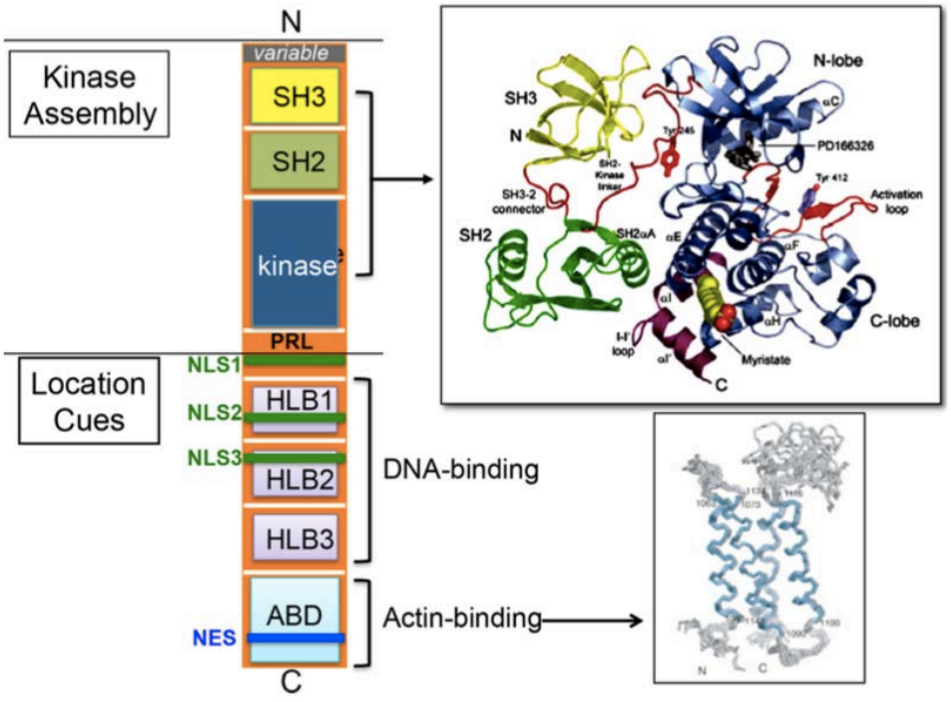

Figure 2.8.1. ABL domains and their structures. 'N' refers to the N terminal which is a variable. It is a promoter and two ABL variants are encoded by 5' exon. These variants are Type 1a/b (human) and Type I/IV (mouse). SH3 refers to Src homology 3 domain, SH2 refers to Src homology 2 domain and kinase refers to kinase domain (85).

Kharbanda et al. have been defined the first pro-apoptotic role of c-Abl. This is accomplished with the aid of explaining c-Abl knock-out cells are compromised in the apoptotic response to ionizing radiation (86). Because of the inconsistent roles of c-Abl, more extensive functional analysis should be conducted about c-Abl.

2.8.1. Activation of c-Abl kinase

Generally, domain of c-Abl kinase is inactive in cells (87,88). Previous studies exerted that when SH3 domain of c-Abl was deleted or swapped, c-Abl kinase was activated (89,90). The meaning of this that the activity of c-Abl kinase domain is inhibited by SH3 domain. With the aid of interacting with inhibitory proteins, SH3 accomplishes this. SH3 domain is binded by kinase inhibitory proteins. In addition, activity of c-Abl kinase is inhibited by only a few of SH3 binding proteins which are

Pag/MSP23 and Aap1. Also, activity of c-Abl kinase is inhibited by Pag/MSP23 as independent from SH3 domain. Pag/MSP23 accomplishes this by interacting directly with kinase domain (91). In addition to these, activity of c-Abl kinase is inhibited by tumor supressor retinoblastoma protein (Rb). Rb makes possible it with the aid of binding of the ATP-binding lobe of Abl kinase (92). According to these informations, it is obvious that SH3 domain has not an exclusive role in inhibiting activity of kinase. Additionally, c-Abl phosphorylates Abi 1 and 2 which are another binding proteins of SH3 (93). Thus, c-Abl can not inhibited by these proteins. In in-vitro studies, it was observed that adaptor protein Crk26 and RFX113 which was a DNA-binding protein stimulate the activity of c-Abl kinase.

In order to be able to activate c-Abl, many agents that damage to DNA are recognized. One of these are ionizing radiation (IR). Unlike ionizing radiation, it was observed that ultraviolet radiation (UV) can not stimulate the activation of c-Abl (94). Activation of c-Abl kinase activity by IR is associated with the activation of the ataxia-telangiectasia-mutated (ATM) gene (95). SH3 domain of c-Abl is binded by ATM which belongs to phosphatidylinositol-3-kinase like enzymes family (96). c-Abl is phosphorylated by ATM at its serine 465 region in the case of exposing cells to ionizing radiation (95). Although interaction between c-Abl and ATM occurs, activation of c-Abl kinase is seen after ionizing radiation. Therefore it is obvious that instead of interaction between ATM and c-Abl, phosphorylation of c-Abl at serine 465 region is more contributory for activation of c-Abl (85). In addition to ionizing radiation, other agents such as cisplatin and mitomycin-c which damage to DNA causes to activate of c-Abl. In 1995, Khabarda and co-workers indicated that when cis-platin and mitomycin-c treatment was applied to NIH3T3 fibroblast cells, formation of DNA intrastrand crosslinks and mono/bifunctional DNA lesions leading to activate c-Abl occured. (97).

2.8.2. Relationship between c-Abl, Apoptosis and p73

In the continuation of tissue homeostasis and stress response, the process which is called apoptosis is essential. It is also needed for development of organisms. There are many molecular pathways which have been defined as reasons of apoptosis. These

pathways leading to apoptosis have been induced by some modifications such as protein-protein interactions and phosphorylation (84).

Dorsch and his colleagues suggested that c-Abl was shown to have an anti-apoptotic effect. In this study, lymphoid bone marrow culture was performed by through the c-Abl deficient mice and it was shown that the obtained B-cell lines show enhanced sensitivity to apoptosis triggered by growth factor loss (98).

Similarly, Konopka et al. have been exerted that cells without c-Abl showed malfunction in apoptotic response to ionizing radiation (IR). According to this group, IR gives a pro-apoptotic function to c-Abl (87). Coherently, cells which expressed the c-Abl kinase death mutant showed resistance to ionizing radiation- stimulated loss of apoptosis. Variants of oncogenic c-Abl and wt c-Abl acted in contrast with each other. Instead of first exon of c-Abl tyrosine kinase, BCR gene was present in patients with chronic myelogenous leukemia. As a results of this replacement, c-Abl kinase was present an active form. As a result of BCR/ABL expression, proliferation increased, morphologic transformation and anti-apoptotic impacts occured (99).

In addition to anti-apoptotic role of c-Abl, inferences have also been made regarding its pro-apoptotic role. As a result of Yuan an co-workers'study, it was suggested that resistance to ionizing radiation-induced apoptosis exhibited by cells which expressing inactive c-Abl kinase mutant. According to this research group, it was implicated that the c-Abl have a pro-apoptotic role (100).

It is contemplated that the tumor suppressor which is called as p53 is a downstream effector of c-Abl. However, it was observed that apoptosis was stimulated by c-Abl independent from p53 status. Direct interaction between p53 and c-Abl was only recognized in in-vitro study. In addition, although over-expression conditions were available, c-Abl did not significantly phosphorylate p53 (101). Unlike to this, it was shown that p73 is preferable candidate. p73 is belong to p53 family. Additionally, c-Abl can phosphorylate the p73 in-vitro and in-vivo. It was observed that apoptosis in different cell lines is induced by p73 (102). In fibroblasts, p73 should be over-producted and it should come together with c-Abl to be able to stimulate apoptosis. When p73 exposure to ionizing radiation, it is tyrosine phosphorylated (103). p73 includes motif which is a PxxP interacting with SH3 domain of c-Abl. Additionally, p73 act as a substrate of c-Abl (102).

When DNA-damage is occured by ionizing radiation, p73 start to accumulate in c-Abl dependent mode. In addition, when p73 accumulates and become modified, the transcription of the downstream pro-apoptotic genes is provided by p73 (101).

2.8.3. Relationship between c-Abl and DNA Repair Activities

To be able to support balance between variety and genomic stability, DNA proceedings have vital role. These DNA transactions include DNA recombination, repair and replication also. c-Abl can involve into DNA proceedings with the aid of its DNA binding site.

In response to damage of DNA, c-Abl is activated and it interacts with components which are functioning in double strand break (DSB) repair. Some of these components are phosphorylated by c-Abl while some of them phosphorylate it. In response to DNA damage, there is a mutual interaction between c-Abl and ATM (ataxia- telangiectasia mutated protein kinase) (104). It has been also observed that there was a direct interaction between c-Abl and DNA-PK (protein kinase). Non-homologous end joining repair process (NHEJ) is regulated by these DNA-PKs (protein kinases). When DNA-PKs are phosphorylated by c-Abl, complex of DNA-PK-Ku80 protein separetes from DNA. Because of this phosphorylation, NHEJ repair reduces also (87). Ku80 is an another protein that connects the ends of DNA double strand breaks. This protein is also required for non-homologous end joining repair (NHEJ). BRCA1 is an another player that participate in mechanism which response to double strand breaks. When cells are subject to ionizing radiation, interaction between c-Abl and BRCA1 is inhibited (105). It has been observed that interaction between c-Abl and Rad51 occurs. In recombination, this protein is responsible for exchange of strand. Activity of DNA strand exchange of Rad51 is inhibited by c-Abl in response to DNA damage (106). In additon to Rad51, c-Abl phosphorylates also Rad52 which is an another homologous recombination protein (107). In response to DNA damage, c-Abl interacts also with WRN which is a helicase functioning in DNA metabolism processes (108).

These data from studies show that c-Abl may play a role in regulating DNA repair. When DNA damage occurs and it becomes too dangerous, it can not to be repaired. In this situation, pro-apoptotic pathway is activated by c-Abl.

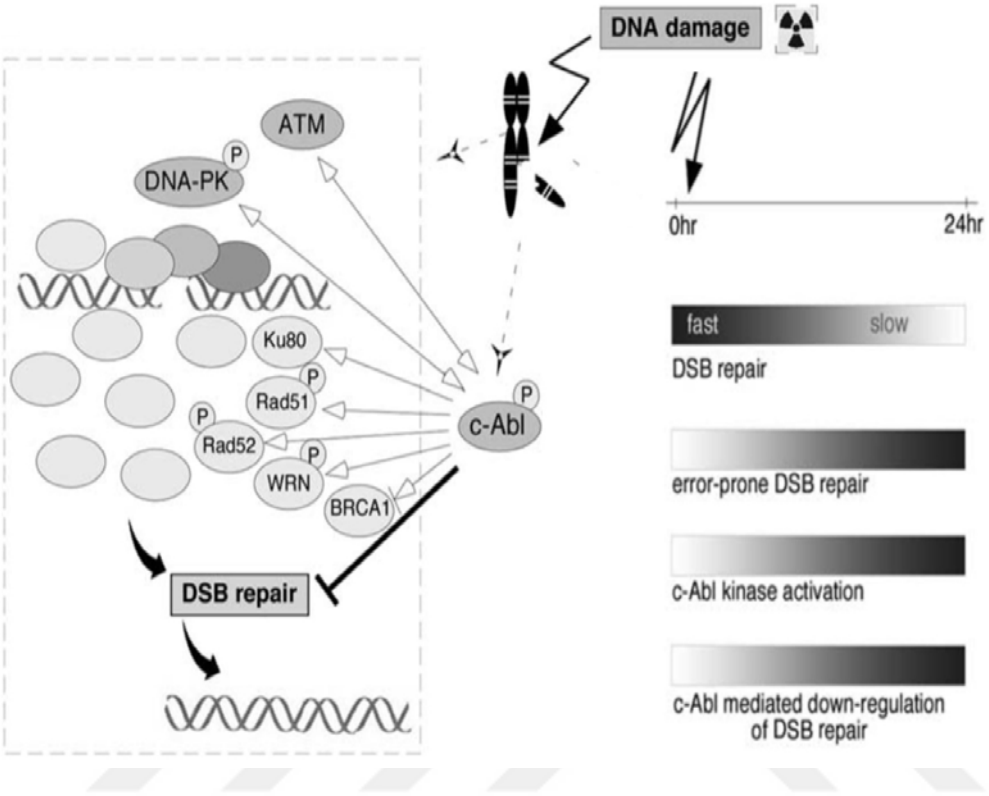

Figure 2.8.3.1. Regulation mechanism of double strand break (DBS) repair by c-Abl in response to DNA damage (104).

2.9. Oncogenic Function of YAP is Antagonized by c-Abl

Keshet et. al have been studied relationship between DNA damage response pathway and Hippo pathway. As a result of this study, it was exerted that there was a change in the function of protein that acts as a proto-oncoprotein. This proto-oncoprotein started to behave as a tumor supressor. In order to be able to target particular genes, YAP enters into nucleus. In human cancers, YAP is defined as an oncogene. It is in conjuction with TEAD family. Also, pro-proliferative and antiapoptotic target genes are activated by YAP (7).

Under the situations of DNA damage, to be able to response to damage of DNA, p73 is targeted by YAP. Thus, expression of proapoptotic genes is stimulated. In this way, cellular death axis is initiated. When damage of DNA occurs, c-Abl is activated. Then, tyrosine residues on p73 and YAP are phosphorylated by activated c-Abl (103,109).

When YAP is tyrosine phosphorylated, death axis is supported at two levels. When YAP is tyrosine phosphorylated, death axis is supported at two levels. Firstly, if p73-mediated death axis is enhanced, death axis is supported. Secondly, if accumulation of p73 is is supported, death axis is provided. Additionally, if Runx which refers to the Runt-associated transcription factor is coactivated, expression of p73 E3 ligase (Itch) is regulated by YAP. After c-Abl phosphorylates YAP, it get out from association of Runx. Therefore, accumulation of p73 is supported by YAP (110). In this way, c-Abl alters the behaviour of YAP. YAP starts to coactivates the accumulated p73 instead of activating E3 ligase. When E3 ligase is activated, degredation of p73 is induced.

Similarly, altering in behaviour of YAP was observed when TEAD transcription factor is targeted. Survival axis is controlled by nuclear YAP/TEAD complex. This complex accomplishes control with the aid of stimulating transcription of a range of genes. These set of genes are involved in two different activities. One of these activities are to provide cell proliferation. Another activity is to inhibit apoptosis. As a result of both of these activities which are YAP regulated, cell population enhances. However, to be able response to DNA damage, c-Abl is activated. When this occurs, YAP which is tyrosine phosphorylated can bind TEAD. However, survival axis is not induced by YAP in this situation (6). As a result of this process, oncogenic activity of YAP is removed. Death axis is stimulated by modified YAP with the aid of p73. Thus, oncogene behaviour of YAP is switched into tumor supressor behaviour by activated c-Abl.

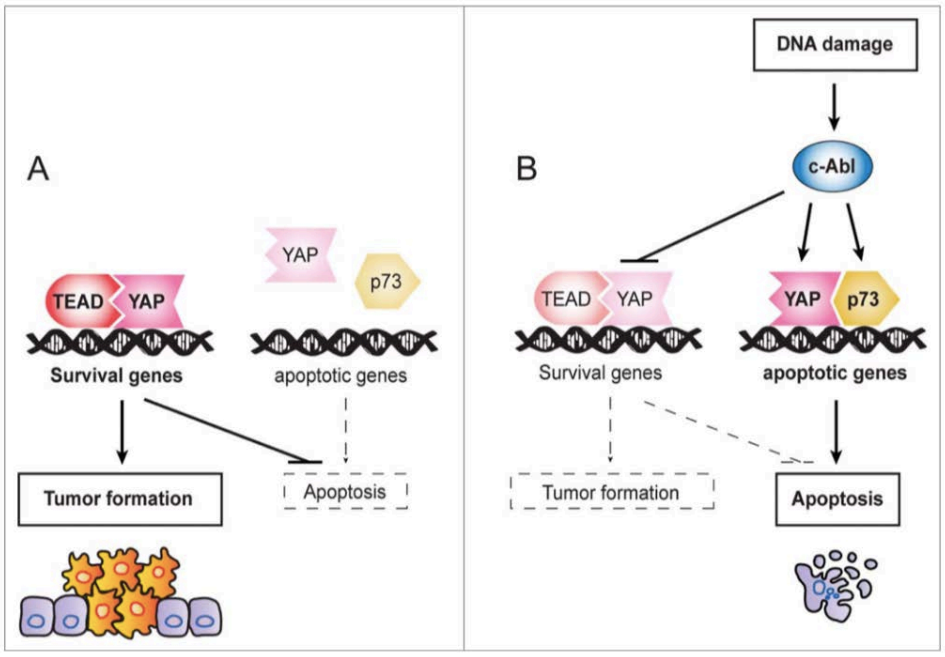

Figure 2.9.1. c-Abl antagonizes oncogene behaviour of YAP into tumor supressor behaviour with the aid of phosphorylation (6).

Although YAP performs critical role in GC proliferation and c-Abl transforms the YAP function from oncogenic to tumor suppressor, the correlation between the YAP and c-Abl in ovarian granulosa cells is still unknown. In order to clarify this obscurity, we suggest that DNA-damage stimulate c-Abl activation may lead to switch in the function of YAP from pro-proliferative form to pro-apoptotic form in mouse ovarian GCs. Thus, we aimed to exert the changes in the expressions of YAP and p73 after DNA damage induces c-Abl activation *in vitro* mouse ovarian granulosa cells.

3.MATERIALS AND METHODS

3.1. Animals and Experimental Design

A total of 8-weeks old 27 female Balb/C mice were gained from YUDETAM with the approval of Yeditepe Ethical Committee and these mice were randomly assigned to one of two groups. 3 mice, 6 ovaries were used for each primary granulosa cell culture. Food and water were available ad libitum. All experimental procedures were approved by the YUDETAM. All experimental procedures were performed in YUDETAM and Histology Laboratory of Yeditepe University. General outline of primary granulosa cell culture and post procedures were shown below in Figure 3.1.1.

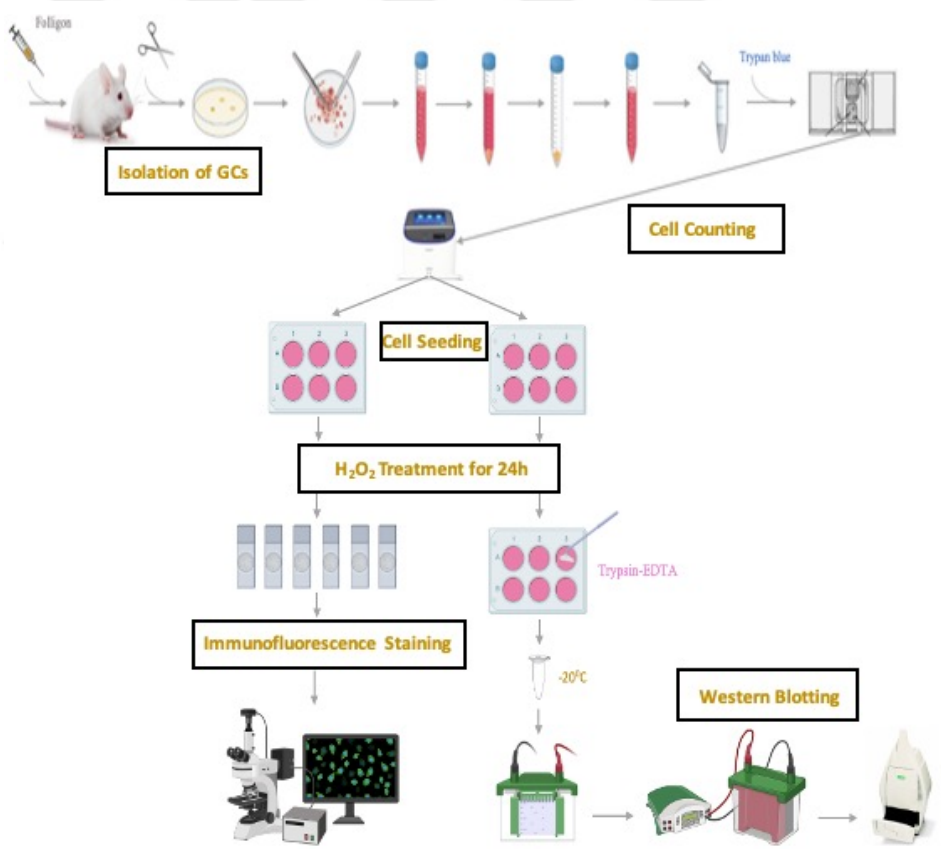

Figure 3.1.1. General outline of primary granulosa cell culture and post procedures.

3.2. Tissue Processing

Ovaries which were obtained from mice were fixed by neutral formalin solution (Formalin, Buffered, Fisher Scientific, SF100-4) for 12h. After the fixation process, ovaries were washed in three times for 10 minutes. Afterward, ovaries were dehydrated in increasing alcohol(ethanol) series. Then, ovaries were washed with xylene and these ovaries were embedded in paraffin by using paraffin embedding station (Leica, EG 1160). After then, ovaries were cut into 5 mm histological sections with the aid of using microtome (Leica, RM 2245). Lastly, sections were mounted on poly-lysine glass slides.

3.3. Double Immunofluorescence Staining of Mouse Ovary Sections

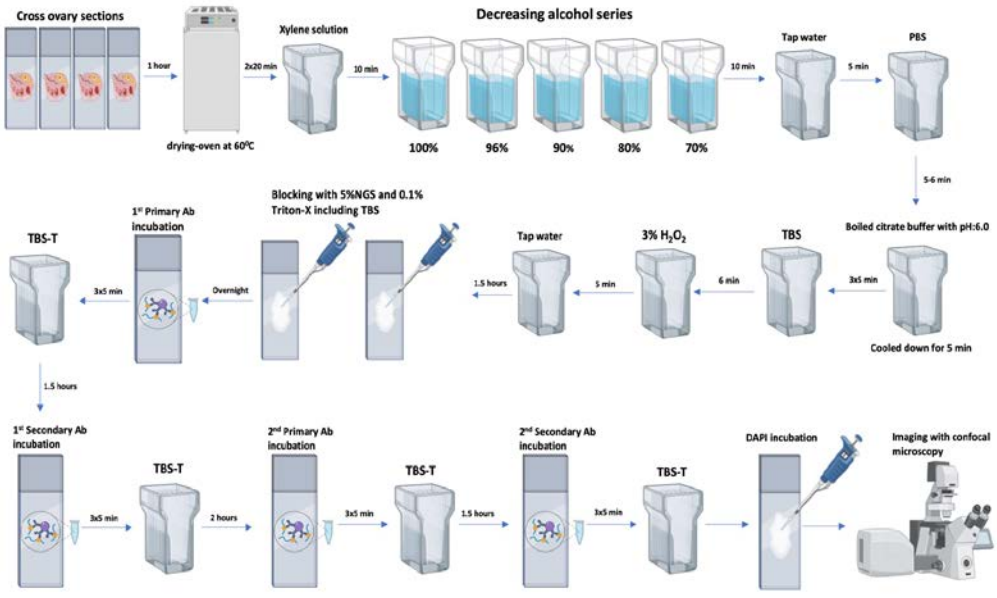

Figure 3.3.1. General outline of double immunofluorescence staining of mouse ovary sections.

Three mouse ovary slides were stained for c-Abl-YAP, p73-YAP, p73-c-Abl double staining, and one slide was stained for phospho c-Abl and phospho YAP staining. Slides were placed into drying oven at 60^0C for 1 hour. Then, slides were kept in xylene solution for 20 minutes in two times. Then the sections were kept for 10 minutes in decreasing alcohol series which were 100%, 96%, 90%, 80% and 70% respectively.

Following this, sections were washed by tap water for 10 minutes. Then, sections were washed by PBS for 5 minutes. Sections were placed into citrate buffer (pH:6.0) which was boiled in microwave for 5-6 minutes. Then, sections were cool down at room temperature for 5 minutes. Sections were washed by water for 5 minutes and then washed by TBS for 5 minutes in three times. Then, sections were kept in 3% H_2O_2 solution (97ml ethanol, 3ml H_2O_2) for 6 minutes. After sections were washed by water for 5 minutes, 5% NGS and 0.1% Triton-X-100 including 15ml of TBS was prepared as blocking solution. Then, sections were drawn by pap-pen and blocked by blocking solution for 1.5 hours at room temperature. Then, sections were incubated with primary antibodies for overnight at 4^0C. Primary antibodies were YAP (YAP rabbit, Cell signalling, D8H1X, #14074) that was prepared in 1:100 dilution rate, p73 (p73 rabbit mAb, Cell signalling, D3G10, #14620) that was prepared in 1:250 dilution rate, phospho YAP (Anti- YAP1, phospho Y357 rabbit, abcam, ab62751) that was prepared in 1:100 dilution rate and phospho c-Abl (p-cAbL rabbit, Cell signalling, #2861S) that was prepared in 1:100 dilution rate. Sections were washed by TBS-T for 5 minutes in three times. Then, phospho c-Abl and phospho YAP sections were counterstained by DAPI. Then, sections were incubated with secondary antibody which was (Goat pAb to Rb IgG, cell abcam, ab150077, alexa-fluor 488) that was prepared in 1:200 dilution rate for 1.5 hours. Then, sections were incubated with second primary antibodies for 2 hours. These antibodies were; YAP (YAP mouse mAb, Cell signalling, 1A12) which was prepared in 1:400 dilution rate and c-Abl (monoclonal anti-c-Abl antibody produced in mouse, clone ABL-148, sigma-aldrich) which was prepared in 1:100 dilution rate. After incubation was completed, sections were washed by TBS-T for 5 minutes in three times. Then sections were incubated with second secondary antibodies at room temperature for 1.5 hours. All slides were incubated with (Goat anti-mouse, abcam, ab175473, alexa-fluor 568) that was prepared in 1:250 dilution rate. Then, sections were washed by TBS-T for 5 minutes in three times. Lastly, sections were counterstained by DAPI (Fluoroshield with DAPI, Sigma-Aldrich, F6057). Then, the observation was performed by using confocal microscope (Zeiss, LSM780).

3.4. Collection of Ovaries

Subcutaneous injection of 1.5ml of folligon including PMSG (Folligon, Chrono-Gest Pregnant mare serum gonadotropin, MSD Animal Health) was conducted in order to stimulate the development of follicles. 48 h after the folligon injection, all mice were sacrified and back skin of mice was grasped using dissection forceps. Large incision in the skin and body wall was made. Ovaries were grasped gently by using forceps and scissor was used to sever ovaries attachment to the uterus. Pair of ovaries were transferred into culture dish including prewarmed dissection medium which is DMEM (Dulbecco's Modified Eagle Medium F-12 Nutrient Mixture, Gibco, 31330-038).

3.5. Isolation of Ovarian Granulosa Cells

Ovaries were dissected under the Zeiss SteREO Discovery.V12 microscope and excess tissues containing adipose tissue and fallopian tube were removed. Then, each ovary was transferred into 60mm cell culture dish. 2ml of DMEM was added into cell culture dish and follicles were punctured under the Zeiss SteREO Discovery.V12 microscope by using insulin needles.

3.6. Primary Culture of Granulosa Cells

Punctured follicles in DMEM were filtered and transferred into 50ml of falcon tube. Then, 2ml DMEM was added into falcon tube. Cells were centrifugated at 4000 rpm for 15 minutes. Then, supernatant will be removed and 2ml of 1X DMEM was added to pellet. Vortex was applied and centrifugation was conducted at 4000 rpm for 10 minutes. Supernatant was removed again and 10% FBS (Fetal Bovine Serum, Gibco, 10270-106) and 1% Pen/Strep including 5ml of DMEM was added to pellet. Pipettage were applied to this mixture.

3.6.1. Cell Counting and Seeding

30uL of sample mixture and 30uL of trypan blue solution (Trypan blue stain 0.4%, Invitrogen by Thermo Fischer Scientific, 1948601) were mixed. Then, 10uL from this mixture was transferred onto cell counting chamber slide (Countess^{TM} Cell Counting Chamber Slides, Invitrogen by Thermo Fischer Scientific, C10228) and live cells were counted by an automated

cell counter (Countess™ II FL Automated Cell Counter, Invitrogen by Thermo Fischer Scientific, AMQAF1000). Then, total cell number was calculated by applying necessary calculations. Then, equal amount of cell was added into each well of two six well plates. Then, cells were incubated at 37°C with 5%CO_2. For the immunofluorescence staining procedure, a round coverslips were placed on the bottom of the wells of one six plate before seeding of cells.

3.7. H_2O_2 Treatment of Cultured Granulosa Cells

In order to be able to activate DNA-damage response of c-Abl, hydrogen peroxide (H_2O_2) treatment was applied to primarly cultured granulosa cells. The adhesion rate and morphology of the cells was checked every 48 hours. Also, medium of cells was changed every two days until density of cells reached 70%. Then H_2O_2 treatment were applied when the rate of cell density and healthy cells reached 70%. H_2O_2 treatment was applied in five different doses which were 2,5μM, 5μM, 10μM, 20μM and 50μM and cells were cultured for 24 hours (111). For control group cultured granulosa cells, there were no H_2O_2 treatment and they were cultured same time period with treatment groups. Additionally, H_2O_2 treatment was applied in new three different doses which were 100μM, 200μM and 400μM. Then, cells were cultured for 24 hours.

3.8. Double Immunofluorescence Staining of Cultured GCs

Round coverslips were placed on the bottom of the plates before seeding of cells were placed in new petri dishes and waited in 4% PFA solution prepared in PBS for 30 minutes. Then, round coverslips were washed with PBS-T in three times for 5 minutes. Then, coverslips were incubated in 0.1%Triton-X-100 solution prepared in PBS for 30 minutes at room temperature. Coverslips were washed with PBS in three times for 5 minutes. Then, humidified filter papers were placed onto 6 different petri dishes. Then, coverslips were placed onto dry filter papers and a circle was drawn on the round of each coverslip with a hydrophobic barrier pen. Then, coverslips were placed onto petri dishes including humidifed filter papers. Coverslips were blocked with 5% normal goat serum solution prepared in PBS-T for 1 hour. Coverslips were incubated with the first primary antibody c-Abl (monoclonal anti-c-Abl antibody produced in mouse, clone ABL-148,

sigma-aldrich) at +4^{o} C for overnight. Coverslips were washed with PBS-T for 5 minutes for 3 times then were incubated with first secondary antibody (goat pAb to Ms Alexa flour-647) for 1,5 hours at room temperature. Then coverslips were washed with PBS-T for 5 minutes for 3 times again. Then, coverslips were incubated with second primary antibody YAP (YAP rabbit, Cell signalling, D8H1X, #14074) for 2 hours at room temperature. Coverslips were washed with PBS-T for 5 minutes for 3 times then were incubated with second secondary antibody (Alexa flour-488 goat anti-rabbit IgG) for 1,5 hours at room temperature. Coverslips were washed with PBS-T for 5 minutes for 3 times. Then, coverslips were mounted with DAPI (Fluoroshield with DAPI, Sigma-Aldrich, F6057) for nucleus staining, the observation was performed by using confocal microscopy (Zeiss, LSM780).

3.8.1. Signal Intensity Measurements

The signal intensities were calculated using the ImageJ program in all photographs taken in the Z- stack. For each treatment group, ten individual cells were choosen. Then, total area and nucleus area of cells were defined. Then, the signal intensities of cAbl and YAP in nucleus area and in the total area of each individual cells were determined. The results were evaluated by using the appropriate statistical program.

3.9. Trypsinization of Granulosa Cells

All growth medium in wells was removed and 1ml of 1X trypsin was added into each well. Cells were incubated in trypsin for 3 minutes and 1ml of DMEM was added into each well. Each well was stripped by cell scraper and samples were transferred into different falcon tubes. Then, 500 µl of 1X trypsin was added into each well and controlled under the light microscope. After 5 minutes, 500 µL of DMEM was added into each well and each well was stripped again by cell scraper. Samples were transferred into same falcon tubes and centrifugation was applied for 10 minutes at 4000 rpm. Then, supernatant was removed and 1 ml of DMEM was added into each falcon tube. Samples were transferred into ependorf tubes. Centrifugation was applied for 6 minutes at 10.000 rpm. Supernatant was removed and 200 µl of RIPA coctail including RIPA lysis buffer, sodium ortho-vanadate, protein inhibitor cocktail (PIC), and 10µl phenylmethylsulphonyl

fluoride (PMSF) (RIPA Lysis Buffer System, SantaCruz Biotechnology, sc-24948A) was added into each eppendorf tube. Then samples were stored at -20ºC.

3.10. Immunoblotting

3.10.1. Isolation of Proteins

Samples including RIPA coctail were resuspended into the ice and all samples were broken down with insulin needles. All samples were waited on the ice for 5 minutes. Then, centrifugation was applied at 14800 rpm for 15 minutes. Then, supernatants were transferred into new eppendorf tubes. Lastly, protein concentrations in each sample were determined by spectrophotometer.

3.10.2. Preparation of Samples

After the total protein concentrations was determined, samples were equalized with distilled water, 5µl LDS sample buffer (NuPAGE LDS Sample Buffer (4X), Invitrogen, NP0007) and 2µl reducing agent (NuPAGE Sample Reducing Agent (10X), Invitrogen (10X), NP0009). Then, each sample mixture was heated at 95ºC for 5 minutes by using Thermal Cycler.

3.10.3. Loading of Samples on Gel

Tape which was on the gel was removed. Then, casette including gel was washed by distilled water. Gel was put into the tank which was filled with running buffer including 950 ml water and 50 ml running buffer (NuPAGE MES SDS Running Buffer (20X), Novex, NP0002). Firstly, all wells were washed by running buffer. Then, 8µL ladder and all samples were loaded into the wells respectively. Then, gel was run at 100-120V and 80W for 2 hours.

3.10.4. Transferring of Proteins to Membrane

After gel electrophoresis was completed, casette including gel removed from the tank. Then, casette was washed by distilled water. Filter papers were placed into transfer buffer including 3 gr Tris (Tris(hydroxymethyl)aminomethane, Thermo Fisher Scientific, 17926), 14.3 gr glycine (Glycin für die Molekularbiologie, BioFroxx, 56-40-6), 200ml

methanol and 800ml distilled water. Also, membrane was activated by methanol for 20 minutes. Then, sandwich model was prepared from bottom to top as two filter papers, membrane, gel and two filter papers respectively. This model was transferred into the tank including transfer buffer. Wet transfer was conducted at 22V and +4°C for overnight.

3.10.5. Blocking

After transfer was completed, membrane was washed by distilled water. Then, membrane was blocked by 5% milk powder in TBS-T for 1 hour at room temperature.

3.10.6. Primary Antibody Incubation

After blocking solution was removed, membrane was incubated with primary antibodies at +4°C overnight. Primary antibodies were diluted with 5% blocking solution. First primary antibody was cAbl (cAbl rabbit mAb, Cell signalling, #2862S) that was prepared in 1:750 dilution rate. Second primary antibody was YAP (YAP rabbit, Cell signalling, D8H1X, #14074) that was prepared in 1:1000 dilution rate. Third primary antibody was p73 (p73 rabbit mAb, Cell signalling, D3G10, #14620) that was prepared in 1:750 dilution rate. Other primary antibodies were phospho-c-Abl (p-cAbL rabbit, Cell signalling, #2861S) that was prepared in 1:1000 dilution rate and phospho-YAP (Anti-YAP1, phospho Y357 rabbit, abcam, ab62751) that was prepared in 1:1000 dilution rate. Also, β-actin (β-actin (H10D10) Mouse mAb, Cell Signaling, #3700) was prepared in 1:1000 as an internal control. Last primary antibody was phospho-histone (Phospho-histone H3(Ser10), (6G3), Mouse mAb, Cell Signaling, #9706) which was prepared in 1:1000 dilution rate. After primary antibody incubation was completed, membrane was washed by TBS-T for 5 minutes for 3 times.

3.10.7. Secondary Antibody Incubation

The membranes were incubated with the appropriate secondary antibodies for 2 hours at room temperature. Anti-rabbit secondary antibody (Anti-rabbit IgG, HRP-linked antibody, Cell Signalling, #7074S) was prepared in 1:500 dilution rate. Anti-mouse secondary antibody (ECL Mouse IgG, HRP-linked whole Ab, Amersham, #NA931V) in

1:500 was prepared in 5% milk powder and used for β-actin. After secondary antibody incubation was completed, membrane was washed by TBS-T for 6 times for 5 minutes.

3.10.8. Detection and Analysis

ECL kit (Pierce ECL Western Blotting Substrate, Thermo Fisher Scientific, 32106) which was a (ECL+Enhancer) mix used in 1:1 dilution rate for one membrane. Mixture was added onto a membrane and ChemiDoc^{TM} MP Imaging System (170-8280) was used to image gel. To obtain the protein bands, calculations were conducted by ImageJ software. Then, results were evaluated using a suitable statistic program.

3.11. Statistical Analysis

Statistical analysis was done using GraphPad Prism 7.0 software program. Two Way ANOVA test was conducted to determine the correlation between parameters. The p value which was lower than 0.05 was called as significant.

4.RESULTS

4.1. Immunofluorescence Data of Mouse Ovary Sections for c-Abl, YAP, p-c-Abl, p-YAP and p73

To observe the localization of c-Abl, YAP, p-c-Abl, p-YAP and p73 in the mouse ovary sections, double immunofluorescence staining was performed.

4.1.1. Double IF Staining of c-Abl and YAP in Mouse Ovarian Follicles

In order to be able to evaluate the function of c-Abl and YAP in ovarian follicular development, double immunofluorescence method was conducted and localization of c-Abl and YAP in mouse ovarian follicles were identified. According to the results, YAP showed low expression in the oocyte and follicular cells in primordial follicles. In the secondary follicles, YAP was expressed in the oocyte and also cytoplasm of follicular cells. Additionally, YAP showed high expression in theca externa cells. Additionally, in the antral follicles, YAP localized in the oocyte and theca externa cells. Similar to localization of YAP in primordial follicles, c-Abl showed expression in the oocyte and follicular cells in primordial follicles. In addition to this, c-Abl showed a very low expression in the oocyte and nucleus of oocyte, while it exerted more clear expression in the follicular cells of the secondary follicles. Moreover, c-Abl was not expressed in the nucleus of oocyte while it was expressed in the follicular cells and theca cells in the antral follicles. There was no immunostaining in negative control slide. (Negative control was inserted in merged part of Figure 4.1.1.1.)

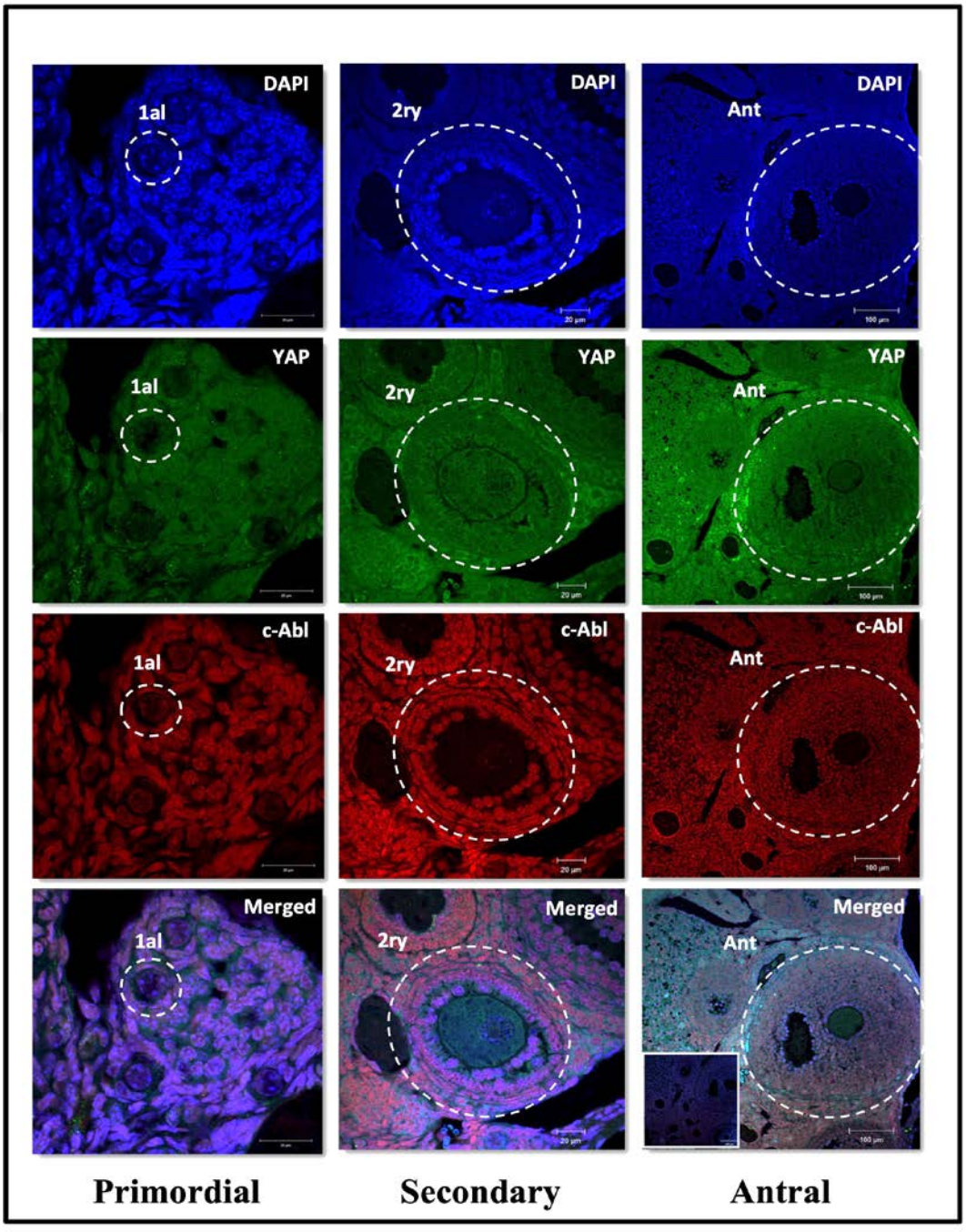

Fig 4.1.1.1. Double immunofluorescence staining of c-Abl and YAP at different stages of follicular development in mouse ovary. DAPI, 4’,6-diamidino-2-phenylindole (1al: primordial follicle, 2ry: secondary follicle, 2ry: secondary follicle, ant: antral follicle.

4.1.2. Double IF Staining of p73 and YAP in Mouse Ovarian Follicles

To show the co-localization of p73 and YAP in mouse ovary cross-sections, double immunofluorescence was performed and co-localization of two proteins was observed in follicles at different stages. According to the confocal representative photomicrographs, p73 exerted low expression in the oocyte of primordial follicles. In primary follicles, p73 showed expression in the oocyte and follicular cells. In secondary follicles, p73 was expressed in the oocyte and the nucleus of oocyte also. Additionally, it was expressed in follicular cells. In the antral follicles, p73 was expressed in the oocyte, nucleus and nucleolus of the oocyte. Addition to this, it showed expression in both granulosa and theca cells. In primordial follicles, YAP was expressed in the nucleus of oocyte. In primary follicles, YAP showed low expression in the nucleus of oocyte and nucleus of follicular cells. In secondary follicles, it was clear that the YAP was not expressed in the oocyte but it was expressed in the follicular cells. Also, it was slightly expressed in oocyte of antral follicle. In antral follicles, YAP showed expression in the granulosa cells and theca cells. There was no immunostaining in negative control slide. (Negative control was inserted in merged part of Figure 4.1.2.1)

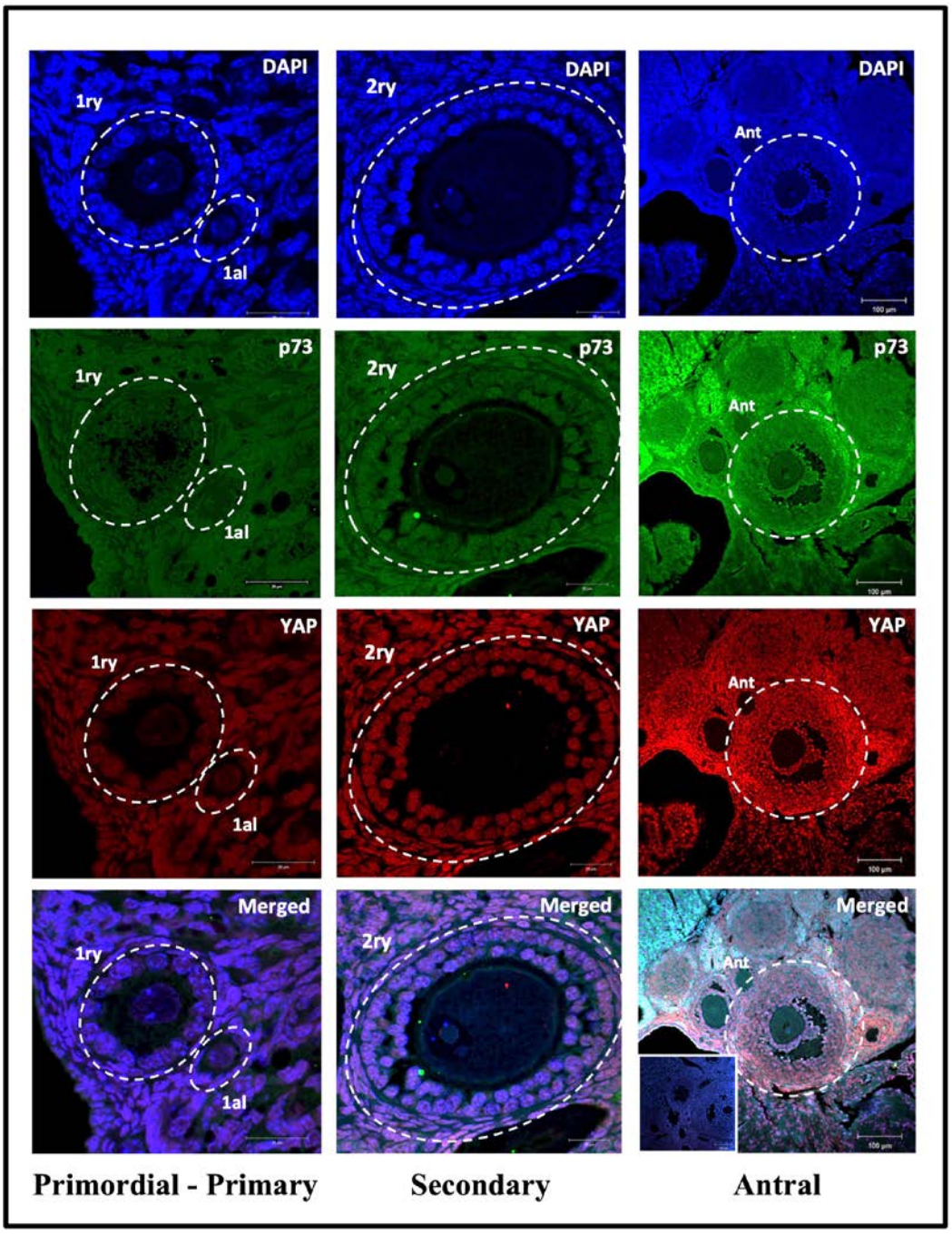

Fig 4.1.2.1. Double immunofluorescence staining of p73 and YAP at different stages of follicular development in mouse ovary. DAPI, 4’,6-diamidino-2-phenylindole. (1al: primordial follicle, 1ry: primary follicle, 2ry: secondary follicle, ant: antral follicle.)

4.1.3 Double IF Staining of p73 and c-Abl in Mouse Ovarian Follicles

In order to analyze the co-localization of p73 and c-Abl in mouse ovary cross-sections, double immunofluorescence was performed also. According to the obtained confocal representative images, it was observed that the p73 showed expression in the oocyte and nucleus of oocytes in early secondary follicles and late secondary follicles. Also, it was showed cytoplasmic localization in the follicular cells of early and late secondary follicles. In addition to being localized in the oocyte, p73 also showed expression in the granulosa and theca cells of antral follicles. c-Abl showed negligible expression in the nucleus of oocyte in early secondary follicles compared to p73. In the late secondary follicle, c-Abl showed expression in follicular cells and showed very weak expression in the oocyte and nucleus of oocyte. Similarly, it was clear that c-Abl was expressed in the follicular cells of antral follicles. Also, it was showed negligible expression in oocyte. There was no immunostaining in negative control slide. (Negative control was inserted in merged part of Figure 4.1.3.1)

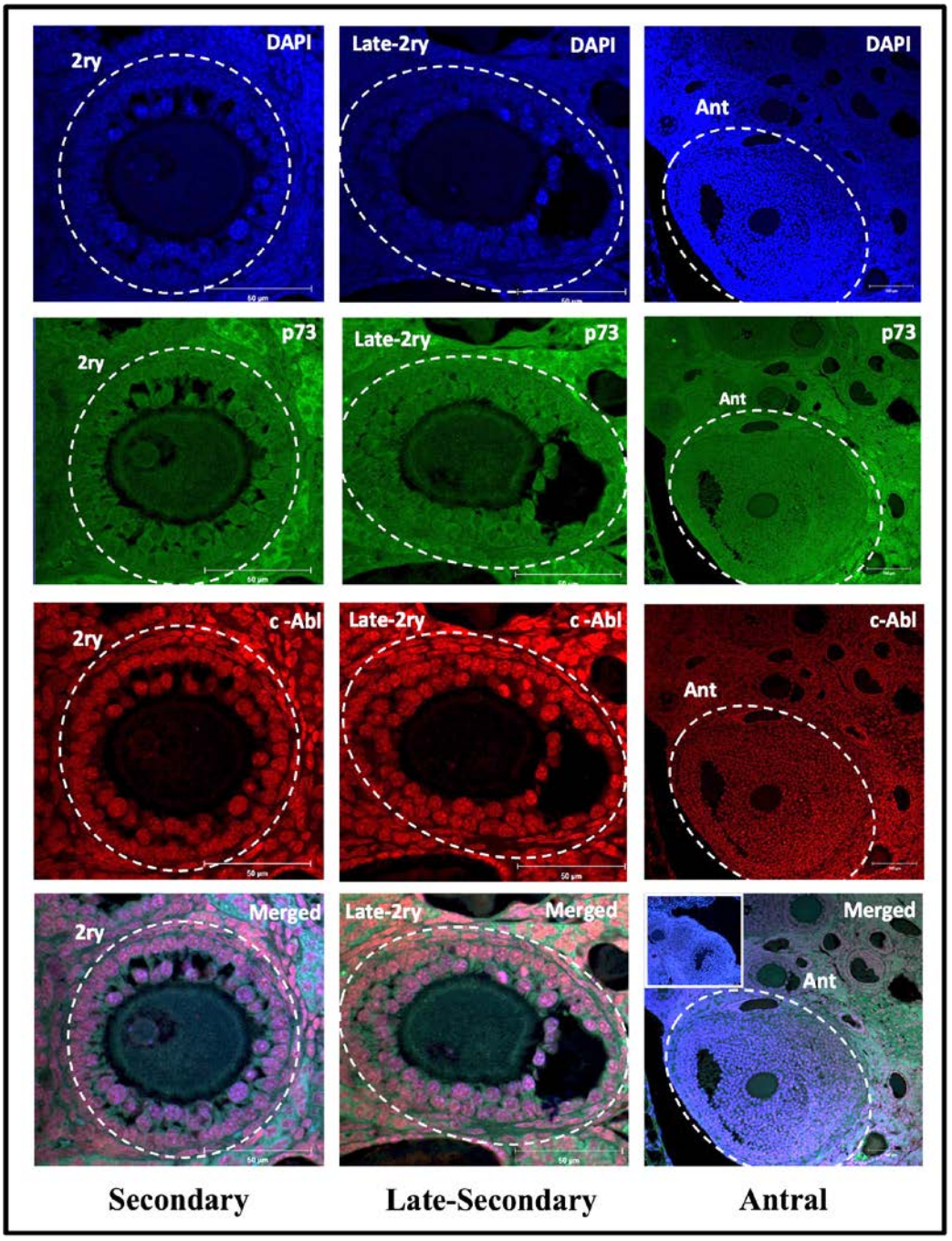

Fig 4.1.3.1. Double immunofluorescence staining of p73 and c-Abl at different stages of follicular development in mouse ovary. DAPI, 4’,6-diamidino-2-phenylindole. (2ry: secondary follicle, ant: antral follicle.

4.1.4. IF Staining of phospho YAP in Mouse Ovarian Follicles

In order to show the expression areas of phospho YAP in mouse ovary sections, immunofluorescence method was applied and confocal representative photomicrographs were obtained. According to these representative images of ovary sections, it was observed that the p-YAP was expressed in the follicular cells and oocyte of the primordial follicles. Moreover, p-YAP was expressed strongly in the oocyte of early secondary follicles. Also, p-YAP expression was observed in the follicular cells and thecal cells. Similarly, it was obvious that the p-YAP showed localization in the oocyte of late secondary and antral follicles. There was no immunostaining in negative control slide. (Negative control was inserted in merged part of Figure 4.1.4.1.)

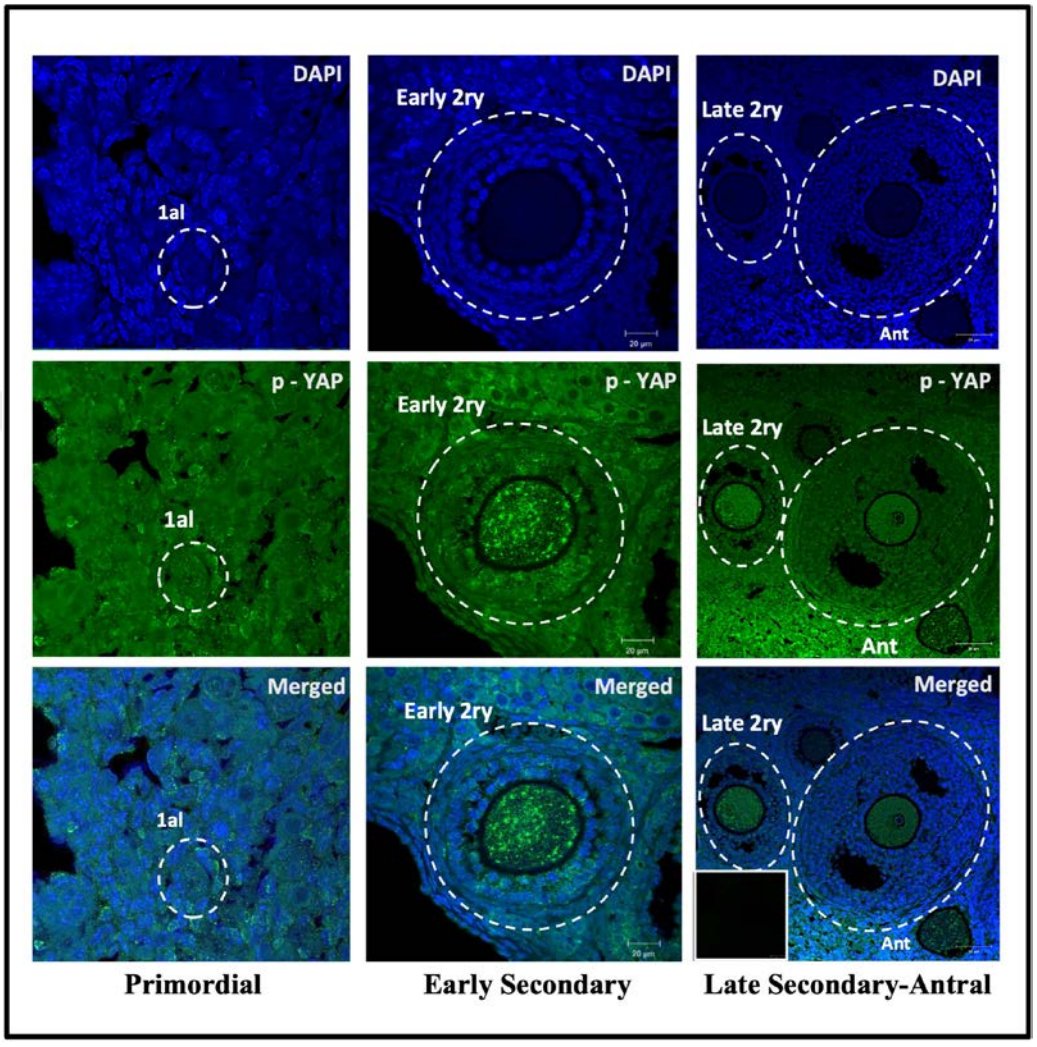

Fig 4.1.4.1. Localization of phospho YAP at different stages of follicular development in mouse ovary. DAPI, 4’,6-diamidino-2-phenylindole. (1al: primordial follicle, 1ry: primary follicle, early 2ry: early secondary follicle, late 2ry: late secondary follicle, ant: antral follicle.

4.1.5. IF Staining of phospho c-Abl in Mouse Ovarian Follicles

To observe the localization of phospho c-Abl in mouse ovary, immunofluorescence staining was performed. According to the results, phospho c-Abl showed expression in the oocyte of early secondary follicle. It was obvious that there was expression in the follicular cells and theca cells of early secondary follicle also. Similarly, phospho c-Abl was expressed in the oocyte and follicular cells of late secondary follicle. Moreover, phospho c-Abl was localized in the oocyte of some antral follicles while it was not expressed in the oocyte of other antral follicles. There was no immunostaining in negative control slide. (Negative control was inserted in merged part of Figure 4.1.5.1.)

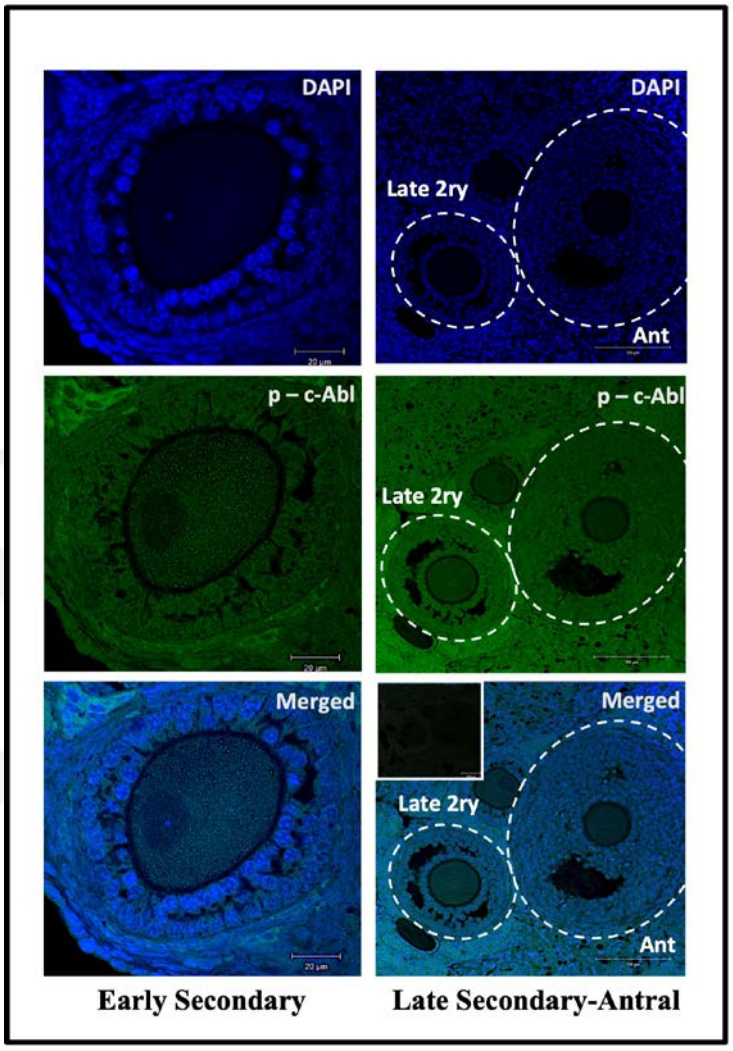

Fig 4.1.5.1. Localization of phospho c-Abl at different stages of follicular development in mouse ovary. DAPI, 4’,6-diamidino-2-phenylindole. (early 2ry: early secondary follicle, late 2ry: late secondary follicle, ant: antral follicle)

4.2. Invert Microscopy and Confocal Microscopy Observations of GCs After 2.5µM,10µM, 20µM and 50µM H_2O_2 Treatment

After GCs treated with 10% FBS including DMEM for 7 days as a positive control group, the morphology of GCs was observed under the inverted microscope. Under the microscope, granulosa cells were observed to showed epithelial-like shape. **(Figure 4.2.1-A)**

To determine the localization of YAP and c-Abl in cultured granulosa cells, double immunofluorescence staining was conducted after 7 days culture. According to the results of double immunofluorescence staining, it was observed that YAP exerted highly nuclear expression in primary cultured granulosa cells. Additionally, it was observed that the c-Abl showed highly nuclear expression in GCs treated with 10% FBS including DMEM. Although both c-Abl and YAP showed highly nuclear expression in GCs, c-Abl exerted more intense nuclear expression in comparision to YAP. There was no staining in negative control slide which inserted in merged part of Fig.4.2.1.-B. **(Figure 4.2.1-B)**

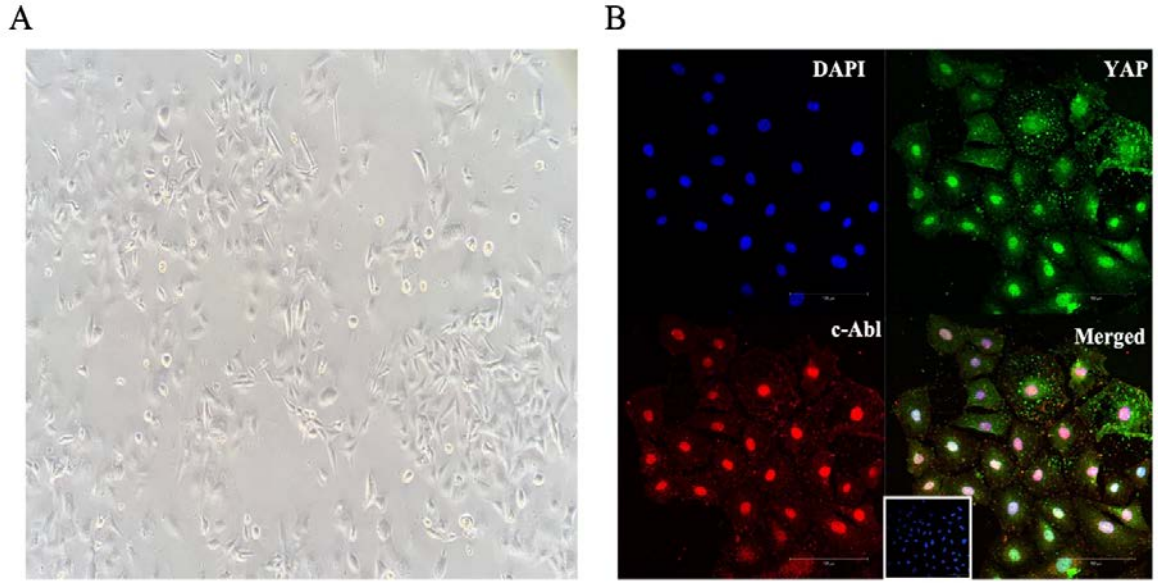

Figure 4.2.1. Observation of primary cultured GCs treated with 10% FBS including DMEM after 7 days as positive control group. **(A)** Image of GCs after 10%FBS including DMEM treatment on inverted microscope at 20X objective. **(B)** Localization of c-Abl and YAP in GCs on confocal microscope at 20X objective. DAPI stained nucleus of cells.

After GCs treated with 10% FBS including DMEM for 7 days and confluency of cells reached to 70%, they are treated with 2.5μM H_2O_2 for 24 hours. Under the inverted microscope, granulosa cells were observed in an epithelial-like shape for control group. In treatment group, most of granulosa cells showed spindle-like or elongated shape. However, some granulosa cells were observed as a rounded shape after treated with 2.5uM H_2O_2. **(Figure 4.2.2.)**

In order to decide the localization of YAP and c-Abl in cultured granulosa cells after 2.5μM H_2O_2 treatment, double immunofluorescence staining was conducted after 7 days culture. According to the double immunofluorescence results, although YAP showed expression in the cytoplasm in a few cells, it was mostly localized in the nucleus of the cells. Similarly, c-Abl exerted higly nuclear expression in the granulosa cells treated with 2.5μM H_2O_2. **(Figure 4.2.3. - Figure 4.2.4.)**

After double immunofluorescence staining was completed, fluorescence intensity ratios of total c-Abl and YAP were measured by Image J and observed as quantitatively. According to the results, fluorescence intensity ratio of YAP in granulosa cells treated with 2.5μM H_2O_2 was significantly lower than in comparision with positive control group. Similarly, fluorescence intensity ratio of c-Abl in granulosa cells treated with 2.5μM H_2O_2 was significantly reduced in comparision with positive control group. Additionally, fluorescence intensity ratios of nuclear c-Abl and nuclear YAP were measured by Image J and observed as quantitatively to determine the shifting of c-Abl and YAP between the nucleus and cytoplasm. According to the results, intensity ratio of nuclear YAP in granulosa cells treated with 2.5μM reduced in comparision with positive control group. There was no significant difference between two groups. Intensity ratio of nuclear c-Abl did not exert difference between two groups. **(Figure 4.2.5.)**

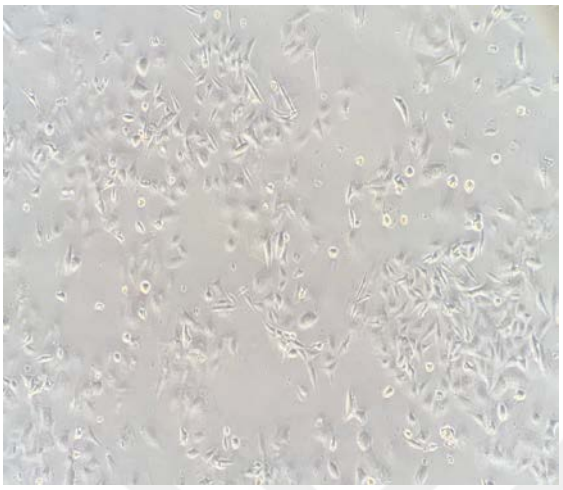

Granulosa cells before 2.5µM H_2O_2 treatment

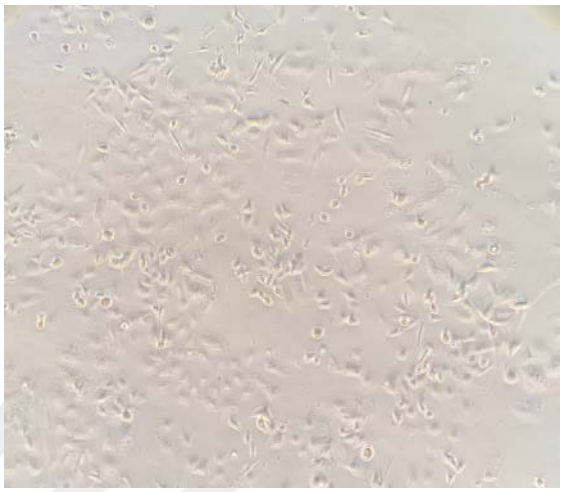

Granulosa cells after 2.5µM H_2O_2 treatment

Figure 4.2.2. Images of GCs before 2.5µM H_2O_2 treatment and 24 hours after 2.5µM H_2O_2 treatment on inverted microscope at 20X objective.

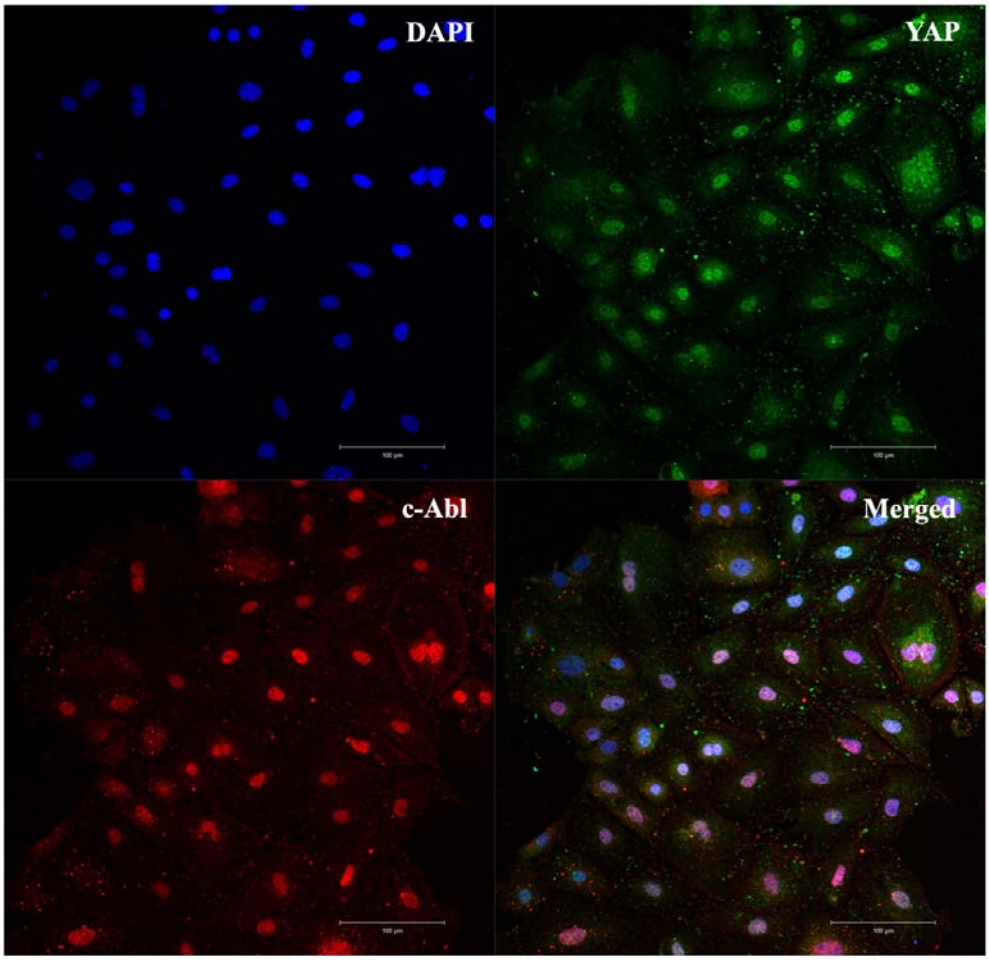

Figure 4.2.3. Localization of c-Abl and YAP in GCs after 2.5μM H_2O_2 treatment on confocal microscope at 20X objective.

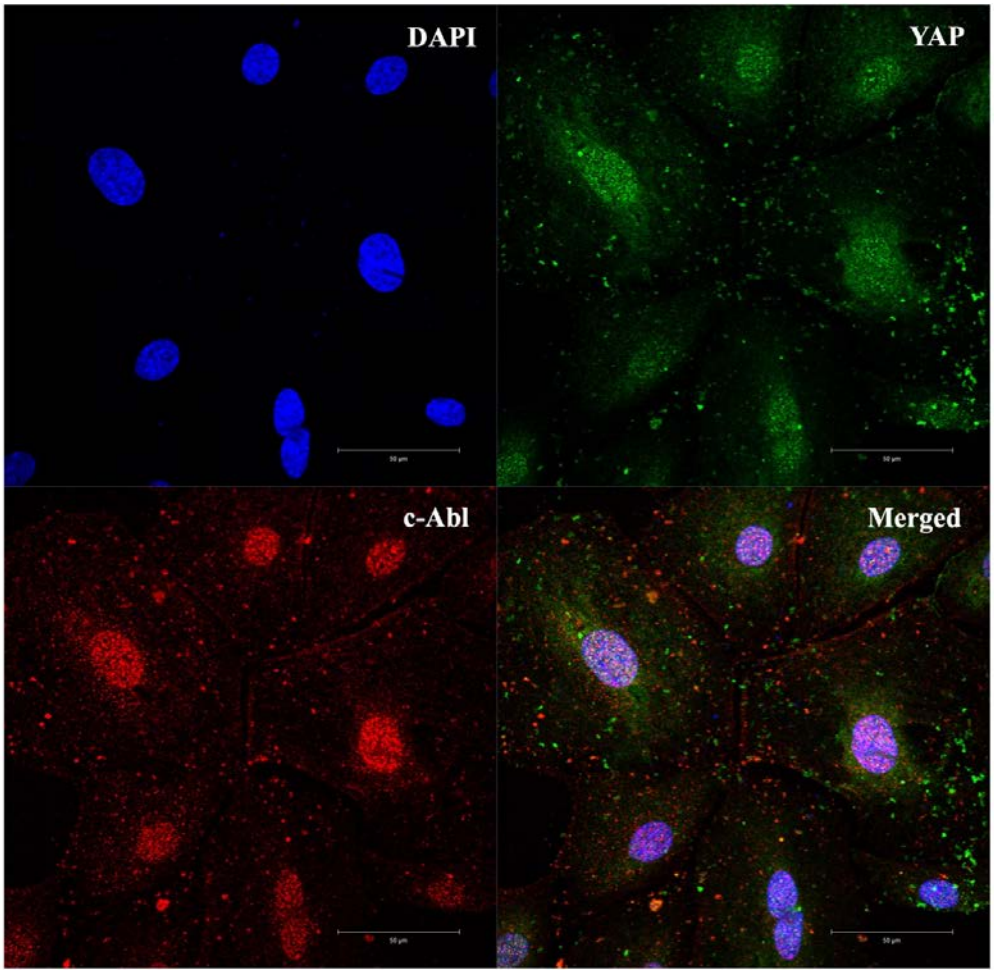

Figure 4.2.4. Localization of c-Abl and YAP in GCs after 2.5μM H_2O_2 treatment on confocal microscope at 63X objective.

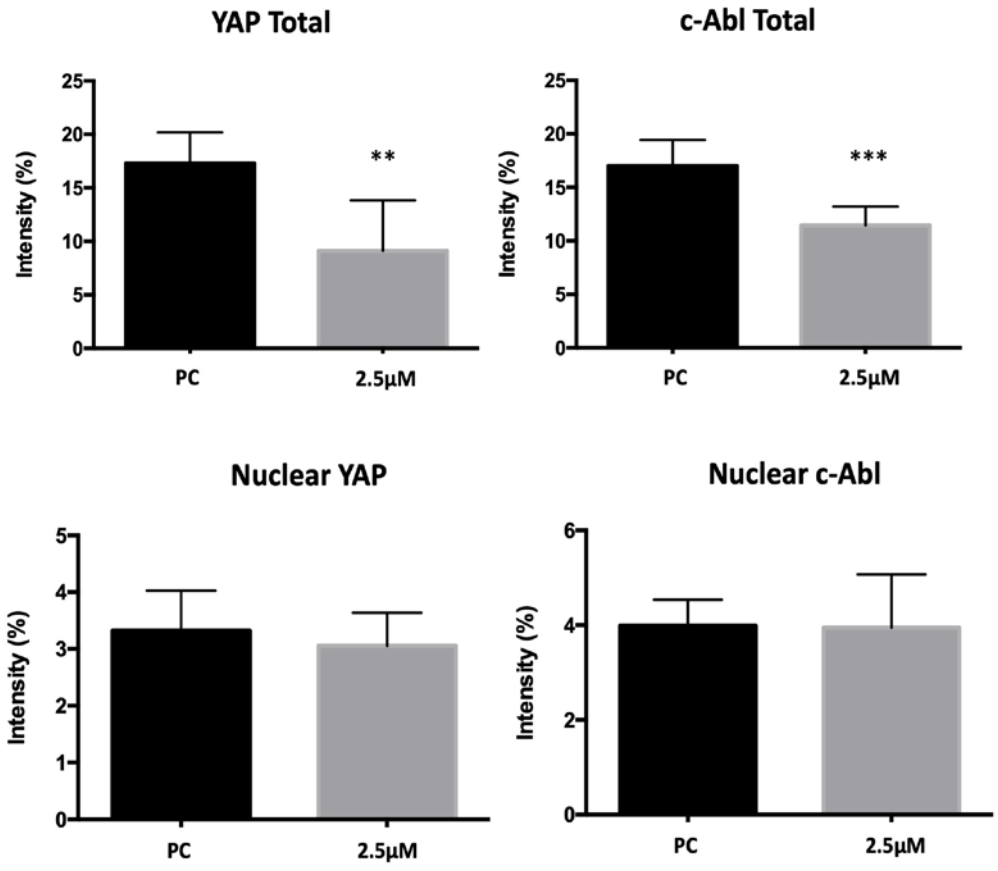

Figure 4.2.5. Total and nuclear fluorescence intensity ratios of c-Abl and YAP in GCs after 2.5µM H_2O_2 treatment.

After GCs treated with 10% FBS including DMEM for 7 days and confluency of cells reached to 70%, they are treated with 5μM H_2O_2 for 24 hours. Then, morphology of cells before and after H_2O_2 treatment was observed under the inverted microscope. Granulosa cells were observed in an epithelial-like and polygonal shape before H_2O_2 treatment. However, in treatment group, the granulosa cells began to lose their normal morphology. Some granulosa cells were observed as a rounded shape and some of them had fibroblast-like shape and elongated shape after treated with 5μM H_2O_2. **(Figure 4.2.6.)**

To determine the localization of YAP and c-Abl in cultured granulosa cells after 5μM H_2O_2 treatment, double immunofluorescence staining was conducted after 7 days culture. According to the obtained results, c-Abl was localized in the nucleus to a certain extent. Also, YAP exerted nuclear expression in the granulosa cells treated with 5μM H_2O_2. **(Figure 4.2.7.- Figure 4.2.8.)**

To determine the fluorescence intensity ratios of total c-Abl and YAP, measurement was applied by Image J and intensity ratios were observed as quantitatively. In granulosa cells treated with 5μM H_2O_2, intensity ratio of YAP significantly reduced im comparision to positive control group. Similarly, fluorescence intensity ratio of c-Abl in granulosa cells treated with 5μM H_2O_2 was significantly reduced in comparision with positive control group. Also, fluorescence intensity ratios of nuclear c-Abl and YAP were measured and compared between positive control and 5μM H_2O_2 treatment group. The intensity ratio of nuclear YAP in granulosa cells treated with 5μM H_2O_2 did not show difference in accordance to positive control. However, intensity ratio of c-Abl showed reduced intensity in the treatment group in comparision to positive control group treated with 10% FBS including DMEM. **(Figure 4.2.9.)**

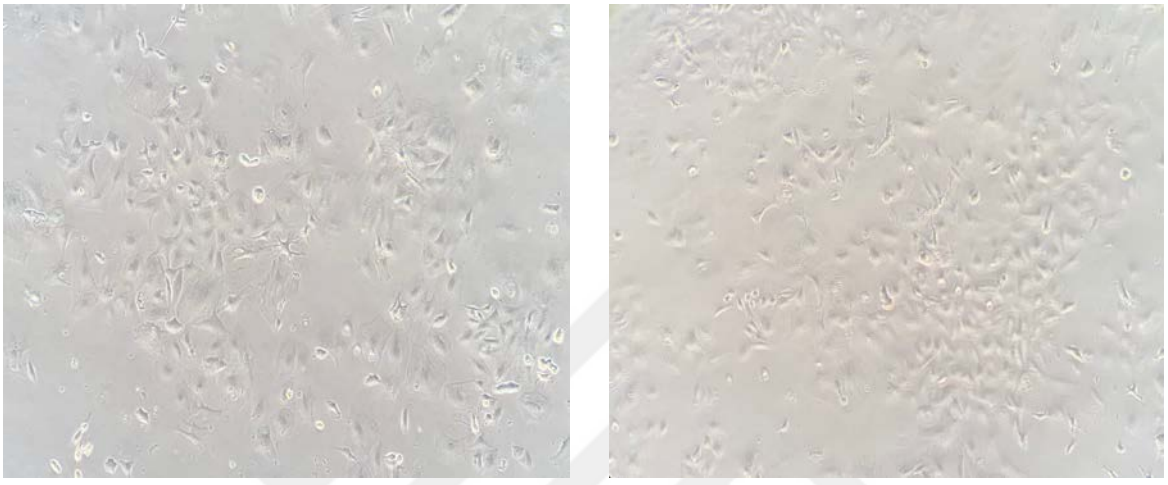

Granulosa cells before 5µM H_2O_2 treatment **Granulosa cells after 5µM H_2O_2 treatment**

Figure 4.2.6. Images of GCs before 5µM H_2O_2 treatment and 24 hours after 5µM H_2O_2 treatment on inverted microscope at 20X objective.

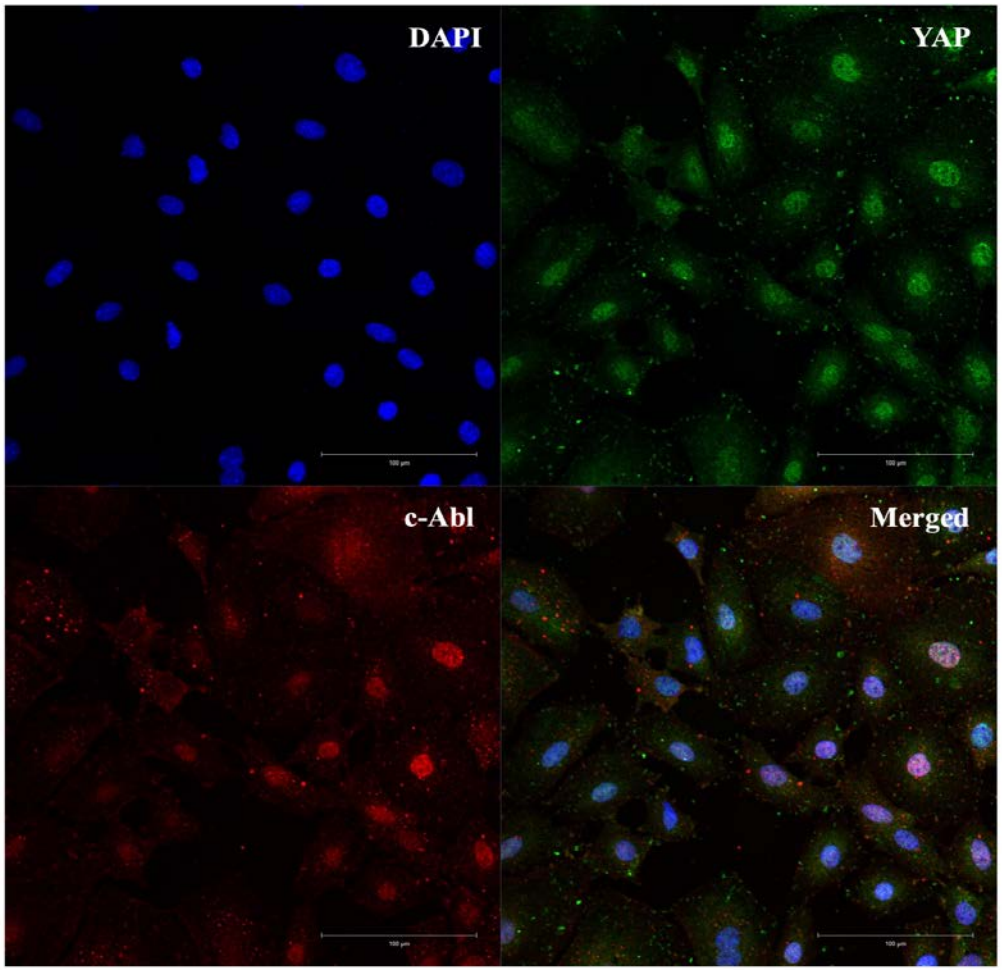

Figure 4.2.7. Localization of c-Abl and YAP in GCs after 5μM H_2O_2 treatment on confocal microscope at 20X objective.

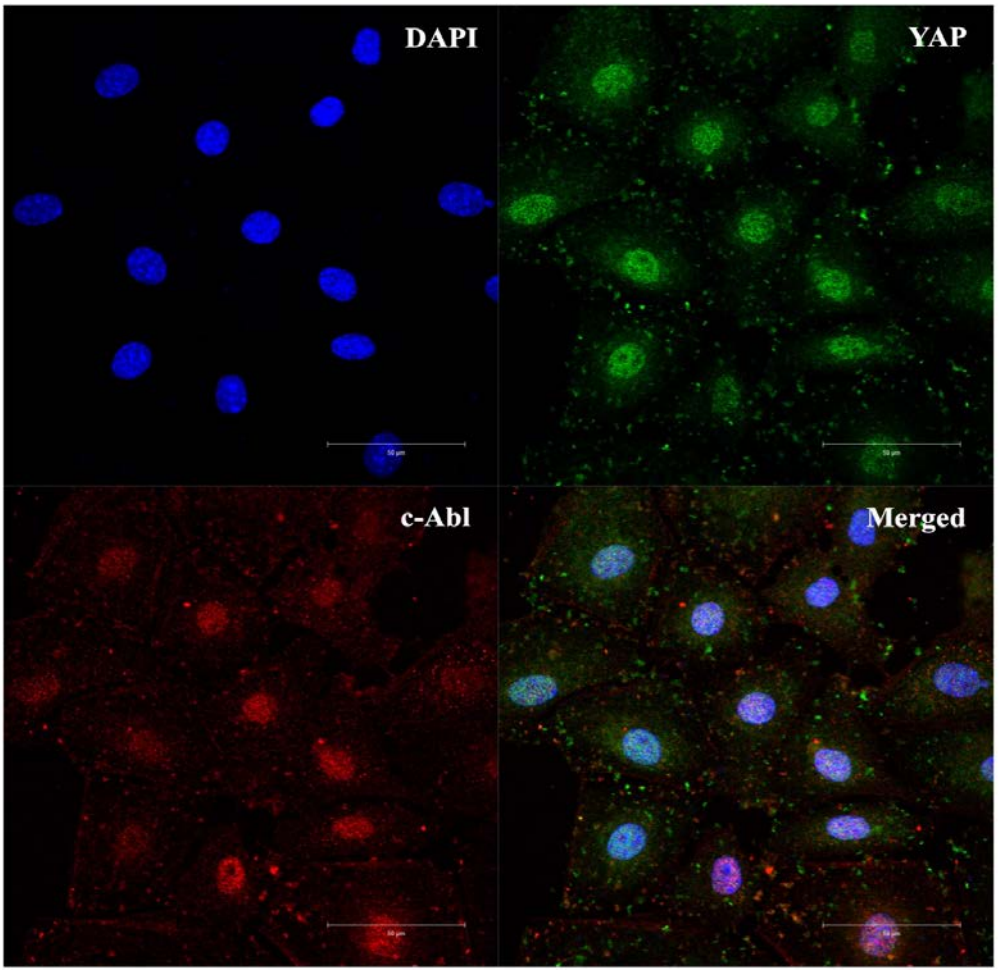

Figure 4.2.8. Localization of c-Abl and YAP in GCs after 5μM H_2O_2 treatment on confocal microscope at 63X objective.

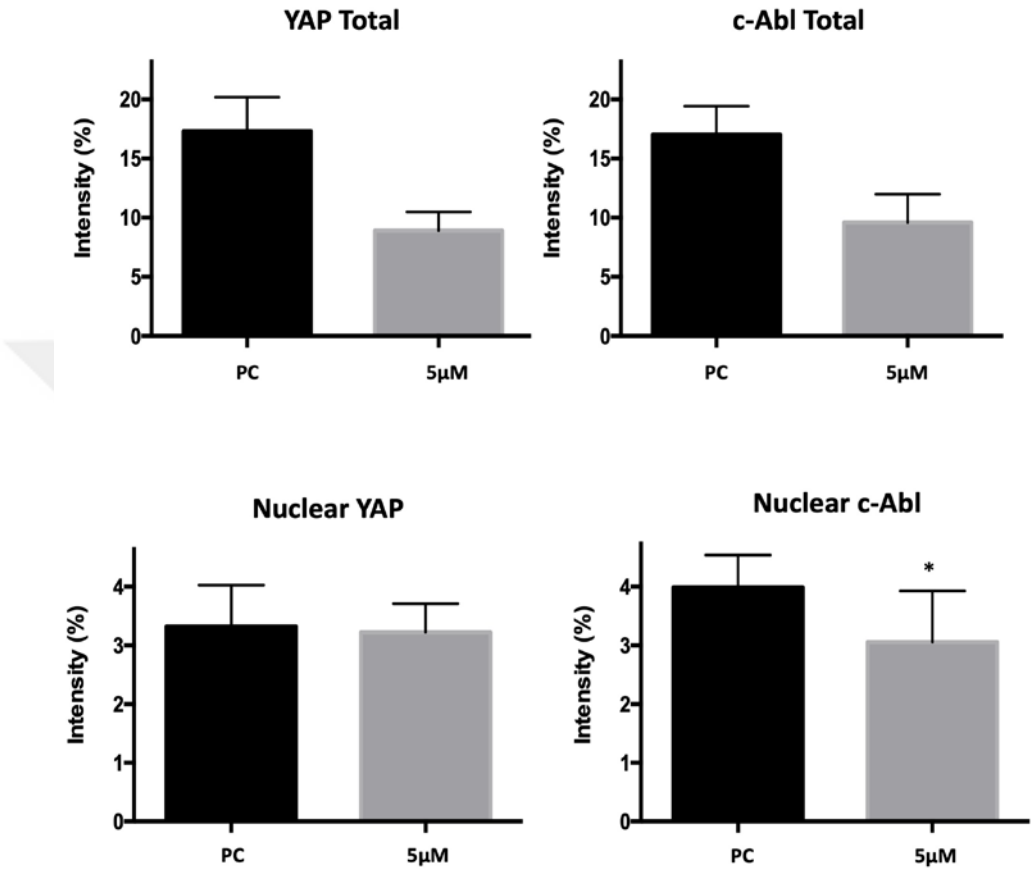

Figure 4.2.9. Total and nuclear fluorescence intensity ratios of c-Abl and YAP in GCs after 5μM H_2O_2 treatment.

After GCs treated with 10% FBS including DMEM for 7 days and confluency of cells reached to 70%, they are treated with 10μM H_2O_2 for 24 hours. Morphology of granulosa cells before and after H_2O_2 treatment was observed by the inverted microscope. According to the results, granulosa cells were observed in polygonal shaped in positive control group. When cells were treated with 10μM H_2O_2 for 24 hours, they start to lose their normal morphology. Some cells were observed as rounded shape and elongated shape. **(Figure 4.2.10.)**

To determine the localization of YAP and c-Abl in cultured granulosa cells after 10μM H_2O_2 treatment, double immunofluorescence staining was conducted. According to the obtained images, it was obvious that the granulosa cells were not in contact. Cell to cell interactions might be inhibited in granulosa cells treated with 10μM H_2O_2. According to the immunofluorescence results, c-Abl was localized in the cytoplasm to a certain extent. On the other hand, YAP was localized in the nucleus of some granulosa cells treated with 10μM H_2O_2. Also, YAP was localized in the cytoplasm of some granulosa cells treated with 10uM H_2O_2. **(Figure 4.2.11.- Figure 4.2.12.)**

Fluorescence intensity ratios of c-Abl and YAP were determined by the Image J as quantitatively. According to the results, density ratios of both YAP and c-Abl did not differ significantly in positive control group and cells treated with 10μM H_2O_2. The intensity ratio of nuclear YAP in granulosa cells treated with 10μM H_2O_2 decreased in accordance to positive control. A significant difference was observed between the treatment and positive control groups for the nuclear intensity ratio of c-Abl. Intensity ratio of c-Abl showed reduced intensity in the granulosa cells treated with 10uM H_2O_2 in comparision to positive control group treated with 10% FBS including DMEM. Moreover, cells treated with 10μM H_2O_2 showed higher intensity ratio of nuclear YAP than the c-Abl since the YAP showed higher localization in the nucleus in accordance to c-Abl. **(Figure 4.2.13.)**

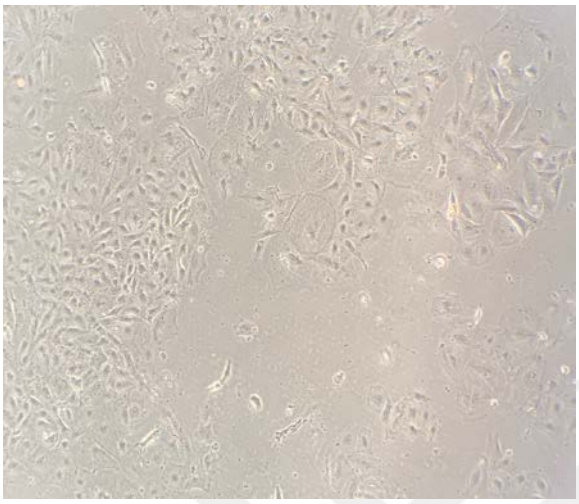

Granulosa cells before 10μM H_2O_2 treatment

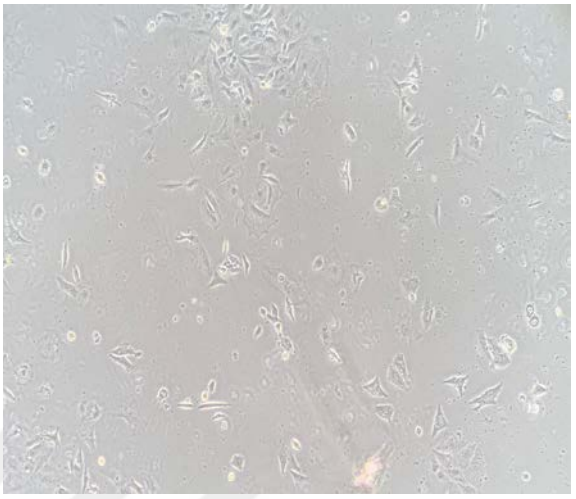

Granulosa cells after 10μM H_2O_2 treatment

Figure 4.2.10. Images of GCs before 10μM H_2O_2 treatment and 24 hours after 10μM H_2O_2 treatment on inverted microscope at 20X objective.

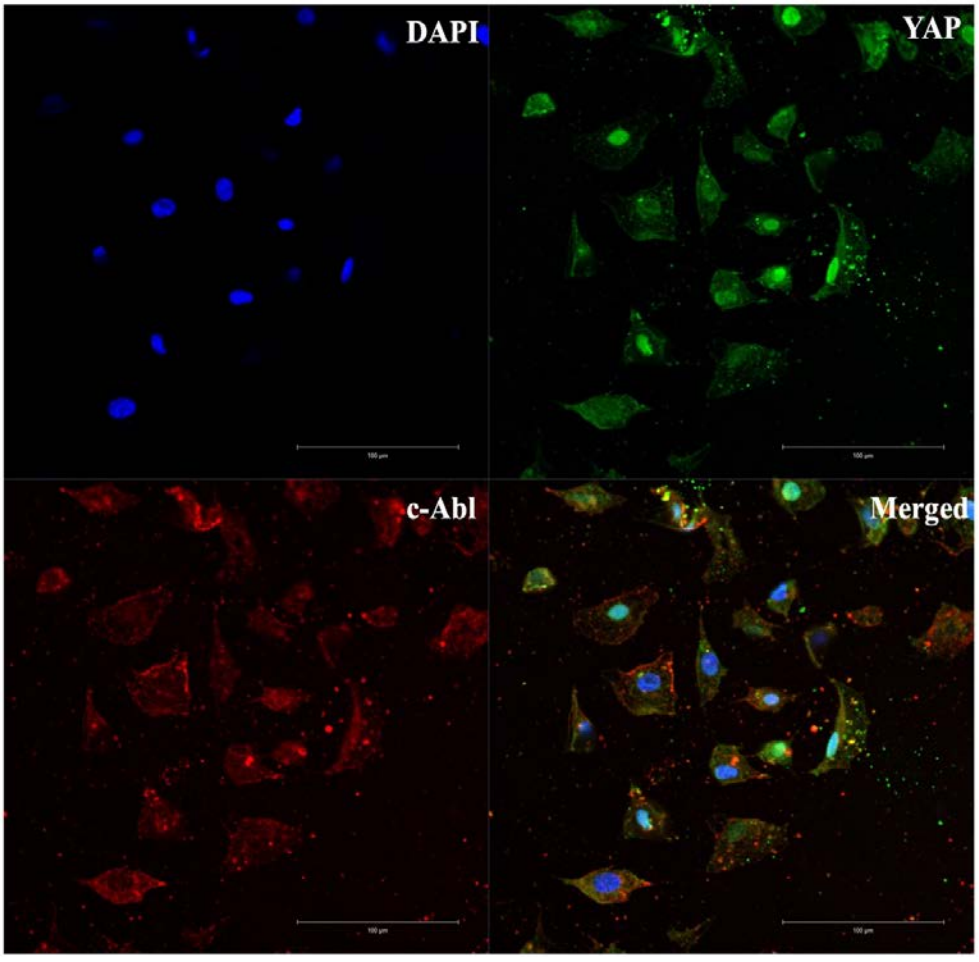

Figure 4.2.11. Localization of c-Abl and YAP in GCs after 10μM H_2O_2 treatment on confocal microscope at 20X objective.

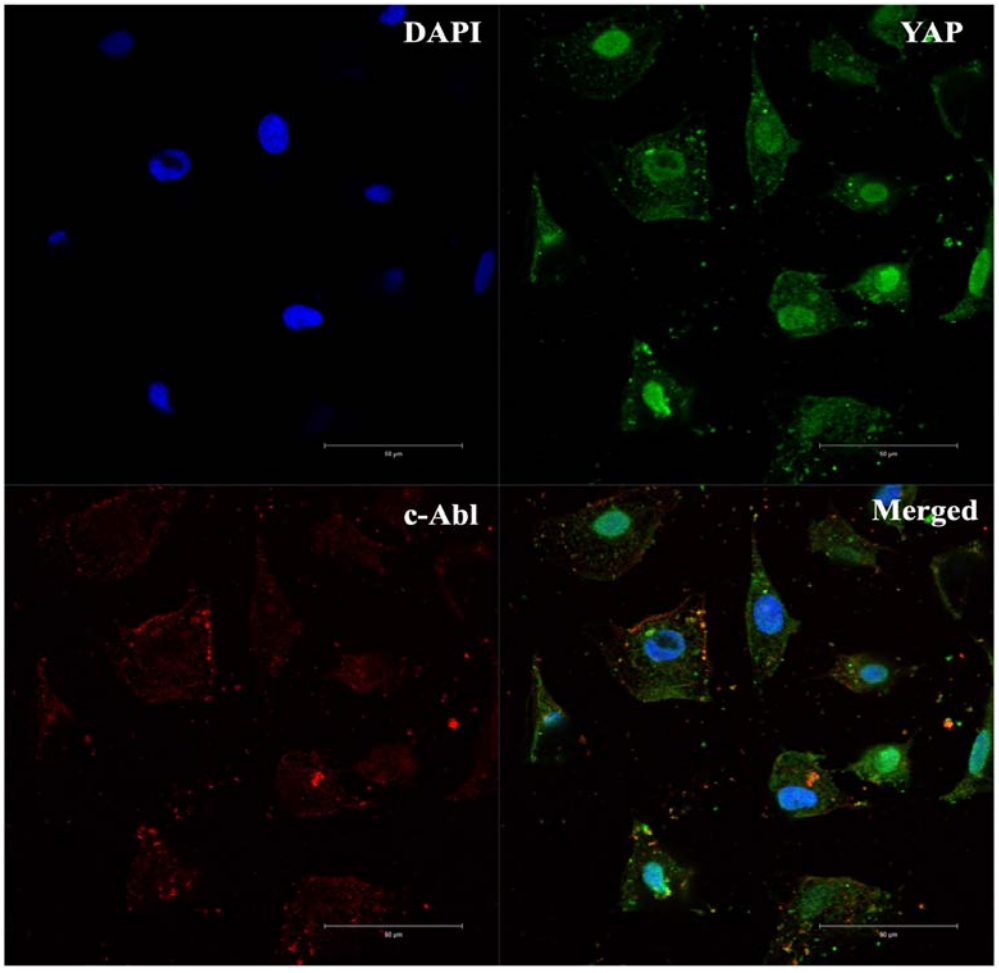

Figure 4.2.12. Localization of c-Abl and YAP in GCs after 10μM H_2O_2 treatment on confocal microscope at 63X objective.

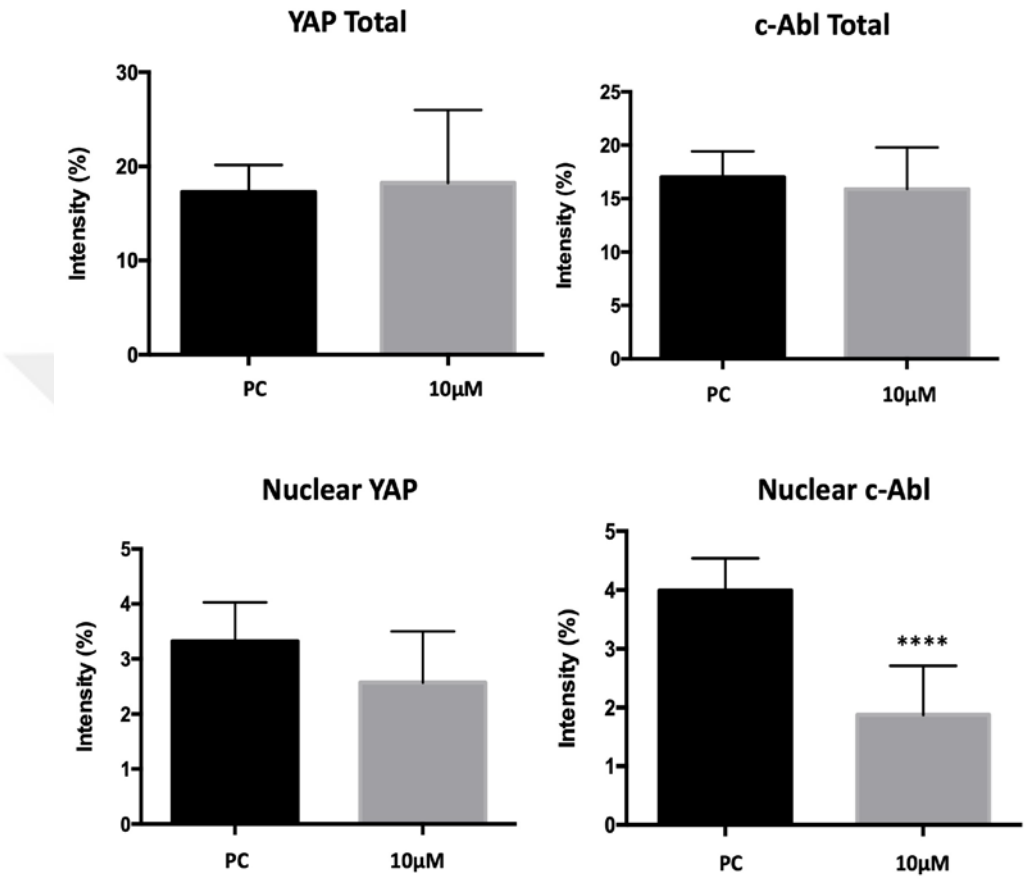

Figure 4.2.13. Total and nuclear fluorescence intensity ratios of c-Abl and YAP in GCs after 10μM H_2O_2 treatment.

After GCs treated with 10% FBS including DMEM for 7 days and confluency of cells reached to 70%, they are treated with 20μM H_2O_2 for 24 hours. Then, morphology of granulosa cells was observed under the inverted microscope. When the granulosa cells were treated with 20μM H_2O_2, some of these cells were observed as rounded shape and some of them observed as spindle shape. However, before cells treated with 20μM H_2O_2, they showed normal morphology. **(Figure 4.2.14.)**

After cells treated with 20μM H_2O_2, double immunofluorescence was performed to observe the localization of YAP and c-Abl in cultured granulosa cells. According to the immunofluorescence results, it was observed that the granulosa cells were in contact. YAP showed nuclear expression in the most of granulosa cells although it showed cytoplasmic localization in few granulosa cells. Addition to the localization of YAP, it was obvious that c-Abl showed high localization in the cytoplasm of granulosa cells. However, a few granulosa cells showed nuclear localization of c-Abl. **(Figure 4.2.15.-Figure 4.2.16.)**

Fluorescence intensity ratios were observed as quantitatively. According to the results, intensity ratio of total YAP decreased in low density in compare with granulosa cells non-treated with H_2O_2. On the other hand, intensity ratio of c-Abl did not show significant decrement in accordance to positive control group. Additionally, fluorescence intensity ratios of nuclear YAP and nuclear c-Abl were measured and observed. It was obvious that there was significant difference in the intensity ratio of nuclear c-Abl between the positive control group and cells treated with 20μM H_2O_2. Also, intensity ratio of nuclear YAP was similar in H_2O_2 treated cells and positive control group. Additionally, cells treated with 20μM H_2O_2 showed higher intensity ratio of nuclear YAP than the nuclear c-Abl. So, it was clear that the YAP showed higher nuclear localization than c-Abl. **(Figure 4.2.17.)**

Granulosa cells before 20μM H_2O_2 treatment

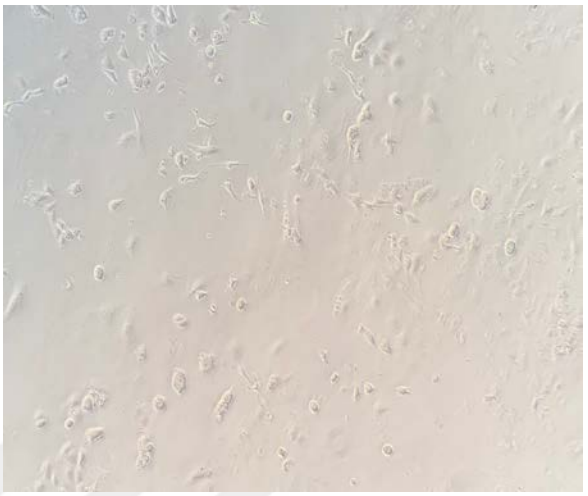

Granulosa cells after 20μM H_2O_2 treatment

Figure 4.2.14. Images of GCs before 20μM H_2O_2 treatment and 24 hours after 20μM H_2O_2 treatment on inverted microscope at 20X objective.

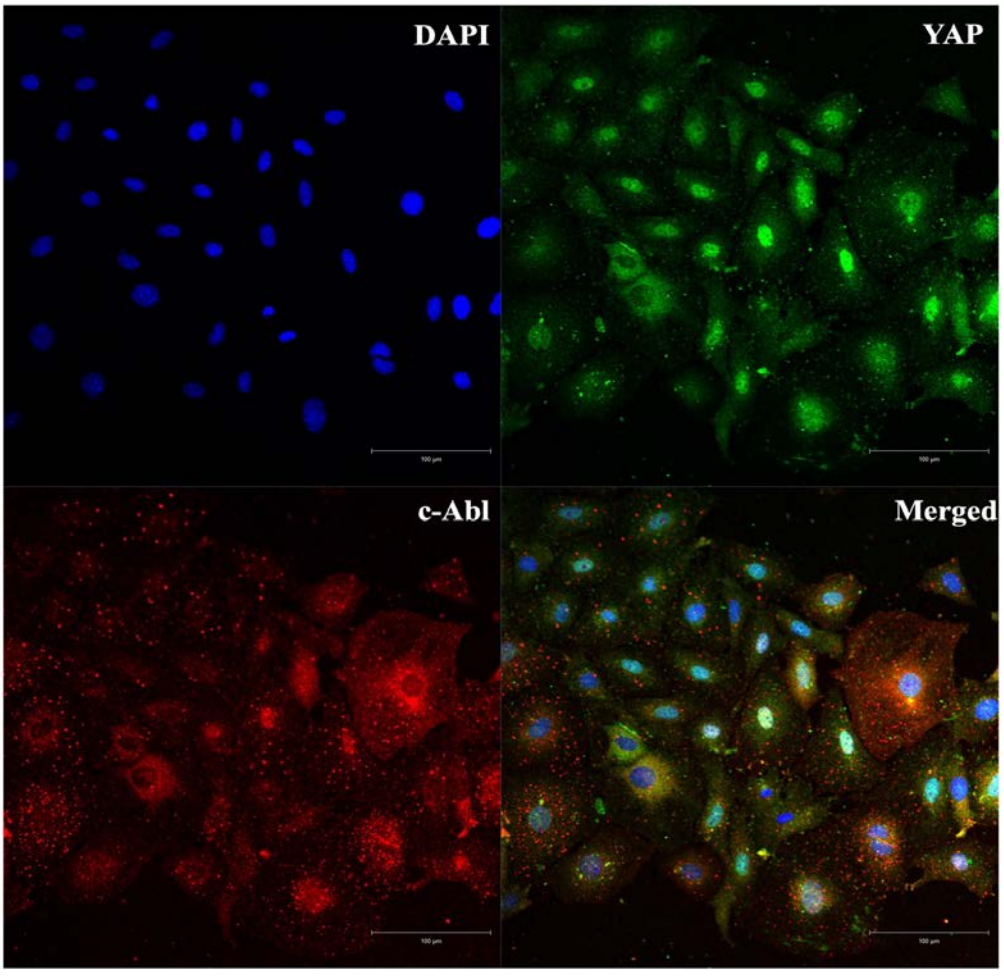

Figure 4.2.15. Localization of c-Abl and YAP in GCs after 20μM H_2O_2 treatment on confocal microscope at 20X objective.

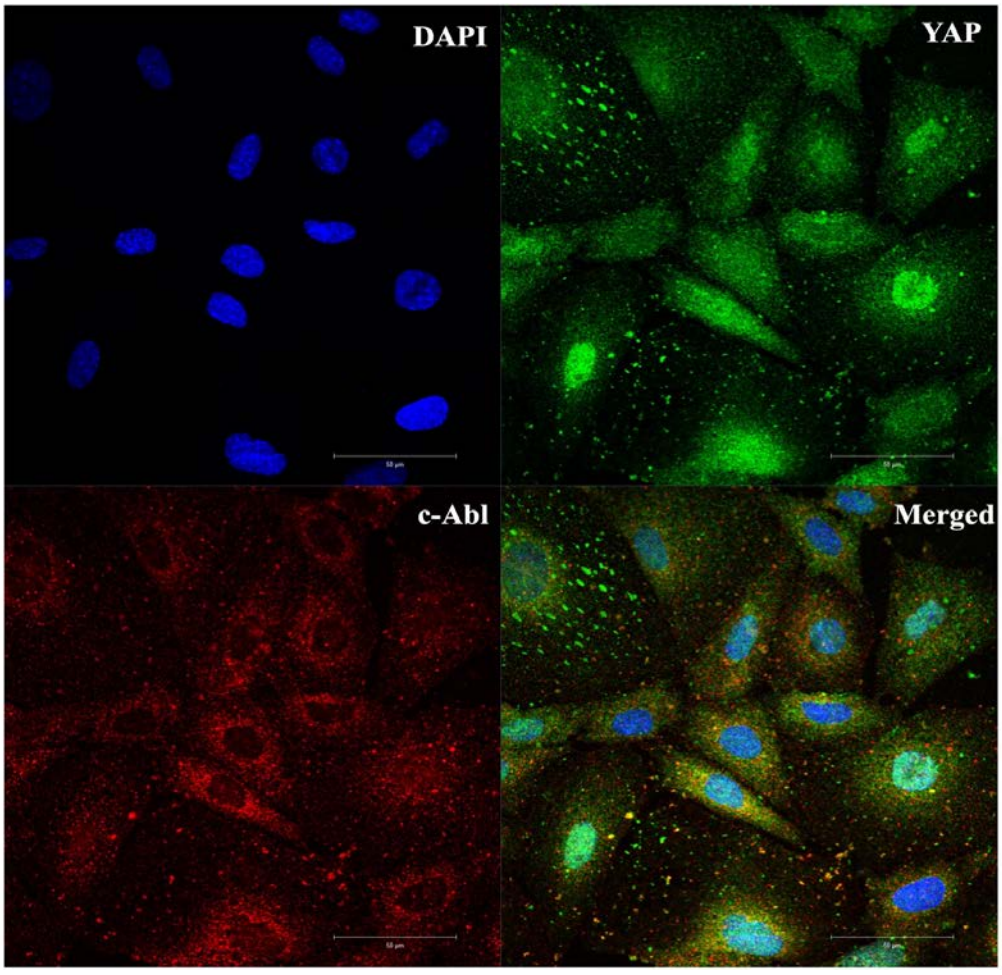

Figure 4.2.16. Localization of c-Abl and YAP in GCs after 20μM H_2O_2 treatment on confocal microscope at 63X objective.

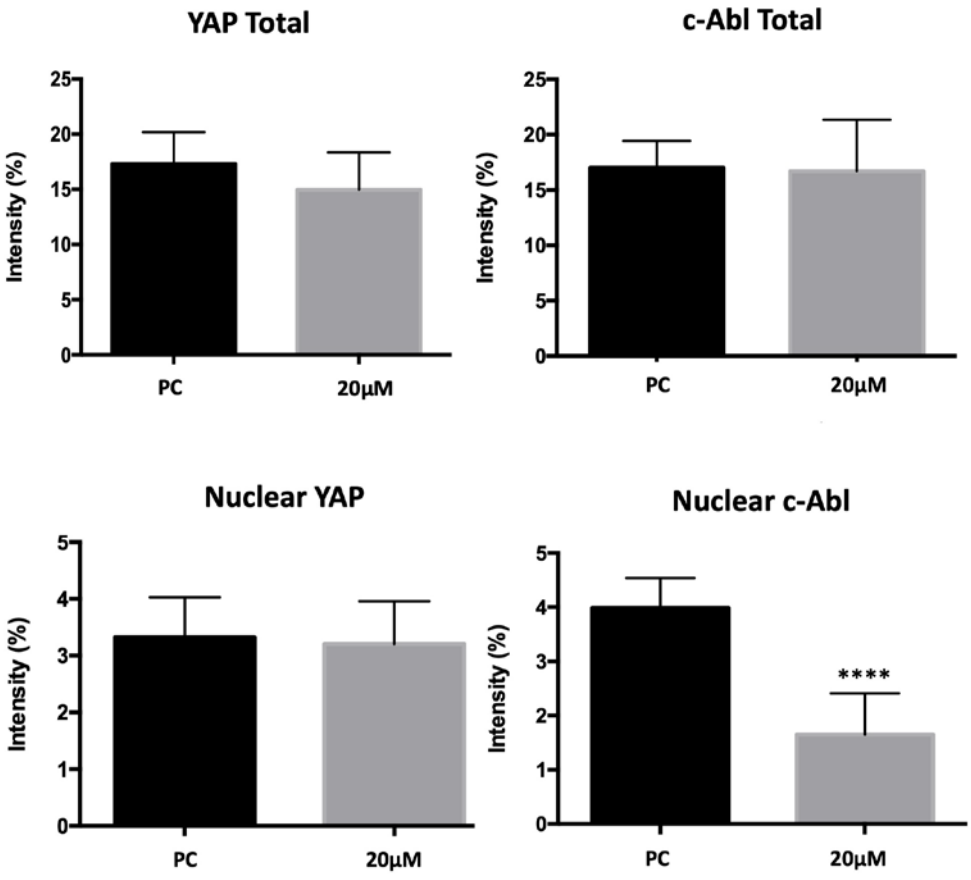

Figure 4.2.17. Total and nuclear fluorescence intensity ratios of c-Abl and YAP in GCs after 20μM H_2O_2 treatment.

After GCs were treated with 50μM H_2O_2 for 24 hours, under the inverted microscope, granulosa cells showed more elongated and spindle-like morphology in treatment group. **(Figure 4.2.18.)**

For the determination of expression sites of YAP and c-Abl, double immunofluorescence staining was conducted after 50μM H_2O_2 treatment. It was observed that the cells did not contact each other too much. Interestingly, c-Abl was not observed to be localized in the any area of granulosa cells. However, YAP exhibited expression in the cytoplasm, albeit at a low intensity in granulosa cells. In addition to this, YAP did not show nuclear localization in granulosa cells. **(Figure 4.2.19.- Figure 4.2.20.)**

In order to decide the fluorescence intensity ratios of total c-Abl and YAP, intensity ratios were observed as quantitatively also. In granulosa cells treated with 50μM H_2O_2, intensity ratio of YAP significantly reduced in comparision to positive control group. Since the c-Abl was not observed to be localized in the any area of granulosa cells, fluorescence intensity ratio of c-Abl also was not observed in granulosa cells treated with 50μM H_2O_2. When the nuclear fluorescence intensity ratios were compared between treatment and control group, it was observed that the intensity ratio of YAP significantly reduced in treatment group in compare with control group. The nuclear intensity ratio of c-Abl was not observed in the treatment group. **(Figure 4.2.21.)**

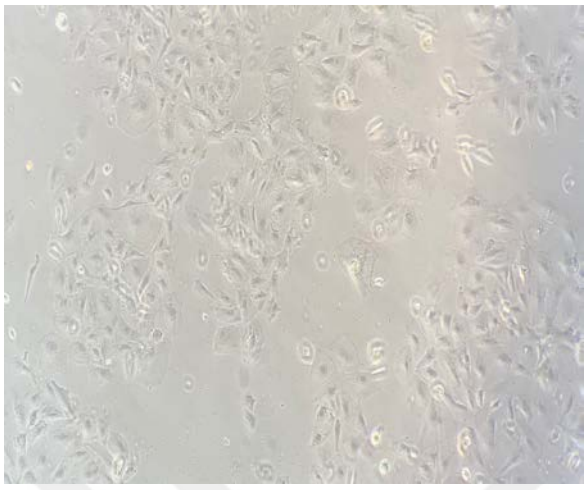

Granulosa cells before 50µM H_2O_2 treatment

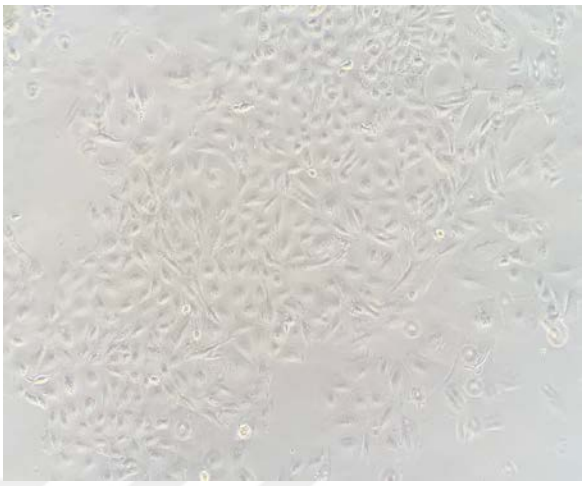

Granulosa cells after 50µM H_2O_2treatment

Figure 4.2.18. Images of GCs before 50µM H_2O_2 treatment and 24 hours after 50µM H_2O_2 treatment on inverted microscope at 20X objective.

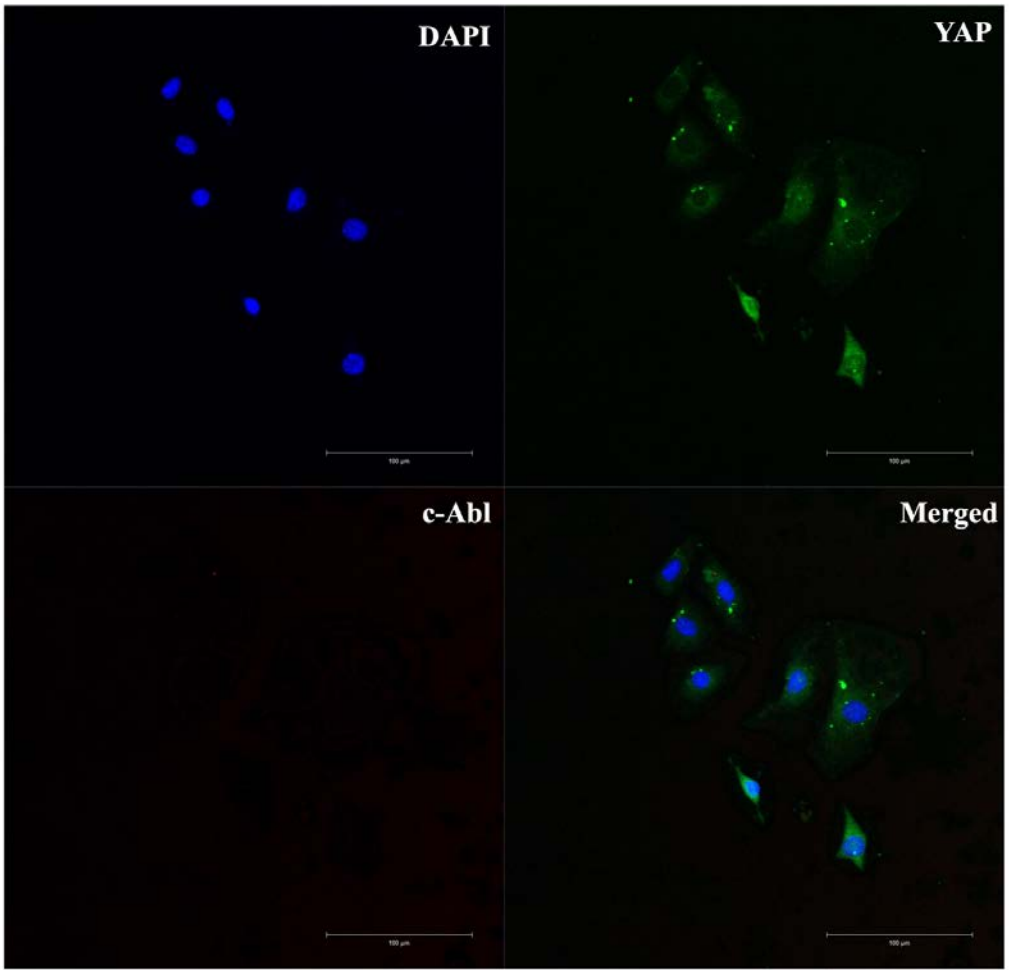

Figure 4.2.19. Localization of c-Abl and YAP in GCs after 50μM H_2O_2 treatment on confocal microscope at 20X objective.

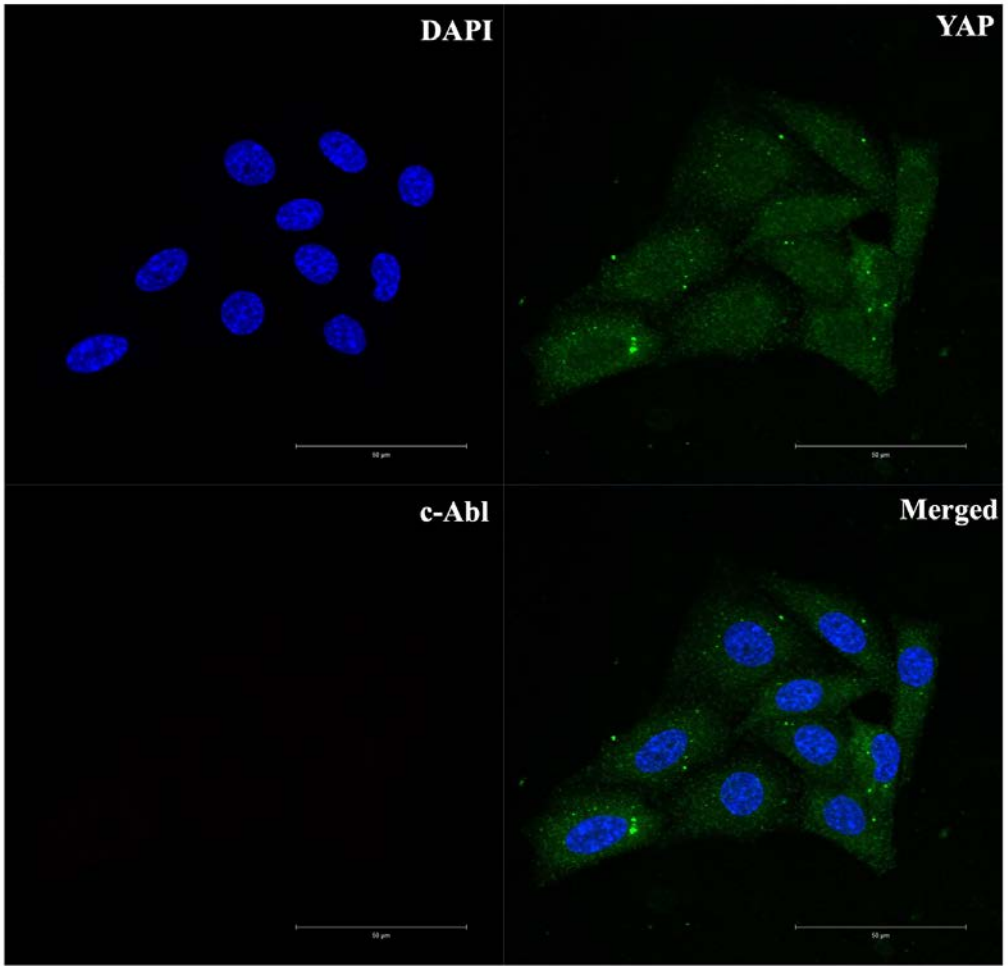

Figure 4.2.20. Localization of c-Abl and YAP in GCs after 50μM H_2O_2 treatment on confocal microscope at 63X objective.

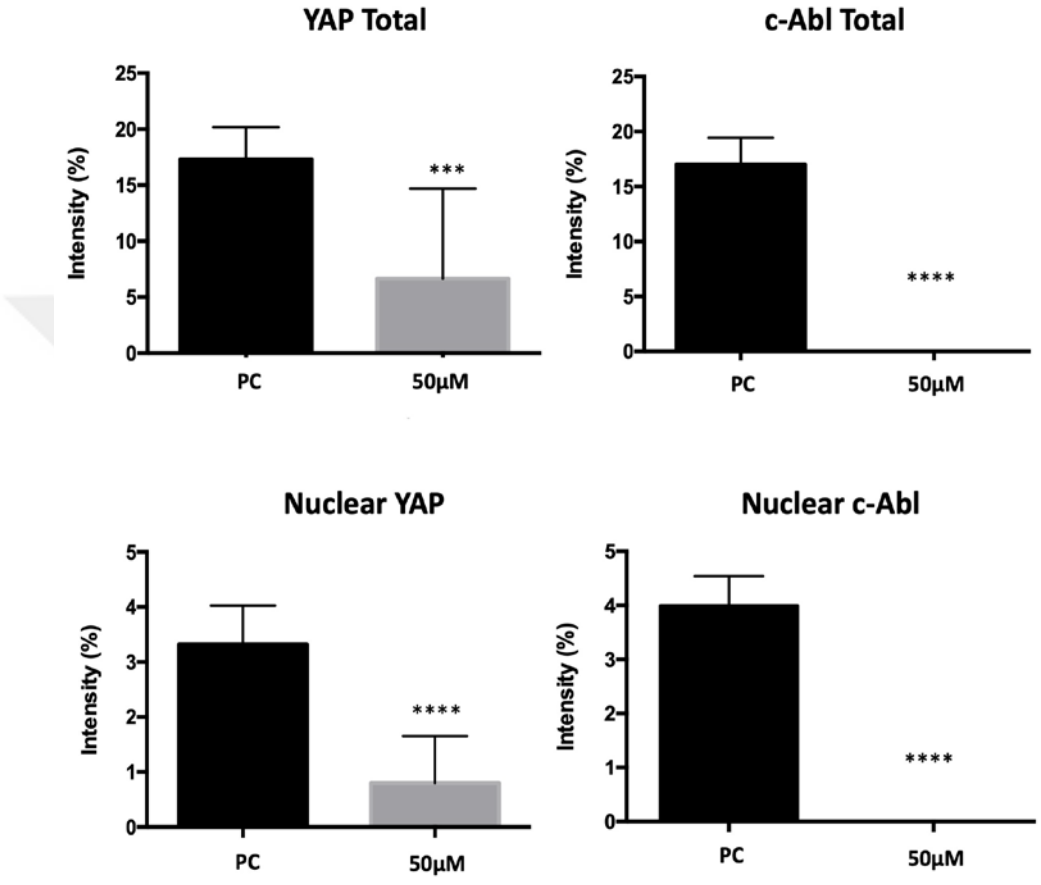

Figure 4.2.21. Total and nuclear fluorescence intensity ratios of c-Abl and YAP in GCs after 50µM H_2O_2 treatment.

4.3. Invert Microscopy and Confocal Microscopy Observations of GCs After 100µM, 200µM and 400µM H_2O_2 Treatment

In order to be able to show how YAP and c-Abl would respond to higher H_2O_2 doses, new culture of granulosa cells have been started.

Firstly, GCs were treated with 10% FBS including DMEM for 7 days as a positive control group. Then, the morphology of GCs was observed by the inverted microscope. Under the microscope, granulosa cells were observed to exerted epithelial-like shape and polygonal shape. **(Figure 4.3.1.-A)**

To decide the expression areas of YAP and c-Abl in cultured granulosa cells, double immunofluorescence staining was conducted after 7 days culture. It was obvious that YAP showed nuclear localization in primary cultured granulosa cells. In addition to this, c-Abl showed also expression nucleus of GCs treated with 10% FBS including DMEM. There was no staining in negative control slide which inserted in merged part of Fig.4.3.1.-B. **(Figure 4.3.1.-B)**

A **B**

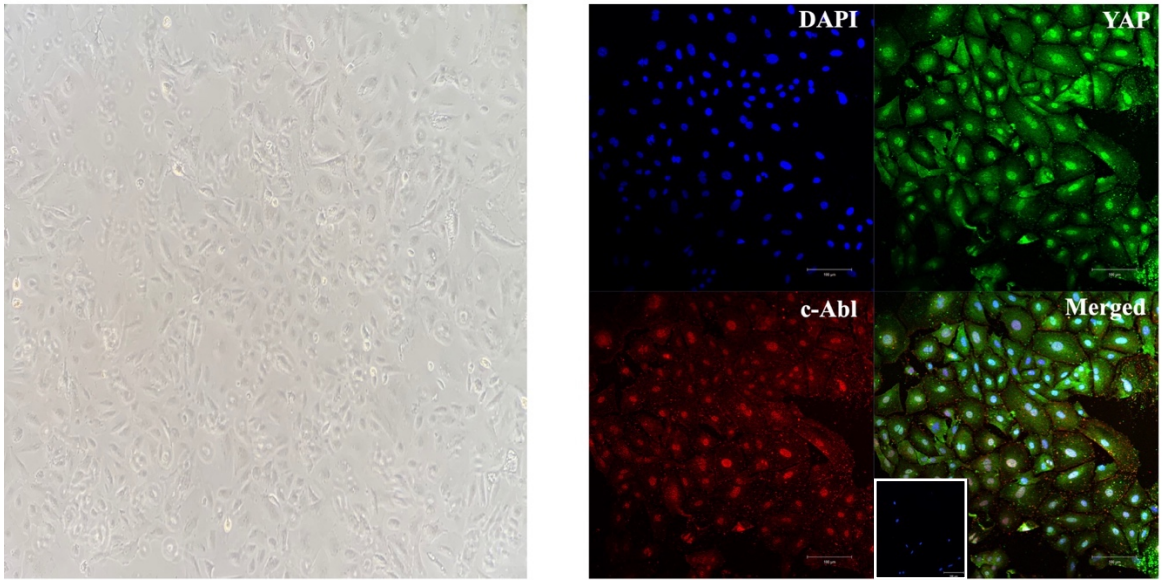

Figure 4.3.1. Observation of primary cultured GCs treated with 10% FBS including DMEM after 7 days as positive control group. (A) Image of GCs after 10%FBS including DMEM treatment on inverted microscope at 20X objective. (B) Localization of c-Abl and YAP in GCs on confocal microscope at 20X objective. DAPI stained nucleus of cells.

After GCs treated with 10% FBS including DMEM for 7 days and confluency of cells reached to 70%, cells were treated with 100μM H_2O_2. After 100uM H_2O_2 treatment, granulosa cells were observed as rounded and some of them showed spindle-like shape. However, most of the cells which were not treated with 100μM H_2O_2, showed normal morphology. **(Figure 4.3.2)**

To decide the expression patterns of YAP and c-Abl in primarly cultured granulosa cells, double immunofluorescence staining was performed after 100μM H_2O_2 treatment. According to the results, it was obvious that the YAP exerted localization both in the nucleus of some granulosa cells and the cytoplasm of some granulosa cells. On the other hand, c-Abl showed higher cytoplasmic localization and no nuclear localization. Additionally, cells have interactions between each other. **(Figure 4.3.3.- Figure 4.3.4.)**

Fluorescence intensity ratios were also observed as quantitatively. According to the results, intensity ratio of total YAP reduced significantly in GCs treated with 100μM H_2O_2 in compare with non-treated cells. On the other hand, intensity ratio of total c-Abl showed significant increment in the granulosa cells treated with 100μM H_2O_2 in compare with non-treated cells. Additionally, the fluorescence intensity ratios of nuclear YAP and c-Abl were compared. According to the results, it was obvious that the intensity ratio of nuclear YAP increased in the cells treated with 100μM H_2O_2 in compare with non-treated granulosa cells. However, the nuclear intensity ratio of c-Abl exert significant decrement in the cells treated with 100μM H_2O_2 in compare with non-treated granulosa cells. **(Figure 4.3.5.)**

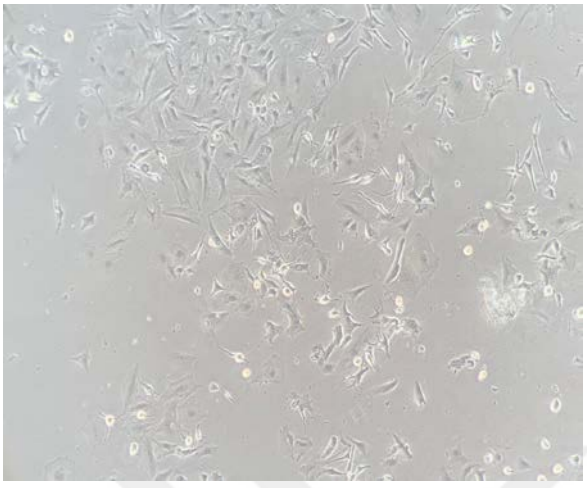

Granulosa cells before 100 µM H_2O_2treatment

Granulosa cells after 100µM H_2O_2treatment

Figure 4.3.2. Images of GCs before 100µM H_2O_2 treatment and 24 hours after 100µM H_2O_2 treatment on inverted microscope at 20X objective.

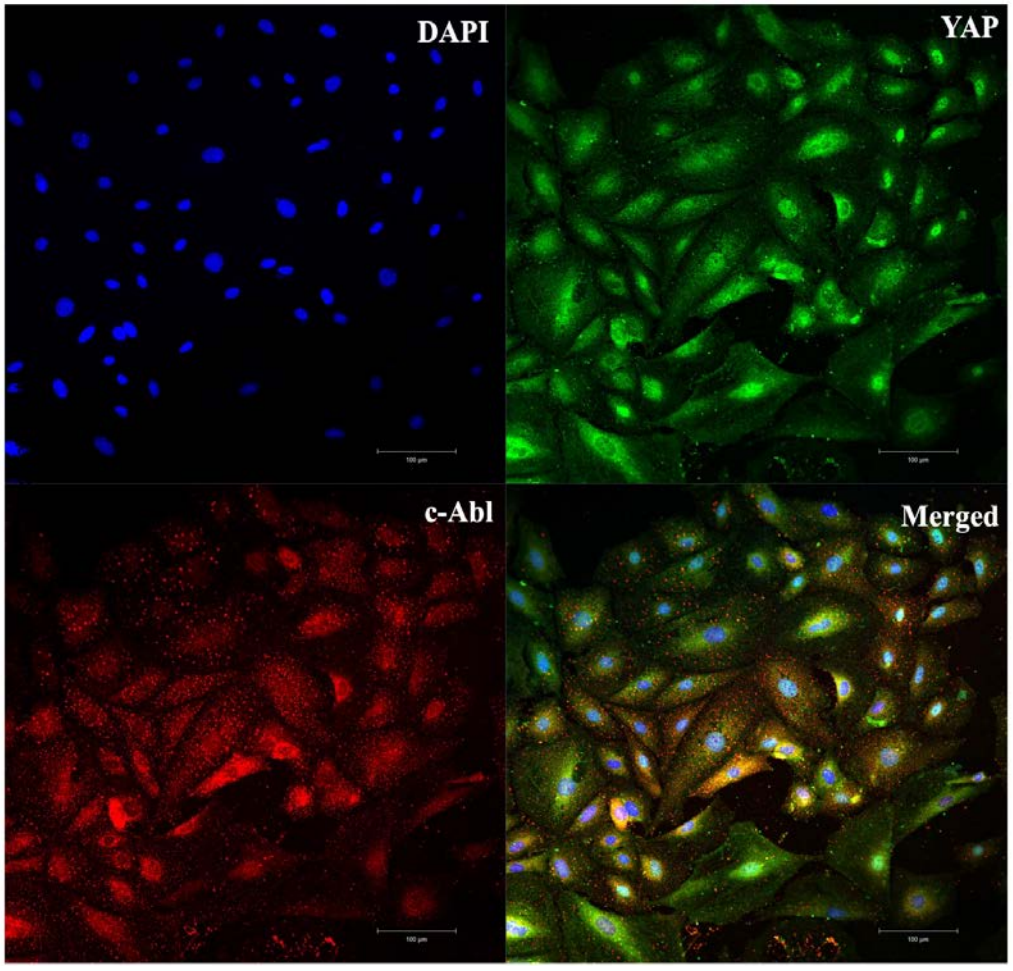

Figure 4.3.3. Localization of c-Abl and YAP in GCs after 100μM H_2O_2 treatment on confocal microscope at 20X objective.

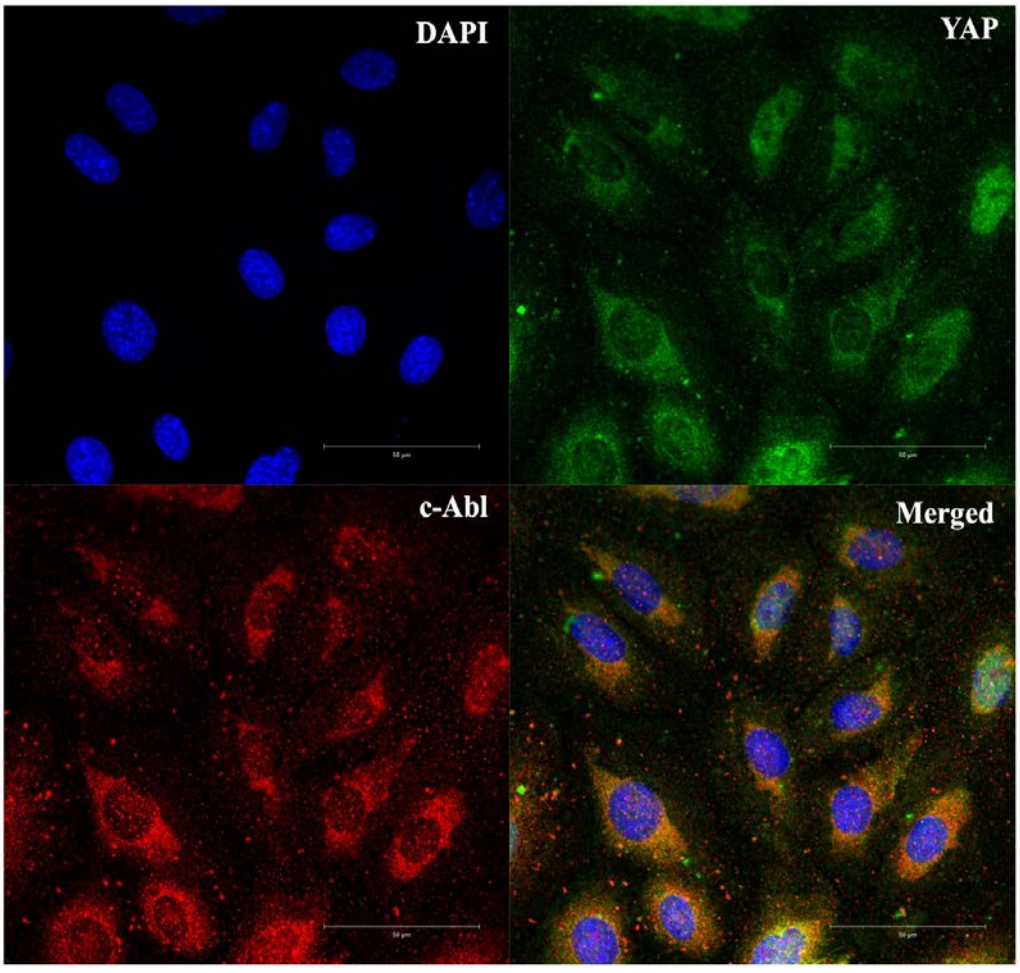

Figure 4.3.4. Localization of c-Abl and YAP in GCs after 100μM H_2O_2 treatment on confocal microscope at 63X objective.

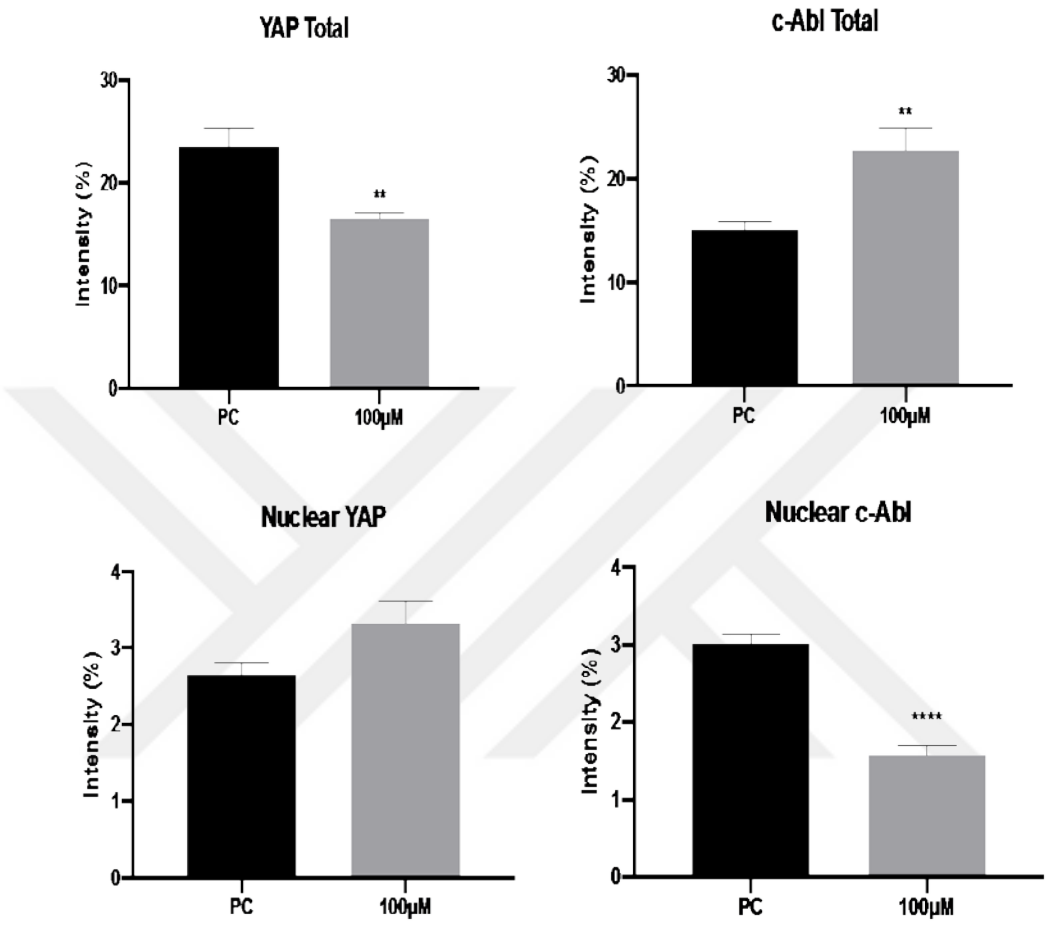

Figure 4.3.5. Total and nuclear fluorescence intensity ratios of c-Abl and YAP in GCs after 100µM H_2O_2 treatment.

After GCs were treated with 200μM H_2O_2, morphology of cells was observed under the inverted microscope. Granulosa cells were observed in epithelial-like shape and polygonal shape before 200μM H_2O_2 treatment. However, it was observed that there were more elongated granulosa cells in the treatment group. **(Figure 4.3.6.)**

To decide the localization of YAP and c-Abl, double immunofluorescence staining was conducted after 200μM H_2O_2 treatment too. According to the results, it was obvious that YAP showed high nuclear localization in the granulosa cells. Similarly, c-Abl was mostly localized in the nucleus, but did not exhibit as strong nuclear localization as YAP. Additionally, most of the cells were in contact with each other. **(Figure 4.3.7.-Figure 4.3.8.)**

Fluorescence intensity ratios were determined as quantitatively. According to the results, the intensity ratio of total YAP decreased in GCs treated with 200μM H_2O_2 in accordance to positive control group. However, there was no significant difference between control and treatment group. In addition to this, the intensity ratio of total c-Abl increased significantly in GCs treated with 200μM H_2O_2 in accordance to positive control group. When the fluorescence intensity ratios of nuclear YAP were compared, intensity ratio of YAP decreased slightly in accordance to control group. On the other hand, intensity ratio of c-Abl decreased significantly in accordance to control group. **(Figure 4.3.9.)**

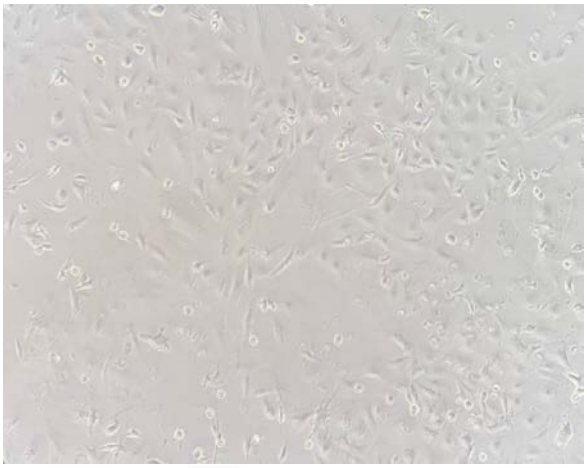

Granulosa cells before 200μM H_2O_2 treatment

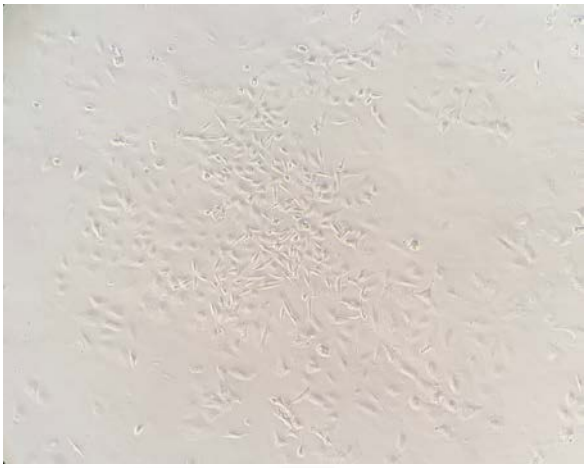

Granulosa cells after 200μM H_2O_2 treatment

Figure 4.3.6. Images of GCs before 200μM H_2O_2 treatment and 24 hours after 200uM H_2O_2 treatment on inverted microscope at 20X objective.

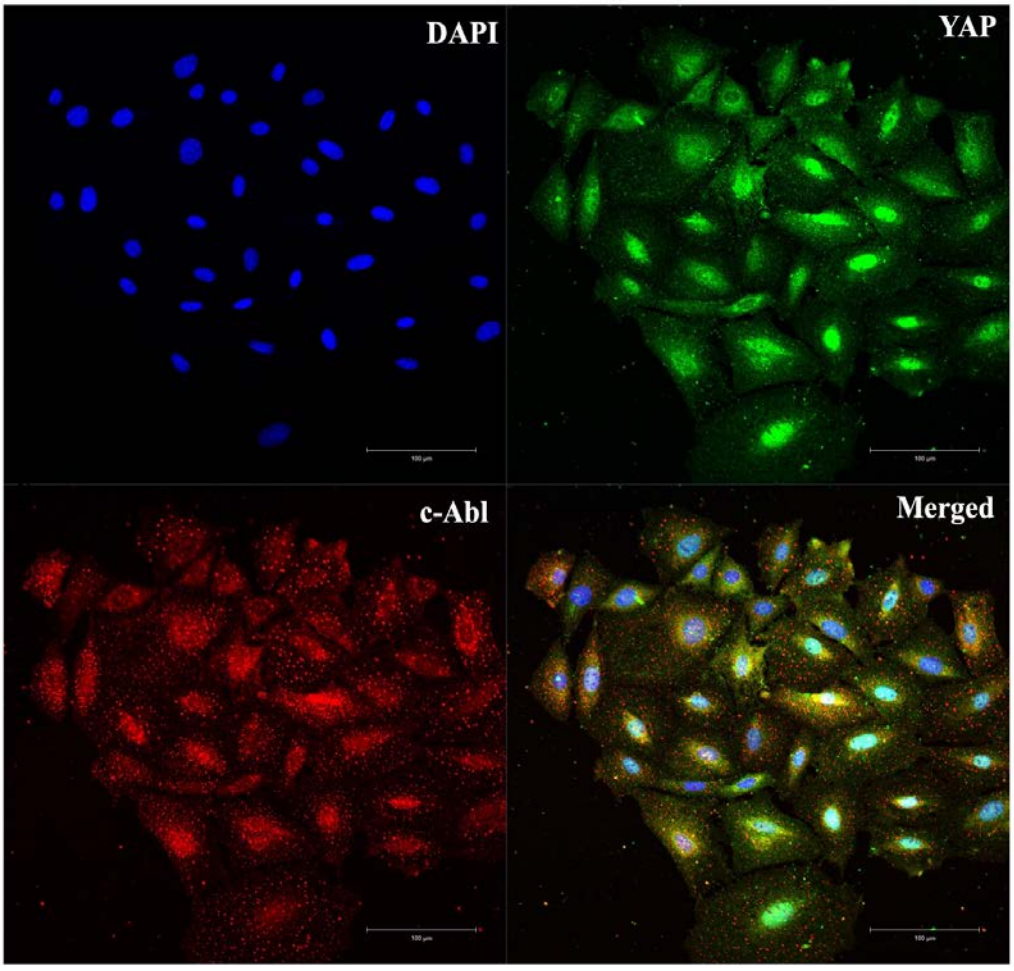

Figure 4.3.7. Localization of c-Abl and YAP in GCs after 200μM H_2O_2 treatment on confocal microscope at 20X objective.

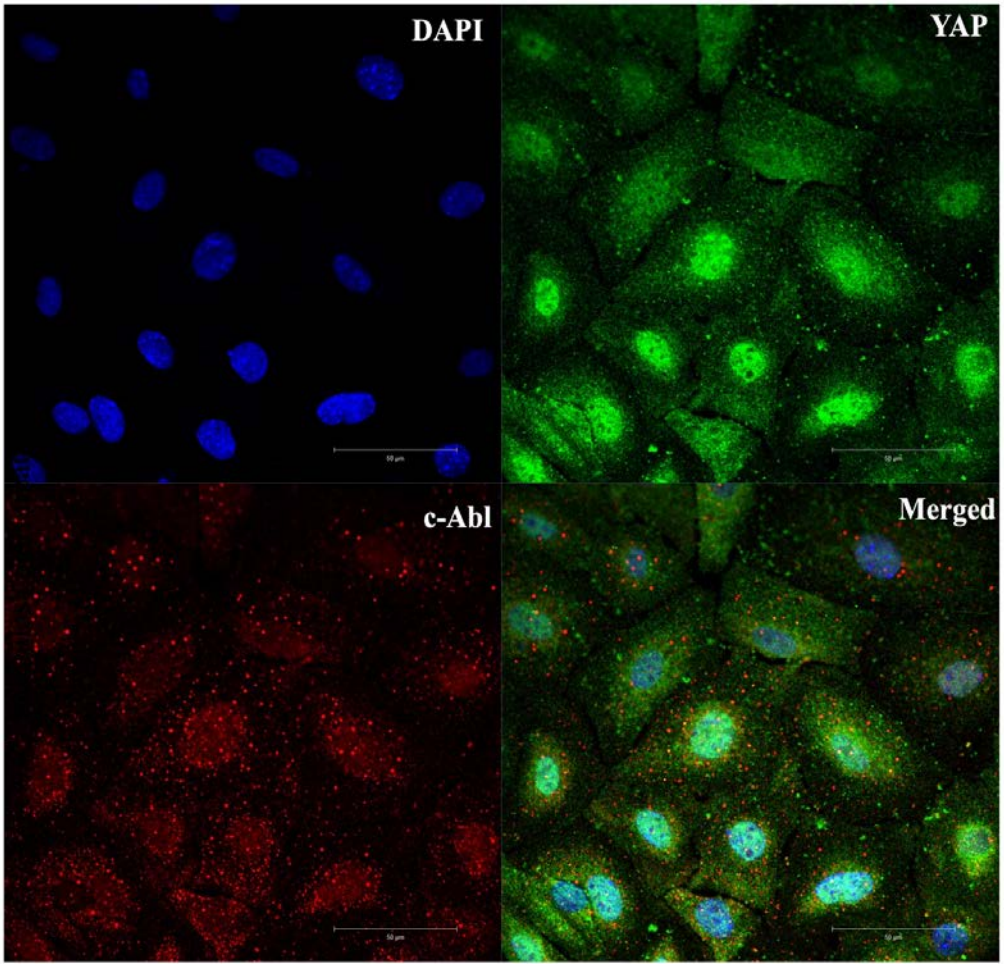

Figure 4.3.8. Localization of c-Abl and YAP in GCs after 200μM H_2O_2 treatment on confocal microscope at 63X objective.

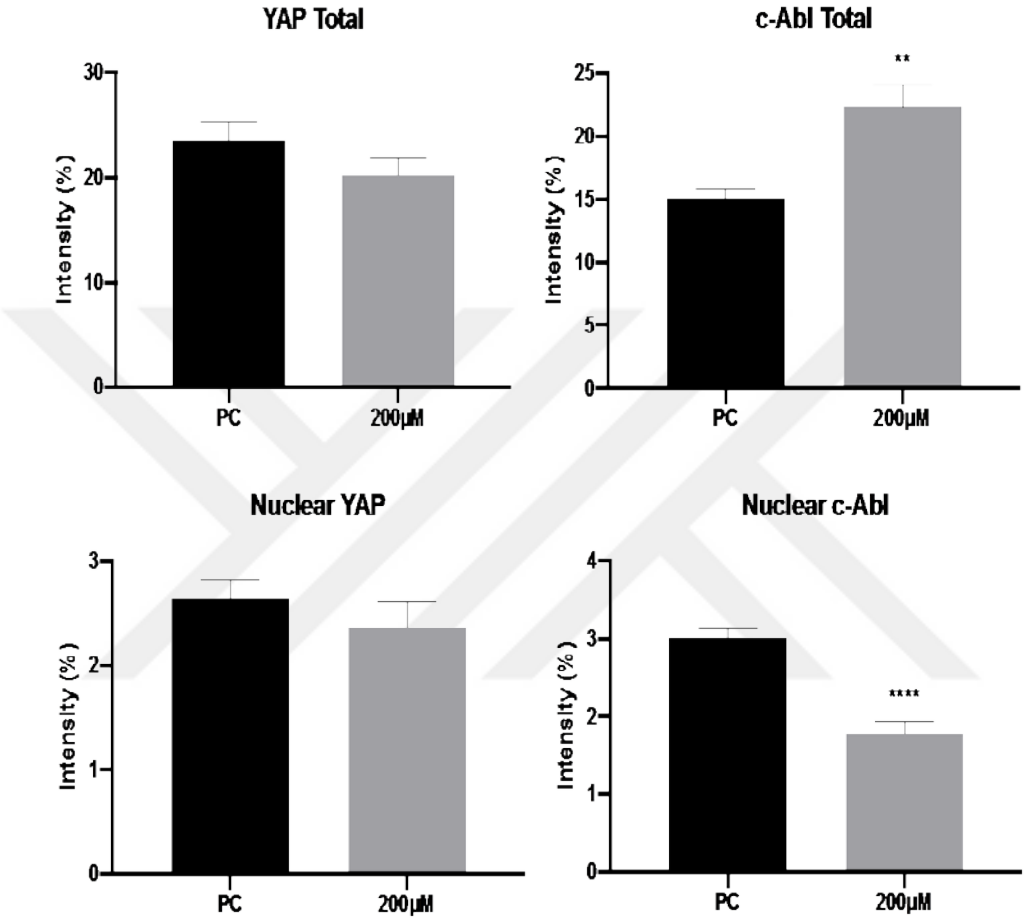

Figure 4.3.9. Total and nuclear fluorescence intensity ratios of c-Abl and YAP in GCs after 200µM H_2O_2 treatment.

After GCs were treated with 400uM H_2O_2, morphology of cells was observed. After 400μM H_2O_2 treatment was applied, there were more rounded granulosa cells in compare with control group. Granulosa cells were observed in a fibroblast-like or spindle-like shape. Generally, it was observed that as the concentration of H_2O_2 increased, the number of GCs in the area decreased and the cells began to return more elongated form and show more spindle-like shape. **(Figure 4.3.10.)**

To decide the localization sites of YAP and c-Abl in the granulosa cells treated with 400μM H_2O_2, double immunofluorescence staining was performed. According to the results, it was observed that YAP highly localized in the nucleus of GCs. In addition to this, c-Abl was also localized mostly in the nucleus rather than the cytoplasm of cells. **(Figure 4.3.11.- Figure 4.3.12.)**

When the fluorescence intensity ratios of total YAP and total c-Abl were compared with positive control, it was observed that intensity ratio of YAP decreased slightly in GCs treated with 400μM H_2O_2 in compare with positive control group though there was no significant difference. Additionally, intensity ratio of c-Abl showed significant increment in GCs treated with 400μM H_2O_2. The nuclear fluorescence intensity ratios of c-Abl and YAP were compared also. Although there was no significant difference, it was clear that the intensity ratio of nuclear YAP increased in the cells treated with 400μM H_2O_2 in compare with non-treated GCs. Unlike this, the nuclear intensity ratio of c-Abl decreased significantly in treatment group in compare with non-treated cells. **(Figure 4.3.13.)**

Granulosa cells before 400 µM H_2O_2 treatment

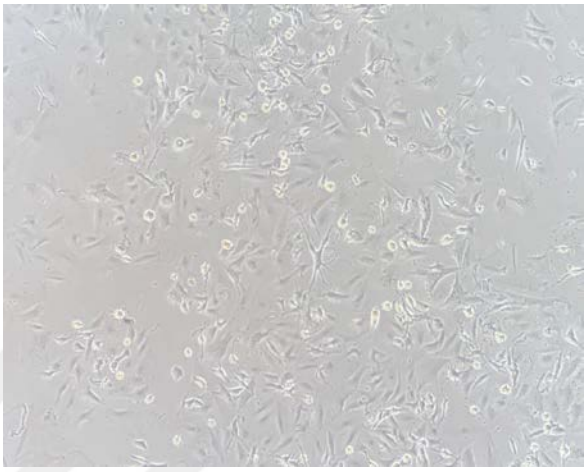

Granulosa cells after 400µM H_2O_2treatment

Figure 4.3.10. Images of GCs before 400µM H_2O_2 treatment and 24 hours after 400uM H_2O_2 treatment on inverted microscope at 20X objective.

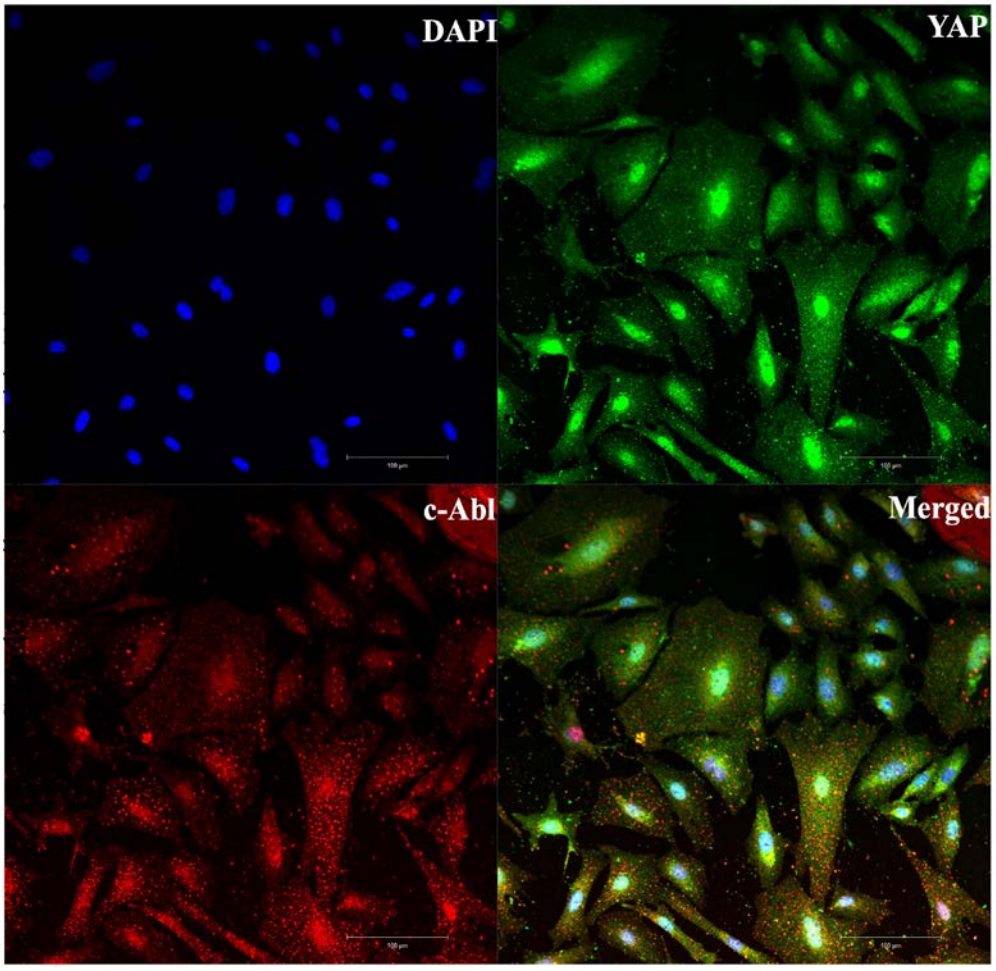

Figure 4.3.11. Localization of c-Abl and YAP in GCs after 400μM H_2O_2 treatment on confocal microscope at 20X objective.

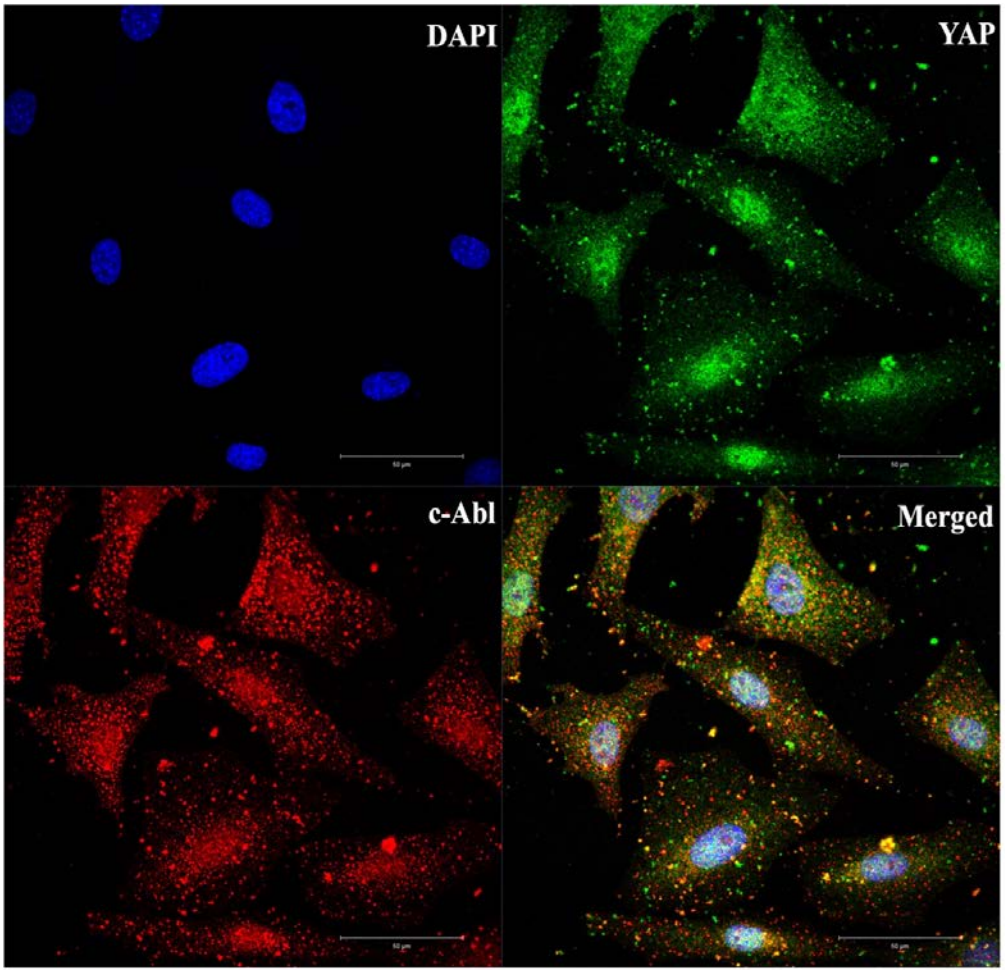

Figure 4.3.12. Localization of c-Abl and YAP in GCs after 400μM H_2O_2 treatment on confocal microscope at 63X objective.

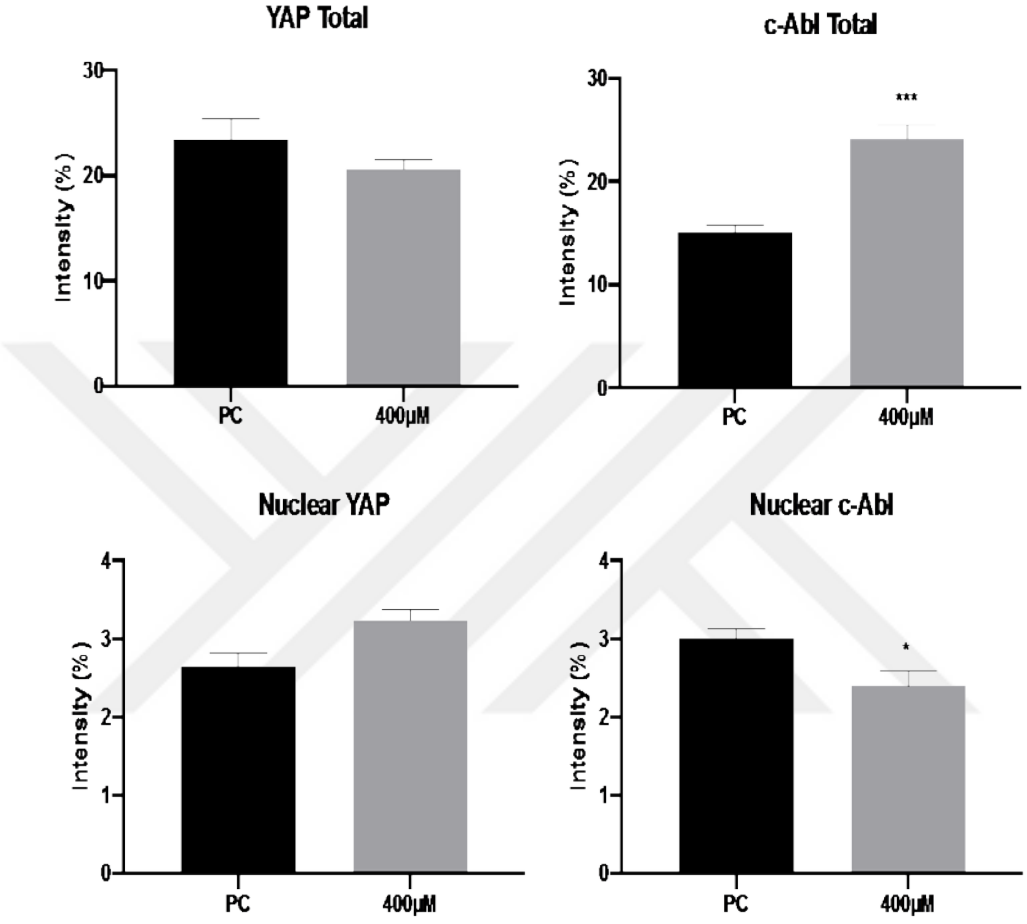

Figure 4.3.13. Total and nuclear fluorescence intensity ratios of c-Abl and YAP in GCs after 400µM H_2O_2 treatment.

To be able to compare shuttling of c-Abl and YAP between cytoplasm and nucleus in whole hydrogen peroxide concentrations, evaluation was performed between all groups. Firstly, shuttling of c-Abl between cytoplasm and nucleus in 2,5μM, 5μM, 10μM, 20μM, 50μM H_2O_2 concentrations was evaluated. According to the results, c-Abl showed expression in mostly nucleus of control granulosa cells and cells treated with 2,5μM and 5μM H_2O_2. The nuclear localization of c-Abl started to decrease from the 10 μM H_2O_2 treatment and the expression of c-Abl completely disappeared at the 50 μM H_2O_2 treatment. Additionally, total expression of c-Abl significantly decreased in cells treated with 2,5μM, 5μM and 50μM H_2O_2 in compare with control group. **(Fig 4.3.18. - A, A')**

When the shuttling of c-Abl between cytoplasm and nucleus in 100μM, 200μM and 400 μM H_2O_2 concentrations was observed, it was obvious that the c-Abl showed decreased nuclear localization in GCs treated with 100μM, 200μM and 400 μM H_2O_2 in compare with positive control group. Additionally, total expression of c-Abl significantly increased in the cells treated with 100μM, 200μM and 400μM H_2O_2 in compare with control group. **(Fig 4.3.18. - B, B')**

Unlike c-Abl, YAP generally localized in the nucleus of granulosa cells in whole groups and nuclear expression of YAP did not decrease with increasing hydrogen peroxide doses. Expression of nuclear YAP only significantly decreased in the granulosa cells treated with 50 μM H_2O_2. Also, total expression of YAP significantly decreased in cells treated with 2,5μM, 5μM and 50μM H_2O_2. **(Fig 4.3.18. - C, C')**

Then, shuttling of YAP between cytoplasm and nucleus in 100μM, 200μM and 400 μM H_2O_2 concentrations was evaluated, it was clear that YAP generally localized in the nucleus of GCs. Nuclear expression of YAP did not exert significant change in GCs treated with 100μM, 200μM and 400 μM H_2O_2 in compare with positive control group. In addition to this, total expression of YAP showed significant decrement in GCs treated with 100 μM H_2O_2 in compare with positive control group. **(Fig 4.3.18. - D, D')**

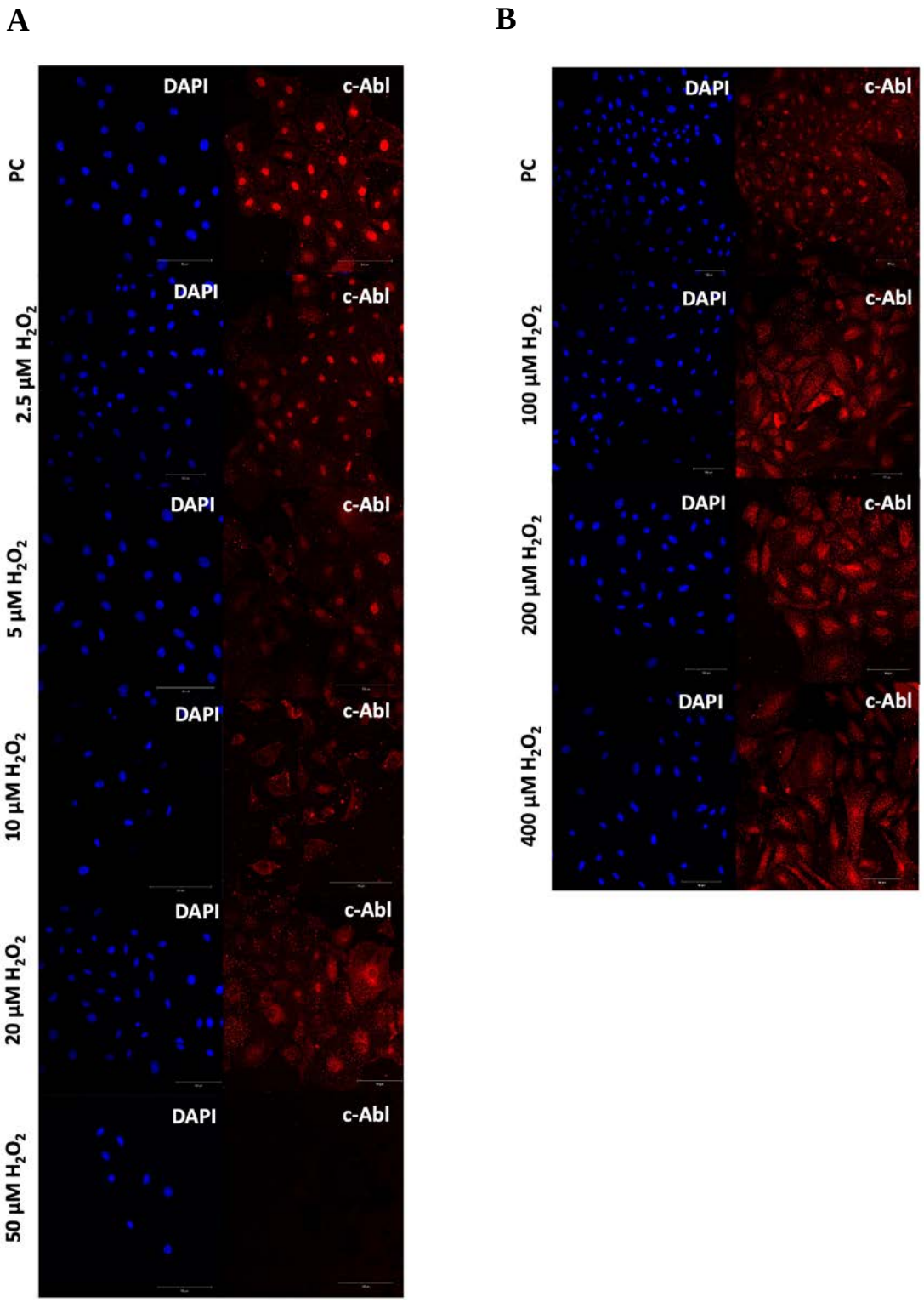
A
B
DAPI
c-Abl
PC
2.5 µM H_2O_2
5 µM H_2O_2
10 µM H_2O_2
20 µM H_2O_2
50 µM H_2O_2
100 µM H_2O_2
200 µM H_2O_2
400 µM H_2O_2

A’

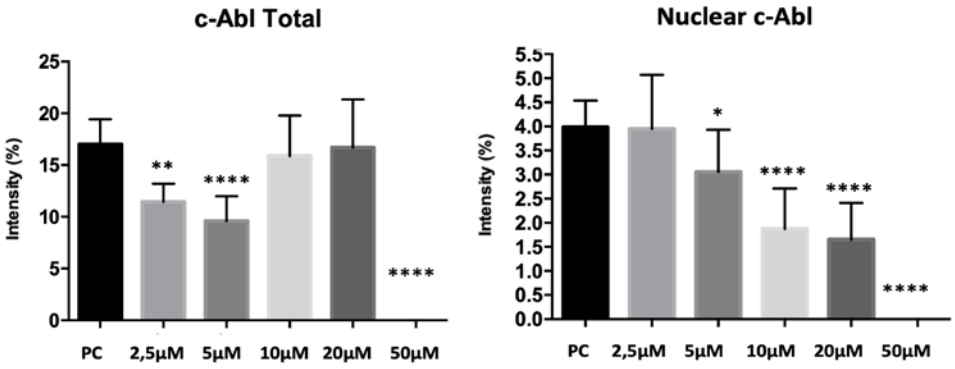
c-Abl Total
Intensity (%)
25
20
15
10
5
0
**
****
****
PC
2,5µM
5µM
10µM
20µM
50µM
Nuclear c-Abl
Intensity (%)
5.5
5.0
4.5
4.0
3.5
3.0
2.5
2.0
1.5
1.0
0.5
0.0
*
****
****
****
PC
2,5µM
5µM
10µM
20µM
50µM

B’

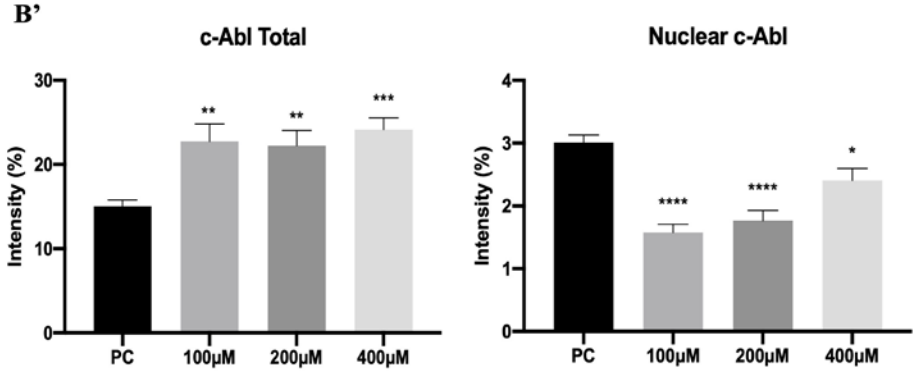
c-Abl Total
Intensity (%)
30
20
10
0
**
**
***
PC
100µM
200µM
400µM
Nuclear c-Abl
Intensity (%)
4
3
2
1
0
****
****
*
PC
100µM
200µM
400µM

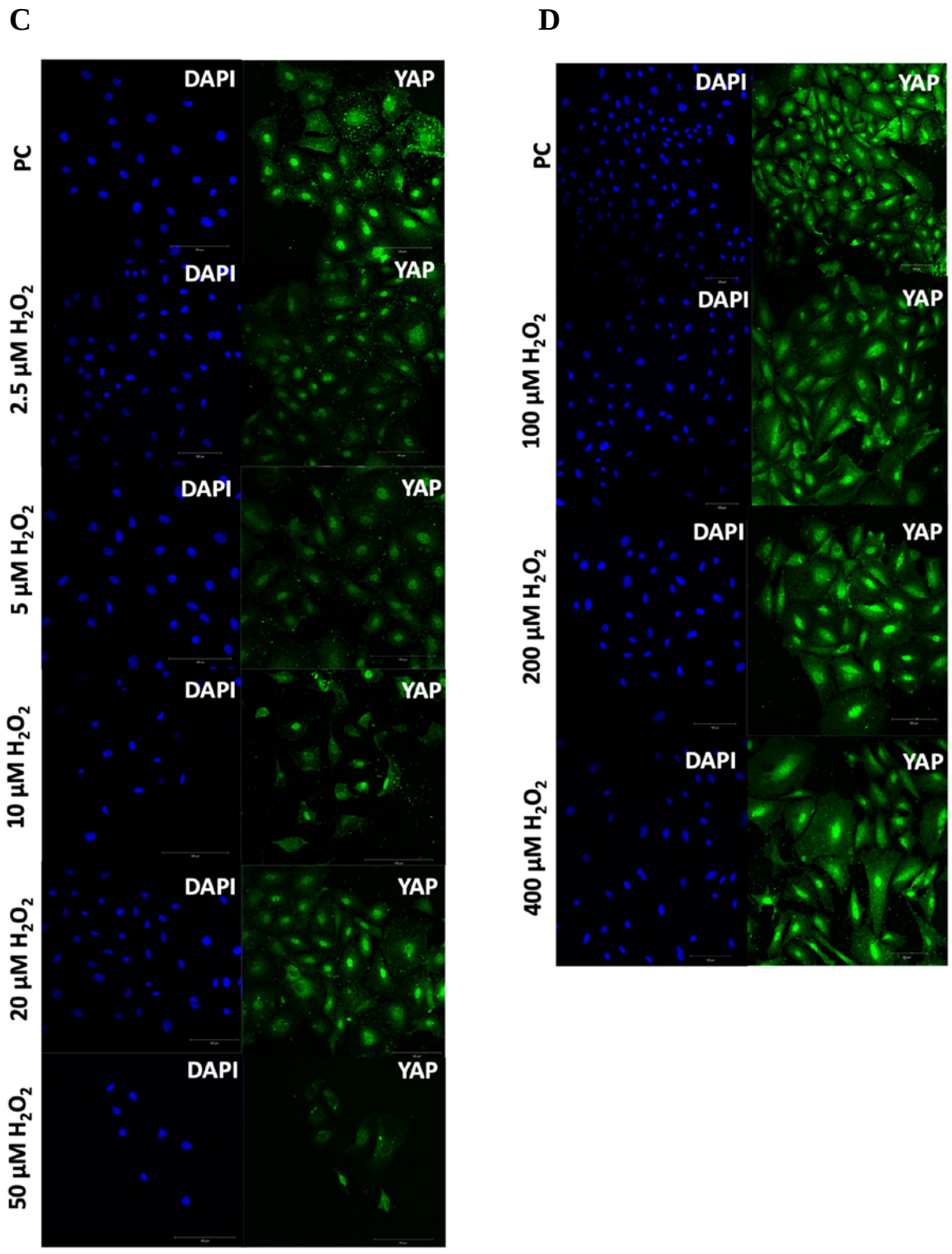
C
D
PC
2.5 µM H_2O_2
5 µM H_2O_2
10 µM H_2O_2
20 µM H_2O_2
50 µM H_2O_2
100 µM H_2O_2
200 µM H_2O_2
400 µM H_2O_2
DAPI
YAP

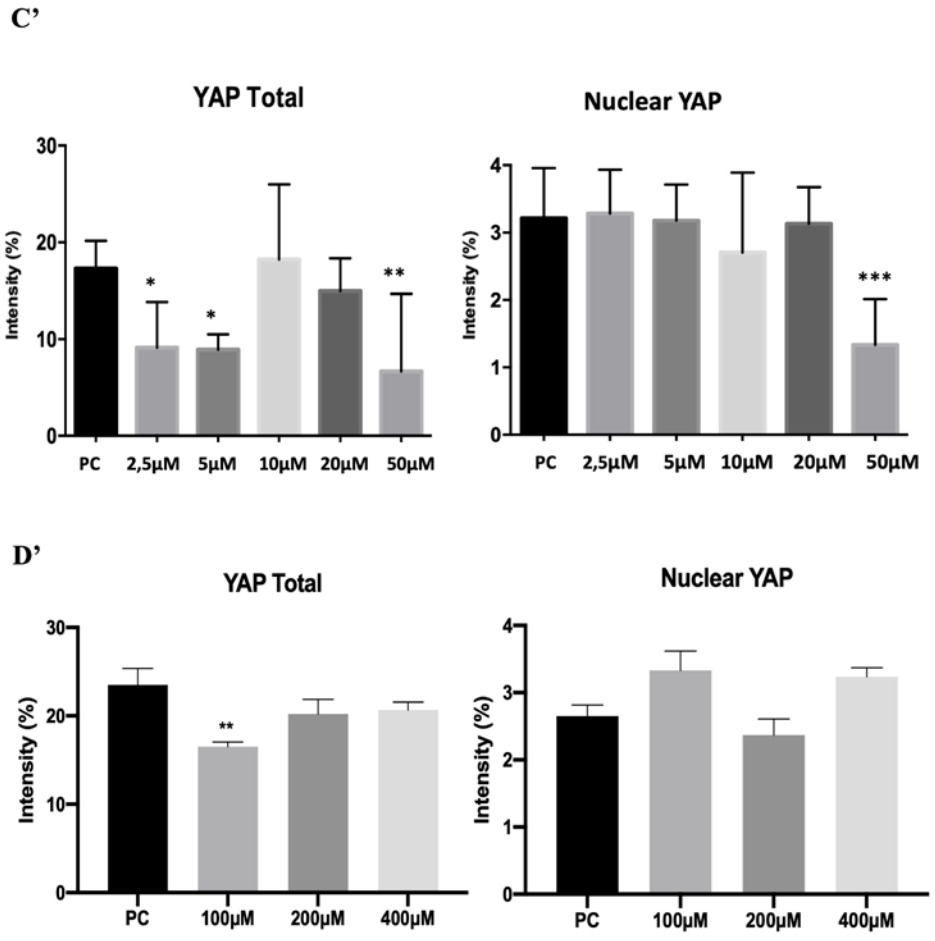

Fig 4.3.18. Comparison of c-Abl and YAP shuttling between cytoplasm and nucleus at all H_2O_2 doses. **(A)** Expression of c-Abl in GCs treated with 2,5µM, 5µM, 10µM, 20µM and 50µM H_2O_2 at 20X objective. **(B)** Expression of c-Abl in GCs treated with 100µM, 200µM and 400µM H_2O_2 at 20X objective. **(A')** Total and nuclear fluorescence intensity ratios of c-Abl in GCs treated with 2,5µM, 5µM, 10µM, 20µM and 50µM H_2O_2. **(B')** Total and nuclear fluorescence intensity ratios of c-Abl in GCs treated with 100µM, 200µM and 400µM H_2O_2. **(C)** Expression of YAP in GCs treated with 2,5µM, 5µM, 10µM, 20µM and 50µM H_2O_2 at 20X objective. **(D)** Expression of YAP in GCs treated with 100µM, 200µM and 400µM H_2O_2 at 20X objective. **(C')** Total and nuclear fluorescence intensity ratios of YAP in GCs treated with 2,5µM, 5µM, 10µM, 20µM and 50µM H_2O_2. **(D')** Total and nuclear fluorescence intensity ratios of YAP in GCs treated with 100µM, 200µM and 400µM H_2O_2.

4.4. Immunoblotting Assay Data

After GCs were treated with 2,5μM, 5μM, 10μM, 20μM, 50μM, 100μM, 200μM and 400 μM H_2O_2 for 24 hours, cells were collected and pellets were immunoblotted to confirm the changes in the c-Abl, YAP, p73 and pHH3 expression at protein level.

4.4.1. Quantification of c-Abl Protein Levels by Normalization Against β-actin

Treated and non-treated granulosa cells were immunoblotted for c-Abl and phospho c-Abl antibodies in the presence of β-actin control protein. According to the results, c-Abl showed band in 135 kDa as expected. Expression levels of c-Abl and phospho c-Abl were quantified by normalization against β-actin. According to the quantification data, protein level of c-Abl down-regulated in GCs treated with 100μM and 200μM H_2O_2 in accordance to control group indicating non-treated granulosa cells. On the other hand, it was observed that the protein level of c-Abl slightly increased in GCs treated with 10μM, 20μM and 50μM H_2O_2 in compare with control group. The most important increase in the protein level of c-Abl was observed in the GCs treated with 2,5μM, 5μM and 400μM H_2O_2 compared to control group. Overall, no increase or decrease in the protein level of c-Abl was observed, dependent on increasing hydrogen peroxide concentrations. **(Fig 4.1.1.1. A and B)**

According to the obtained data, phosphorylated form of c-Abl showed band in approximately 210 kDa. According to the quantification data, protein level of phosphorylated c-Abl clearly down-regulated in GCs treated with 2,5μM, 5μM, 10μM, 20μM and 50μM H_2O_2 in compare with control group. Protein level of phosphorylated c-Abl showed slight decreasing in GCs treated with 100μM H_2O_2 in accordance to control group. On the other hand, protein level exerted clear increasing in GCs treated with 200μM and 400μM H_2O_2 in compare with control group. **(Fig 4.1.1.1. C and D)**

A

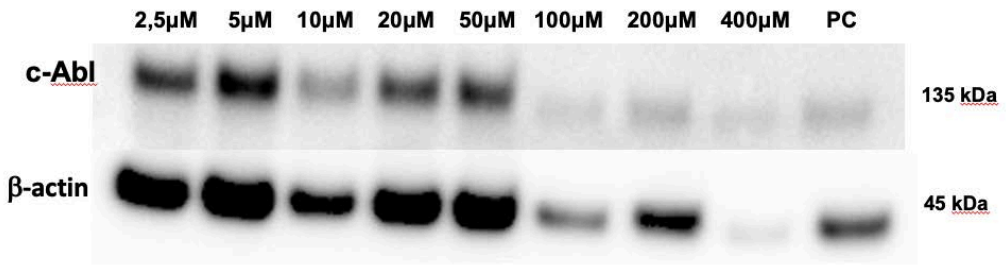
2,5μM
5μM
10μM
20μM
50μM
100μM
200μM
400μM
PC
c-Abl
135 kDa
β-actin
45 kDa

B

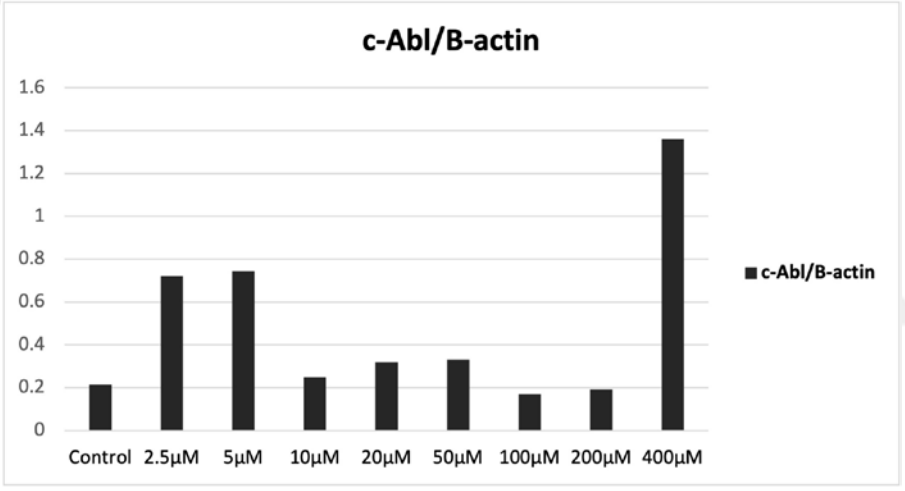
c-Abl/B-actin
1.6
1.4
1.2
1
0.8
0.6
0.4
0.2
0
Control
2.5μM
5μM
10μM
20μM
50μM
100μM
200μM
400μM
c-Abl/B-actin

C

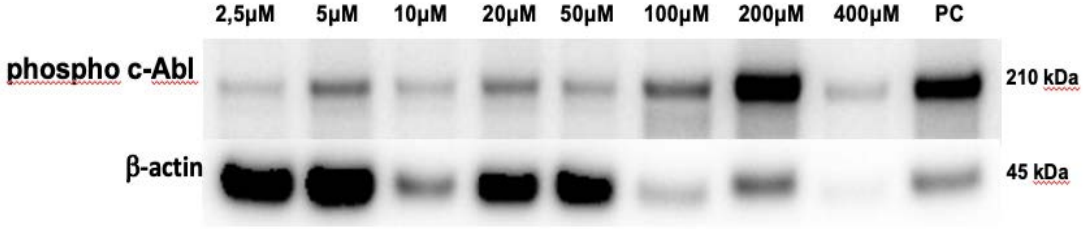
2,5μM
5μM
10μM
20μM
50μM
100μM
200μM
400μM
PC
phospho c-Abl
210 kDa
β-actin
45 kDa

D

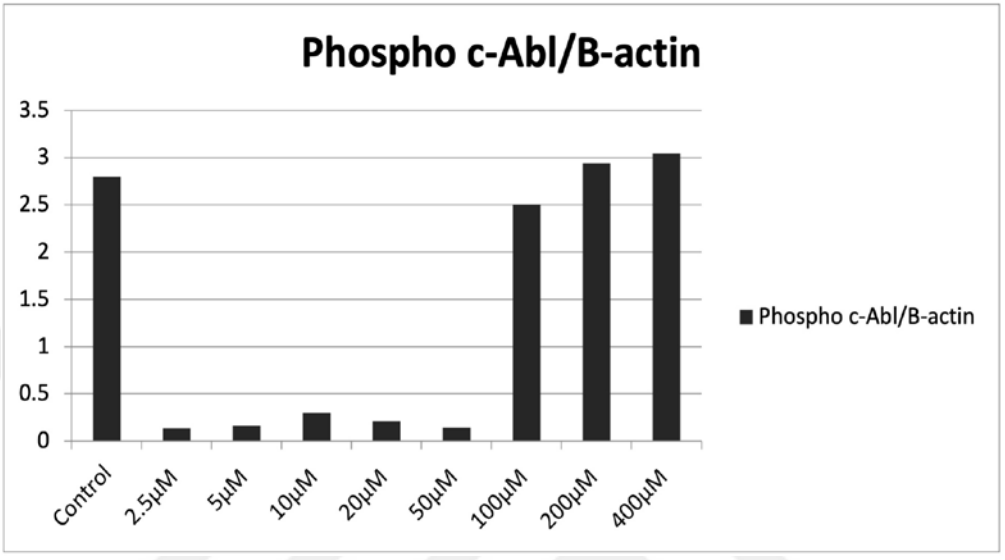

Fig 4.1.1.1. Immunoblotting Assay Data of c-Abl. **(A)** Gel image showing the expression of c-Abl at protein levels in cultured GCs treated with increasing hydrogen peroxide concentrations. **(B)** Quantification of c-Abl protein levels normalized by β-actin. **(C)** Gel image showing the expression of phosphorylated c-Abl at protein levels in cultured GCs treated with increasing hydrogen peroxide concentrations. **(D)** Quantification of phosphorylated c-Abl protein levels normalized by β-actin.

4.4.2. Quantification of YAP Protein Levels by Normalization Against β-actin

Hydrogen peroxide- treated and non-treated GCs were also immunoblotted for YAP and phospho-YAP antibodies in the presence of internal β-actin control protein. According to the results, YAP exerted band in approximately 65 kDa. After the normalization against to β-actin control protein, protein levels of YAP and phosphorylated YAP were quantified. According to the quantification data, YAP exerted decreased levels of protein in GCs treated with 5μM, 10μM, 20μM, 50μM and 200μM

H_2O_2 in compare with control group. On the other hand, it was observed that the protein level of YAP slightly increased in GCs 100µM H_2O_2 in compare with control group. In addition to this, the most significant incrrement in the protein level of YAP was observed in the GCs treated with 2,5µM and 400µM H_2O_2 compared to control group. **(Fig 4.4.2.1. A and B)**

According to the obtained data, phosphorylated form of YAP exerted band in approximately 65 kDa. As a result of a quantification, protein level of phosphorylated YAP slightly decreased in GCs treated with 2,5µM, 5µM, 10µM, 20µM, 50µM and 200µM H_2O_2 in accordance to control group. Protein levels of phosphorylated YAP exerted slight increment in GCs treated with 100µM H_2O_2 in accordance to control group. Additionally, there was no protein level of phosphorylated YAP in GCs treated with 400µM H_2O_2 in compare with control group. **(Fig 4.4.2.1. C and D)**

A

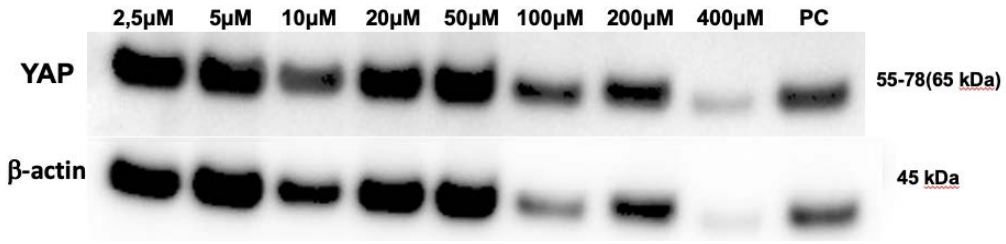

B

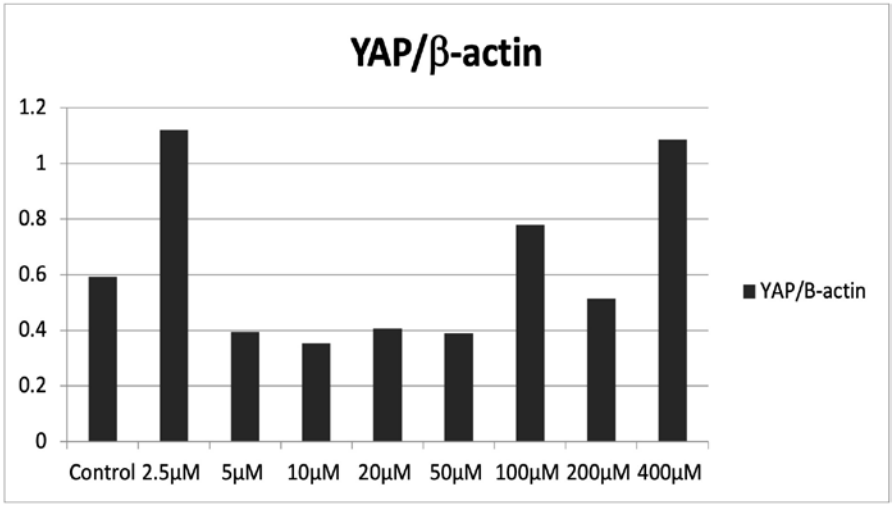

C

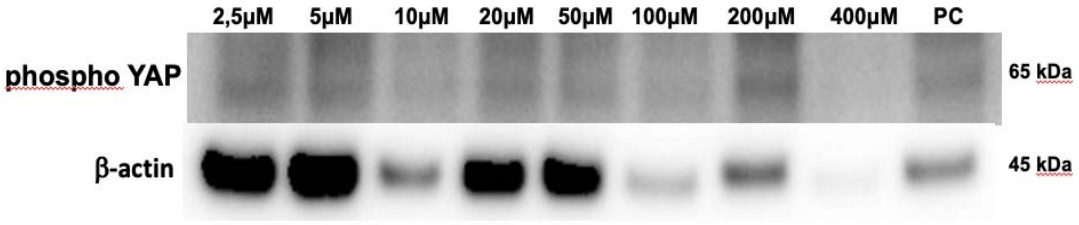

D

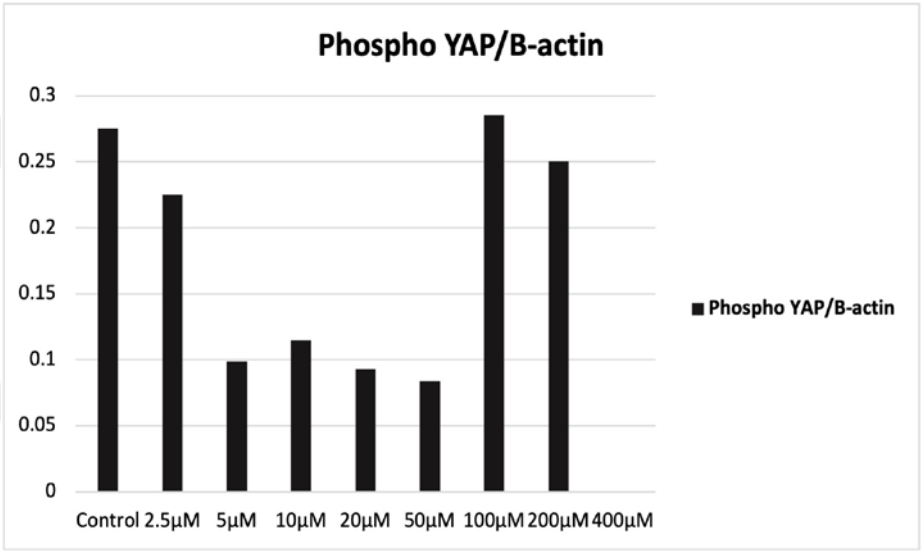

Fig 4.4.2.1. Immunoblotting Assay Data of YAP. **(**A) Gel image showing the expression of YAP at protein levels in cultured GCs treated with increasing hydrogen peroxide concentrations. (B) Quantification of YAP protein levels normalized by β-actin. (C) Gel image showing the expression of phosphorylated YAP at protein levels in cultured GCs treated with increasing hydrogen peroxide concentrations. (D) Quantification of phosphorylated YAP protein levels normalized by β-actin.

4.4.3. Quantification of p73 Protein Levels by Normalization Against β-actin

Hydrogen peroxide-treated and non-treated GCs were also immunoblotted for p73 antibody in the presence of internal β-actin control protein. According to the obtained immunoblotting results, p73 showed band in approximately 80 kDa. According to the quantification data, protein levels of p73 showed slight decrement in GCs treated with 100μM H_2O_2 in compare with control group. Unlike this, it was obvious that the protein levels of p73 slightly increased in GCs treated with 5μM, 10μM, 20μM, 50μM, 200μM and 400 μM H_2O_2 in compare with control group. Additionally, the most significant increment in the protein levels of p73 was observed in the GCs treated with 2,5μM H_2O_2 compared to control group. **(Fig 4.4.3.1. A and B)**

A

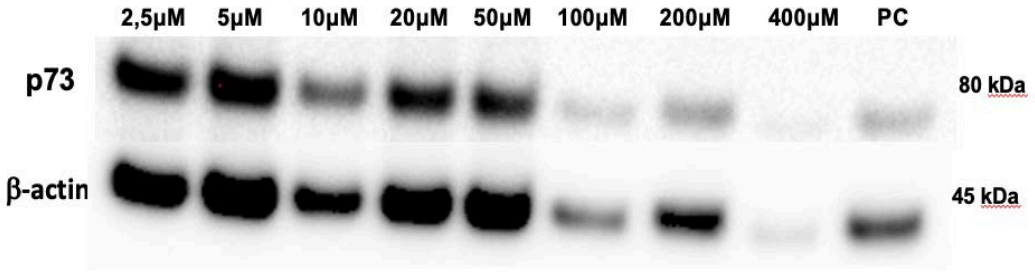

B

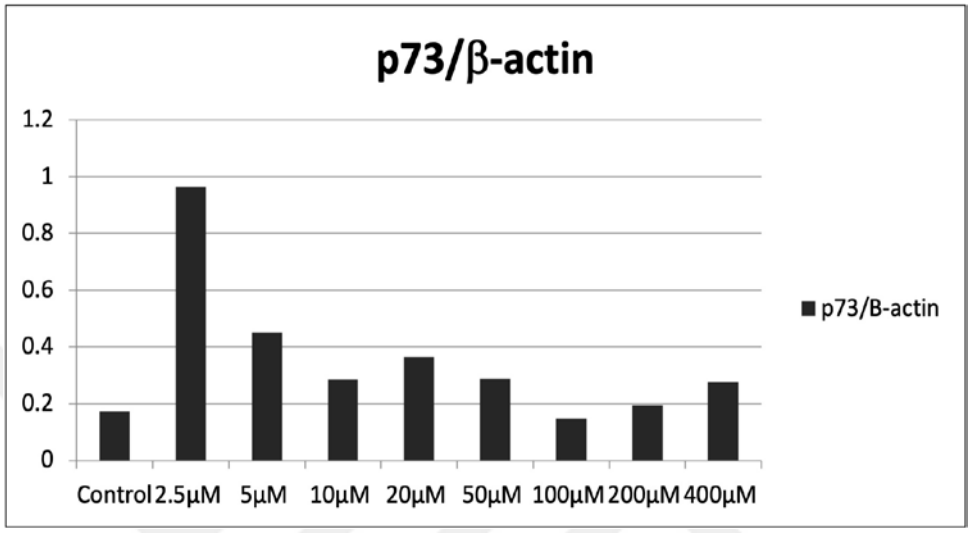

Fig 4.4.3.1. Immunoblotting Assay Data of p73. (A) Gel image showing the expression of p73 at protein levels in cultured GCs treated with increasing hydrogen peroxide concentrations. (B) Quantification of p73 protein levels normalized by β-actin.

4.4.4. Quantification of pHH3 Protein Levels by Normalization Against β-actin

Hydrogen peroxide-treated and non-treated GCs were also immunoblotted for phospho Histone H3 antibody in the presence of β-actin control protein. According to the obtained immunoblotting results, pHH3 exerted band in approximately 17 kDa. According to the quantification data, protein levels of pHH3 showed slight decrement in GCs treated with 100μM and 200μM H_2O_2 in accordance to control group. Unlike this, it was observed that the protein levels of p73 slightly increased in GCs treated with 5μM, 10μM, 20μM, 50μM and 400μM H_2O_2 and in compare with control group. Also, the protein levels of pHH3 in GCs treated with 5μM, 10μM, 20μM, 50μM and 400 μM H_2O_2 were approximately similar. Lastly, the most significant increment in the protein levels of pHH3 was observed in the GCs treated with 2,5μM H_2O_2 in accordance to control group. **(Fig 4.4.4.1. A and B)**

A

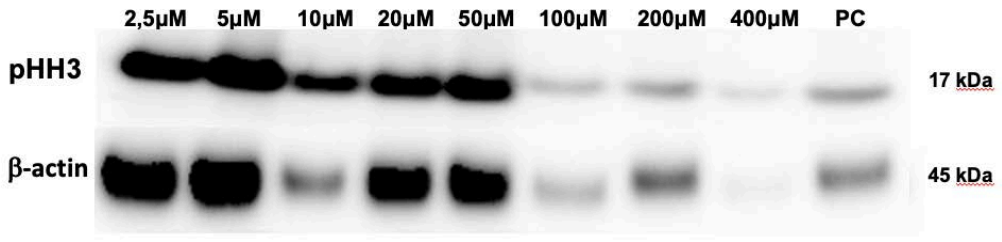

B

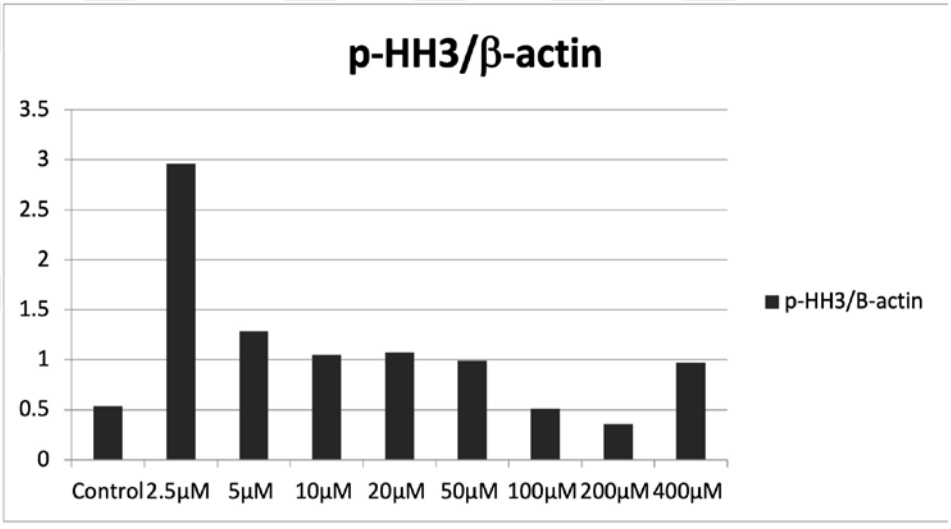

Figure 4.4.4.1. Immunoblotting Assay Data of phospho histone H3. **(A)** Gel image showing the expression of pHH3 at protein levels in cultured GCs treated with increasing hydrogen peroxide concentrations. **(B)** Quantification of pHH3 protein levels normalized by β-actin.

4.4.5. Quantification YAP Protein Levels by Normalization Against p-HH3

To determine the expression of nuclear YAP at protein level, total YAP protein levels were normalized by p-HH3. According to the quantification data, protein levels of nuclear YAP showed decrement in GCs treated with 2.5µM, 5µM, 10µM, 20µM and

50μM H_2O_2 in accordance to control group. On the other hand, it was obvious that the protein levels of nuclear YAP increased in GCs treated with 100μM and 200μM H_2O_2 in compare with control group. Also, the protein level of nuclear YAP in GCs treated with 400 μM H_2O_2 and control group was approximately similar. **(Fig 4.4.5.1. A and B)**

A

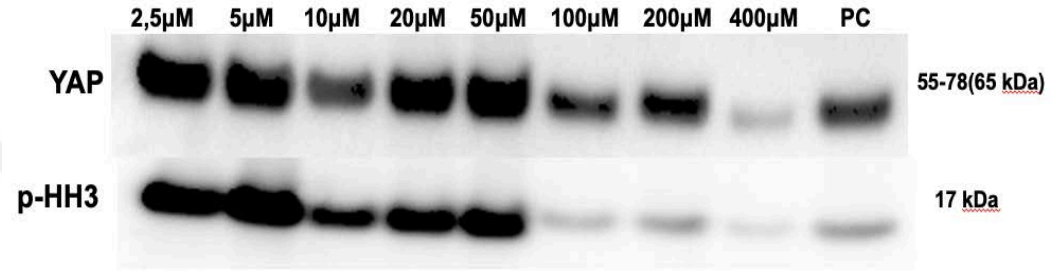

B

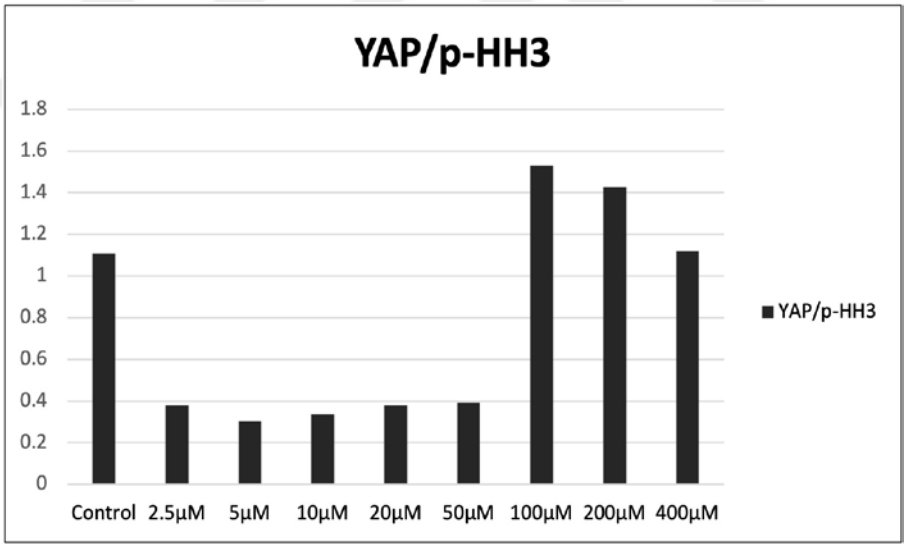

Figure 4.4.5.1. Immunoblotting Assay Data of nuclear YAP. **(A)** Gel image showing the expression of nuclear YAP at protein levels in cultured GCs treated with increasing hydrogen peroxide concentrations. **(B)** Quantification of YAP protein levels normalized by p-HH3.

4.4.6. Quantification c-Abl Protein Levels by Normalization Against p-HH3

To determine the expression of nuclear c-Abl at protein level, total c-Abl protein levels were normalized by p-HH3. According to the quantification data, protein levels of nuclear c-Abl exerted slight decrement in GCs treated with 2.5µM, 5µM, 10µM, 20µM, 50µM and 100µM H_2O_2 in accordance to control group. Unlike this, it was observed that the protein levels of nuclear c-Abl slightly increased in GCs treated with 200µM H_2O_2 in compare with control group. Also, the protein level of nuclear c-Abl significantly increased in GCs treated with 400 µM H_2O_2 in compare with control group. **(Fig 4.4.6.1. A and B)**

A

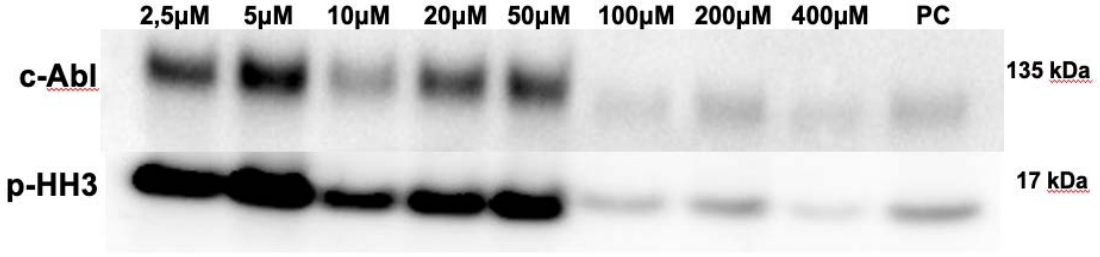

B

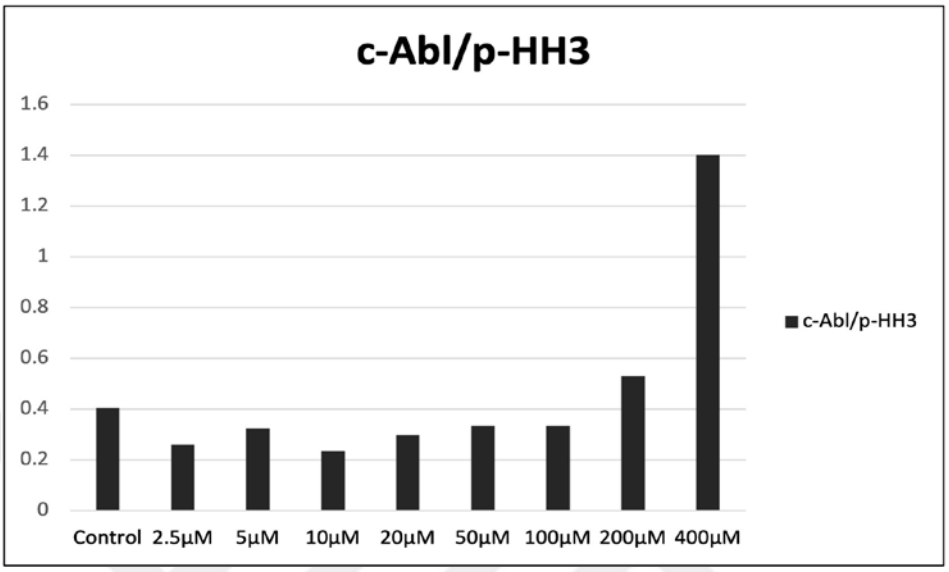

Figure 4.4.6.1. Immunoblotting Assay Data of nuclear c-Abl. **(A)** Gel image showing the expression of nuclear c-Abl at protein levels in cultured GCs treated with increasing hydrogen peroxide concentrations. **(B)** Quantification of c-Abl protein levels normalized by p-HH3.

5. DISCUSSION AND CONCLUSION

GCs are the crucial cell type in the ovarian tissue. These cells provide the physical support and microenvironment necessary for the development and maturation of oocyte. GC proliferation and function are very critical for a healthy follicle development, maturation, ovulation and atresia.

c-Abl regulates the different cellular functions induced by DNA damage. Addition to this, it also functioning in inhibiton of cell growth, cell adhesion and cell migration. In addition to this, cytoplasmic c-Abl performs crucial roles in F-actin dynamics and morphogenesis (112). Activation of cytoplasmic c-Abl functioning in cellular responses stimulated by growth factors, consisting the promotion of DNA synthesis, F-actin assembly and receptor signalling. Previous studies showed that c-Abl have a negative role during proliferation of cells (113,114). However, c-Abl appears to possess antagonistic role, depending on its sub-cellular localization. For instance, G1 phase block of cell cycle is induced by nuclear c-Abl while mitogenesis is supported by cytoplasmic c-Abl. (115,116). We showed before that c-Abl play curicial roles during prenatal and postnatal gonadal development (117) mouse embriyonal and placental development (118). We also showed that c-Abl has important role in mouse GCs *in vivo* and *in vitro* (119).

YAP is a proto-oncoprotein which located in the cell cytoplasm. In cytoplasm it is in an inactivated form. When activated, it translocated to the nucleus. Then, the transcription of survival genes is activated (120). YAP and c-Abl have been known in a relationship which c-Abl alter the function of YAP from oncogenic form to tumor supressor form. Under the DNA damage, c-Abl become activated and in this way YAP and p73 are phosphorylated by the c-Abl. At the end of this process, pro-apoptotic genes are induced and death axis is stimulated (121). Additionally, c-Abl was present in the ionizing radiation signalling pathway which leading to occurence of apoptosis and p73 has been known as a crucial downstream effector in ionizing irradiation pathway (84).

In this study, we aimed to define c-Abl and YAP expression in response to H_2O_2-induced DNA damage in cultured GCs First of all, we defined and confirmed the expression patterns of c-Abl, YAP, phospho c-Abl, phospho YAP and p73 by immunofluorescence staining on ovarian tissue sections. Then, GCs isolated from mouse ovaries were cultured with different concentrations of H_2O_2 for 24 hours. Then, to show

the effect of H_2O_2 on the expression of c-Abl and YAP in GCs, double immunofluorescence staining was performed. Afterwards, immunoblotting assay was conducted to show the protein levels of c-Abl, YAP, phospho c-Abl, phospho YAP, p73 and pHH3.

Firstly, ovarian sections were stained to get a rough idea about the role of c-Abl, YAP, phosphorylated forms and p73 in different stages of ovarian follicles. According to our results, YAP mostly showed localization in the cytoplasm of oocytes instead of nucleus while it also showed expression in granulosa cells and theca externa. Similarly, Abbassi et. al have been demonstrated that YAP was expressed in all stages of oocyte development and it was generally localized in the cytoplasm and excluded from the nucleus (122). In consistent with our results, Xiangmin and his co-workers have been reported that YAP1 showed the expression in the GCs and it has crucial function in the proliferation, differentiation and survival of GCs. They also showed that YAP1 was localized in the nucleus of granulosa cells in the adult human follicles that were from primary stage to pre-ovulatory stage (83). According to the results, when the localization of c-Abl was evaluated, it was found that while it was generally localized in the cytoplasm of oocytes, it was localized very weak in the nucleus and also in granulosa cells and theca cells. Interestingly, it was not expressed in the oocyte of antral follicles. Similarly, except antral follicles, we before indicated that the c-Abl was expressed in the granulosa cells and oocytes in the primordial, primary, pre-antral and large follicles (119). While p73 was also expressed in oocytes, it was also expressed in granulosa and theca cells which means it may have been important role during follicular development and oocyte maturation. Similarly, Santos and his colleagues showed p73 localization in the granulosa cells and they suggested that p73 was necessary for ovarian follicular development (123).

To determine the shuttling of c-Abl and YAP between the cell nucleus and cytoplasm in response to oxidative stress induced DNA damage, cultured GCs were treated with different concentrations of H_2O_2 which were 2,5μM, 5μM, 10μM, 20μM, 50μM. H_2O_2 has been known as one of the major reactive oxygen species (ROS). It has been known that the granulosa cells are highly sensitive cells to reactive oxygen species such as H_2O_2 which induces the GCs apoptosis. (124).

According to the confocal representative images, YAP exerted shuttling between the nucleus and cytoplasm of granulosa cells in applied H_2O_2 concentrations. YAP was mostly localized in the nuclei of granulosa cells in the groups treated with 2.5 µM and 5 µM H_2O_2. In the group treated with 10 µM H_2O_2, it showed both cytoplasmic and nuclear localization. Moreover, YAP was localized in the nucleus of the granulosa cells at 20 µM H_2O_2, while it exhibited cytoplasmic localization in the group treated with 50 µM. These results provide strong evidence that the YAP was in generally active form which means it was localized in the nucleus of cells in all concentrations except 50 µM. According to the Michele and his colleagues, contact of cells and cell density affected the localization of YAP. When cells were seeded at low density, higher nuclear YAP expression was observed (125). Therefore, the contact of the cells with each other and the low seeding density of the granulosa cells might also have affected the high nuclear localization of YAP in granulosa cells regardless of H_2O_2 concentrations. In 2.5 µM and 5 µM H_2O_2 concentrations, YAP showed both nuclear and cytoplasmic expression. In addition to this, in 50 µM of H_2O_2 concentration, YAP showed mostly cytoplasmic localization instead of nuclear localization. Covalent modification might have lead to occurence of this cytoplasmic localization of YAP at 50 µM of H_2O_2 concentration. Because, when the upstream kinases of Hippo signalling pathway activated, YAP is phosphorylated. In this way, YAP change its location, it is translocated from the nucleus to the cytoplasm. This translocation leading to inhibition of its activity (43).

Similarly, c-Abl was also localized in both nucleus and cytoplasm of GCs treated with 2,5µM, 5µM, 10µM, 20µM, 50µM H_2O_2 concentrations. c-Abl was mostly localized in the nucleus of GCs in the groups treated with 2.5 µM and 5 µM H_2O_2 concentrations. Sun and coworkers suggested that cytoplasmic form but not nuclear form of the c-Abl was activated in response to H_2O_2 (126). Since c-Abl was activated against to H_2O_2, we expected that the activation of cytoplasmic c-Abl would also increase increasing H_2O_2 concentrations in GCs. As expected, nuclear localization of c-Abl decreased in GCs treated with 10 µM H_2O_2. Moreover, at the 20µM H_2O_2 group, although c-Abl was localized in both nucleus and cytoplasm, it exhibited more intense expression in the cytoplasm. Interestingly, c-Abl was not expressed GCs treated with 50 µM H_2O_2.

In consistent with Sun and co-workers, the nuclear localization of c-Abl decreased 5μM, 10μM, 20μM and 50μM H_2O_2 concentrations in accordance to control which means c-Abl can be activated in response to oxidative stress induced by increased H_2O_2 concentrations. According to the Sun and coworkers, releasing of mitochondrial cytochrome c is induced by the H_2O_2 (126). Thus, mitochondrial cytochrome-c which participate to the life-providing role of ATP production may have been released from mitochondria of GCs treated with 5μM ,10μM and 20μM H_2O_2 to the cytosol due to receiving apoptotic stimulus by oxidative stress. In this way, proapoptotic pathways may have been trigerred in response to H_2O_2 treatment in mouse GCs.

Subsequently, GCs were cultured again and treated with higher doses since the c-Abl did not show any expression in the 50μM group. For this time, GCs treated with 100 μM, 200 μM and 400 μM H_2O_2 concentrations. According to the results, nuclear localization of c-Abl decreased significantly in treated GCs in compare with positive control group although nuclear localization of c-Abl increased dependent on rising H_2O_2 concentrations which might be showed that the cytoplasmic c-Abl was activated by H_2O_2 treatment. This results provide convincing evidence that c-Abl might respond to these concentrations and cytoplasmic form of c-Abl was activated by high concentrations of H_2O_2. Additionally, these results provide strong evidence that the reason c-Abl was not expressed in the 50 μM group was not dependent on hydrogen peroxide dose. In addition to these, YAP showed mostly nuclear localization in the GCs treated with 100 μM, 200 μM and 400 μM H_2O_2 concentrations. The production of ROS is generated during normal cellular metabolism, as a consequence of this procedure, ROS give damage to DNA and proteins (127,128). Beside DNA damage, ROS also induce apoptosis. The study has been shown that c-Abl phosphorylates protein kinase C (PKC) in H_2O_2 treated cells (129). The results demonstrate that the only cytoplasmic form of c-Abl is activated in the cellular response to H_2O_2. Another study showed that H_2O_2 induces mitochondrial cytochrome c release and apoptosis by a c-Abl-dependent mechanism (126).

In our study, we aimed to cause DNA damage by creating stress with H_2O_2 in granulosa cells and to reveal the relationship between c-Abl and YAP. To determine whether c-Abl is activated by H_2O_2, granulosa cells exposed to H_2O_2 were subjected to immunoflourescence and immunoblotting assay. Overall, H_2O_2 caused increased c-Abl

cytoplasmic entry in granulosa cells. Oxidative stress is known to activate c-Abl kinase activity (126) and c-Abl/p73 proapoptotic pathway. Our next objective was to determine whether oxidative stress induces YAP expression. In other words, we aimed to determine if cytoplasmic form of c-Abl phosphorylates YAP or not, since c-Abl phosphorylates YAP in response to DNA damage in cancer cells. According to the immunofluorescence and immunoblotting assay results, nuclear YAP did not exert significant decrement in H_2O_2 treated GCs in compare with control group. According to the immunoblotting asay data, H_2O_2 treatment decreased the protein level of phosphorylated YAP which meant that YAP was not phosphorylated enough by cytoplasmic c-Abl depending on increasing H_2O_2 treatment. Briefly, cytoplasmic c-Abl did not increase the phosphorylation of YAP depending on H_2O_2 treatment. The reason of this situation might that cytoplasmic c-Abl which is activated in response to oxidative stress in healthy and normal GCs may not be able to adequately phosphorylate YAP. This may be because cytoplasmic c-Abl signalling does not behave similarly in normal and cancer cells, has different functions and is involved in different mechanisms (116).

According to the findings, it was observed that the intracellular distribution of c-Abl decided the area of the response to various type of stresses. Nevertheless, since ROS leads to DNA damage as other cellular members, it could be thought that cells evolved by maintaining a nearly the same response to both genotoxic and oxidative stress (126).

Although our results exerted that c-Abl was displaced between the nucleus and cytoplasm due to H_2O_2, these data did not eliminate the opportunity that localization of c-Abl might also be controlled by mechanisms of retention. For instance, binding with F-actin might prevent nuclear translocation. Additionally, when c-Abl is recruited by DNA binding complexes, this situation might also inhibit nuclear export (130). It was proposed that c-Abl contributes to p73-YAP-dependent cytoskeletal remodeling of GCs and provide a role in GCs for cytoskeletal remodeling induced by H_2O_2.

As a result of this thesis study, our findings exerted that oxidative stress in GCs stimulated the cytoplasmic c-Abl activity, leading to preserved nuclear YAP and increased p73 protein expression through p73/YAP proapoptotic pathway. We suggested that identification of the signaling link between c-Abl and YAP in healthy cells may fill

the gap between oxidative stress and c-Abl/YAP activation-dependent GC proliferation, migration and apoptosis, and also points to new roles of both kinases.

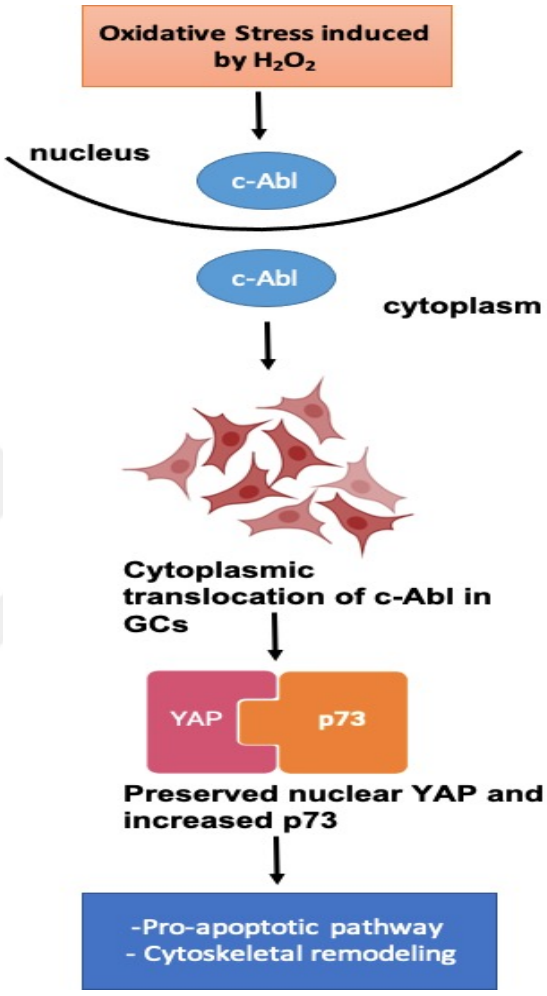

Figure 5.1. Possible relationship between c-Abl and YAP through p73 in response to oxidative stress induced-DNA damage in mouse GCs.

During the follicular development process, the oocyte and GCs show bidirectional communication. GCs contribute to the growth of the follicle with their functions of proliferation, differentiation and steroidogenesis. Also, GCs provide maturation of the oocyte which include nuclear, cytoplasmic, membranous and zona pellucida maturation. Therefore, GCs play very important role in development and ovulation of a healthy follicle with mature oocyte. Within the scope of all these informations, we have been tried to reveal the effect of H_2O_2 on YAP which also plays a role in cell fate, and c-Abl which

interacts with YAP in case of DNA damage, by providing a basis for the formation of oxidative stress in GCs. Overall, this thesis study is the first one in literature that indicates the expression patterns of c-Abl and YAP in GCs under oxidative stress. In the future studies of this thesis, by conducting *in vitro* siRNA-mediated knock-down model, the interaction between c-Abl and YAP under oxidative stress in GCs can be elucidated in detailed molecular mechanism.

6.REFERENCES

1) Plewes MR, Hou X, Zhang P, Wood J, Cupp A and Davis JS. Yes-associated protein (YAP) is required in maintaining normal ovarian follicle development and function. *bioRxiv*, 2018; 406256.
2) Sun T and Diaz FJ. Ovulatory signals alter granulosa cell behavior through YAP1 signaling. *Reproductive Biology and Endocrinology*, 2019b;17: 113.
3) Rouleau GA, Merel P, Lutchman M, et al. Alteration in a new gene encoding a putative membrane-organizing protein causes neuro-fibromatosis type 2. *Nature*, 1993; 363: 515-521.
4) St John MA, Tao W, Fei X, et al. Mice deficient of Lats1 develop soft-tissue sarcomas, ovarian tumours and pituitary dysfunction. *Nat Genet*, 1999; 21: 182-186.
5) Sun T, Pepling ME and Diaz FJ. Lats1 deletion causes increased germ cell apoptosis and follicular cysts in mouse ovaries. *Biology of reproduction*, 2015; 93:22.
6) Keshet R, Adler J, Ricardo Lax I, Shanzer M, Porat Z and Reuven N. c-Abl antagonizes the YAP oncogenic function. 2015a; 22: 935-945.
7) Keshet R, Reuven N and Shaul Y. c-Abl forces YAP to switch sides. *Molecular & cellular oncology*, 2015c; 2: e995006.
8) Hsueh AJ, Kawamura K, Cheng Y and Fauser BC. Intraovarian control of early folliculogenesis. *Endocrine reviews*, 2015; 36: 1-24.
9) Stocco C, Telleria C and Gibori G. The molecular control of corpus luteum formation, function, and regression. *Endocrine reviews*, 2007; 28: 117-149.
10) Emily G and Heba M. Anatomy, Abdomen and Pelvis, Ovary. *StatPearls* [serial online] 2021, Accessed 15.10.21, https://pubmed.ncbi.nlm.nih.gov/31424771/.
11) Chaudhry S and Chaudhry K. Anatomy, Abdomen and Pelvis, Uterus Round Ligament. [serialonline]2021.Accessed14.10.2021,https://www.ncbi.nlm.nih.gov/books/NBK499970/.
12) Morgan C, Sneha S and Megan B. Anatomy, Abdomen and Pelvis, Broad Ligaments. [serial online] 2021, Accessed 15.10. 2021, https://pubmed.ncbi.nlm.nih.gov/29763118/.
13) Marieb, E, Hoehn K, ed. *Anatomy & Physiology*. 3rd ed. Pearson Benjamin Cumming: New York; 2008.
14) Kierszenbaum A and Tres L. *Histology and Cell Biology*. Elsevier Inc: St. Louis; 2020.

15) Mescher A, ed. *Junqueira's Basic Histology Text and Atlas*. 13th ed. McGraw-Hill Education: New York; 2013.
16) Kierszenbaum AL. Cell-cycle regulation and mammalian gametogenesis: a lesson from the unexpected. *Molecular reproduction and development*, 2006; 73: 939-942.
17) Mayo K, Jameson L and Woodruff TK. Eggs in the nest. *Endocrinology*, 2007; 148: 3577-3579.
18) Mhawi AJ, Kanka J and Motlík J. Follicle and oocyte growth in early postnatal calves: cytochemical, autoradiographical and electron microscopical studies. *Reproduction, nutrition, development*,1991; 31:115-126.
19) Albertini DF, Combelles CM, Benecchi E and Carabatsos MJ. Cellular basis for paracrine regulation of ovarian follicle development. *Reproduction*, 2001; 121: 647-653.
20) Wigglesworth K, Lee KB, Emori C, Sugiura K and Eppig JJ. Transcriptomic diversification of developing cumulus and mural granulosa cells in mouse ovarian follicles. *Biology of reproduction*, 2015; 92, 23.
21) Jaffe LA. and Egbert JR. Regulation of mammalian oocyte meiosis by intercellular communication within the ovarian follicle. *Annual review of physiology*, 2017; 79: 237-260.
22) Alam MH and Miyano T. Interaction between growing oocytes and granulosa cells in vitro. 2020; 19: 13-23.
23) Bioxeocotobade.pbworks.com. *bioxeocotobade [licensed for non-commercial use only] / The ovarian and uterine cycles*. [serial online] 2012, Accessed 15.10.21, http://bioxeocotobade.pbworks.com/w/page/51298509/The%20ovarian%20and%20uterine%20cycles
24) Canipari R. Oocyte-granulosa cell interactions. *Human reproduction*, 2000; 6: 279-289.
25) Geissler EN, McFarland EC and Russell ES. Analysis of pleiotropism at the dominant white-spotting (W) locus of the house mouse: a description of ten new W alleles. *Genetics*, 1981; 97: 337-361.
26) Eppig JJ, Wigglesworth K, Pendola F and Hirao Y. Murine oocytes suppress expression of luteinizing hormone receptor messenger ribonucleic acid by granulosa cells. *Biology of reproduction*, 1997; 56: 976-984.
27) Anderson E and Albertini DF. Gap junctions between the oocyte and companion follicle cells in the mammalian ovary. *The Journal of cell biology*, 1976; 71: 680-686.

28) Eppig JJ. Intercommunication between mammalian oocytes and companion somatic cells. *BioEssays: news and reviews in molecular, cellular and developmental biology*, 1991; 13: 569-574.
29) Yan C, Wang P, DeMayo J, et al. Synergistic roles of bone morphogenetic protein 15 and growth differentiation factor 9 in ovarian function. *Molecular endocrinology (Baltimore, Md.)*, 2001;15: 854-866.
30) Mora JM, Fenwick MA, Castle L, et al. Characterization and significance of adhesion and junction-related proteins in mouse ovarian follicles. *Biology of reproduction*, 2012; 86(153):151-114.
31) Wassarman PM and Litscher ES. Biogenesis of the mouse egg's extracellular coat, the zona pellucida. *Current topics in developmental biology*, 2013;102: 243-266.
32) Chiquoine AD. The development of the zona pellucida of the mammalian ovum. *The American journal of anatomy*, 1960;106:149-169.
33) Clarke HJ. Regulation of germ cell development by intercellular signaling in the mammalian ovarian follicle. Wiley interdisciplinary reviews. *Developmental biology*, 2018. p. 7.
34) el-Fouly MA, Cook B, Nekola M and Nalbandov AV. Role of the ovum in follicular luteinization. *Endocrinology*, 1970; 87: 286-293.
35) Liu C, Peng J, Matzuk MM and Yao HH. Lineage specification of ovarian theca cells requires multicellular interactions via oocyte and granulosa cells. *Nature communications*, 2015; 6: 6934.
36) McGrath SA, Esquela AF and Lee SJ. Oocyte-specific expression of growth/differentiation factor-9. *Molecular endocrinology (Baltimore, Md.)*, 1995; 9: 131-136.
37) Otsuka F, McTavish KJ and Shimasaki S. Integral role of GDF-9 and BMP-15 in ovarian function. *Molecular reproduction and development*, 2011; 78: 9-21.
38) Chang HM, Qiao J and Leung PC. Oocyte-somatic cell interactions in the human ovary-novel role of bone morphogenetic proteins and growth differentiation factors. *Human reproduction*, 2016; 23: 1-18.
39) Wu X, Chen L, Brown CA, Yan C and Matzuk MM. Interrelationship of growth differentiation factor 9 and inhibin in early folliculogenesis and ovarian tumorigenesis in mice. *Molecular endocrinology (Baltimore, Md.)*, 2004;18: 1509-1519.
40) Sugiura K, Su YQ, Diaz FJ, et al. Oocyte-derived BMP15 and FGFs cooperate to promote glycolysis in cumulus cells. *Development*, 2007;134: 2593-2603.

41) Su YQ, Sugiura K, Wigglesworth K, et al. Oocyte regulation of metabolic cooperativity between mouse cumulus cells and oocytes: BMP15 and GDF9 control cholesterol biosynthesis in cumulus cells. *Development,* 2008;135: 111-121.

42) Meng Z, Moroishi T and Guan KL. Mechanisms of Hippo pathway regulation. *Genes Dev,* 2016; 30: 1-17.

43) Yu FX and Guan KL. The Hippo pathway: regulators and regulations. *Genes Dev,* 2013;27: 355-371.

44) Boggiano JC, Vanderzalm PJ and Fehon RG. Tao-1 phosphorylates Hippo/MST kinases to regulate the Hippo-Salvador-Warts tumor suppressor pathway. *Developmental cell,* 2011; 21: 888-895.

45) Poon CL, Lin JI, Zhang X and Harvey KF. The sterile 20-like kinase Tao-1 controls tissue growth by regulating the Salvador-Warts-Hippo pathway. *Developmental cell,* 2011; 21: 896-906.

46) Praskova M, Khoklatchev A, Ortiz-Vega S and Avruch J. Regulation of the MST1 kinase by autophosphorylation, by the growth inhibitory proteins, RASSF1 and NORE1, and by Ras. *The Biochemical journal,* 2004; 381: 453-462.

47) Glantschnig H, Rodan GA and Reszka AA. Mapping of MST1 kinase sites of phosphorylation. Activation and autophosphorylation. *The Journal of biological chemistry,* 2002; 277: 42987-42996.

48) Callus BA, Verhagen AM and Vaux D L. (2006) Association of mammalian sterile twenty kinases, Mst1 and Mst2, with hSalvador via C-terminal coiled-coil domains, leads to its stabilization and phosphorylation. *The FEBS journal,* 2006; 273: 4264-4276.

49) Hergovich A, Schmitz D and Hemmings BA. The human tumour suppressor LATS1 is activated by human MOB1 at the membrane. *Biochemical and biophysical research communications,* 2006; 345: 50-58.

50) Yin F, Yu J, Zheng Y, Chen Q, Zhang N and Pan D. Spatial organization of Hippo signaling at the plasma membrane mediated by the tumor suppressor Merlin/NF2. *Cell,* 2013;154: 1342-1355.

51) Chan EH, Nousiainen M, Chalamalasetty RB, Schäfer A, Nigg EA and Silljé HH. The Ste20-like kinase Mst2 activates the human large tumor suppressor kinase Lats1. *Oncogene,* 2005; 24: 2076-2086.

52) Zheng Y, Wang W, Liu B, Deng H, Uster E and Pan D. Identification of happyhour/MAP4K as alternative Hpo/Mst-like kinases in the Hippo kinase cascade. *Developmental cell,* 2015;34: 642-655.

53) Zhao B, Wei X, Li W, et al. Inactivation of YAP oncoprotein by the Hippo pathway is involved in cell contact inhibition and tissue growth control. *Genes & development*, 2007;21: 2747-2761.
54) Liu CY, Zha ZY, Zhou X, et al. The hippo tumor pathway promotes TAZ degradation by phosphorylating a phosphodegron and recruiting the SCF {beta}-TrCP E3 ligase. *The Journal of biological chemistry*, 2010; 285: 37159-37169.
55) Liang N, Zhang C, Dill P, et al. Regulation of YAP by mTOR and autophagy reveals a therapeutic target of tuberous sclerosis complex. *The Journal of experimental medicine*, 2014; 211: 2249-2263.
56) Koontz LM, Liu-Chittenden Y, Yin F, et al. The Hippo effector Yorkie controls normal tissue growth by antagonizing scalloped-mediated default repression. *Developmental cell*, 2013; 25: 388-401.
57) Camargo FD, Gokhale S, Johnnidis JB, et al. (2007) YAP1 increases organ size and expands undifferentiated progenitor cells. *Current biology: CB*, 2007; 17: 2054-2060.
58) Yu FX, Meng Z, Plouffe SW and Guan KL. Hippo pathway regulation of gastrointestinal tissues. *Annual review of physiology*, 2015;77: 201-227.
59) Pan D. The hippo signaling pathway in development and cancer. *Dev Cell*, 2010; 19: 491-505.
60) McClatchey AI and Giovannini M. Membrane organization and tumorigenesis--the NF2 tumor suppressor, Merlin. *Genes & development*, 2005; 19: 2265-2277.
61) Li W, Cooper J, Zhou L, et al. Merlin/NF2 loss-driven tumorigenesis linked to CRL4(DCAF1)-mediated inhibition of the hippo pathway kinases Lats1 and 2 in the nucleus. *Cancer cell*, 2014; 26: 48-60.
62) Zhang N, Bai H, David KK, et al. The Merlin/NF2 tumor suppressor functions through the YAP oncoprotein to regulate tissue homeostasis in mammals. *Dev Cell*, 2010;19: 27-38.
63) Yu J, Zheng Y, Dong J, Klusza S, Deng WM and Pan D. Kibra functions as a tumor suppressor protein that regulates Hippo signaling in conjunction with Merlin and Expanded. *Developmental cell*, 2010;18: 288-299.
64) Saburi S, Hester I, Fischer E, et al. Loss of Fat4 disrupts PCP signaling and oriented cell division and leads to cystic kidney disease. *Nature genetics*, 2008; 40: 1010-1015.
65) Couzens AL, Knight JD, Kean MJ, et al. Protein interaction network of the mammalian Hippo pathway reveals mechanisms of kinase-phosphatase interactions. *Science signaling*, 2013; 6: 302.
66) Zhang L, Tang F, Terracciano L, et al. NDR functions as a physiological YAP1 kinase in the intestinal epithelium. *Current biology*, 2015; 25: 296-305.

67) Tang F, Gill J, Ficht X, et al. The kinases NDR1/2 act downstream of the Hippo homolog MST1 to mediate both egress of thymocytes from the thymus and lymphocyte motility. *Science signaling*, 2015; 8: ra100.

68) Tamaskovic R, Bichsel SJ, Rogniaux H, Stegert MR and Hemmings BA. Mechanism of Ca2+-mediated regulation of NDR protein kinase through autophosphorylation and phosphorylation by an upstream kinase. *The Journal of biological chemistry*, 2003;278: 6710-6718.

69) Bichsel SJ, Tamaskovic R, Stegert MR. and Hemmings BA. Mechanism of activation of NDR (nuclear Dbf2-related) protein kinase by the hMOB1 protein. *The Journal of biological chemistry*, 2004; 279: 35228-35235.

70) Kohler RS, Schmitz D, Cornils H, Hemmings BA and Hergovich A. Differential NDR/LATS interactions with the human MOB family reveal a negative role for human MOB2 in the regulation of human NDR kinases. *Molecular and cellular biology*, 2010; 30: 4507-4520.

71) Barry ER, Morikawa T, Butler BL, et al. Restriction of intestinal stem cell expansion and the regenerative response by YAP. *Nature*, 2013; 493: 106-110.

72) Zhou D, Conrad C, Xia F, et al. Mst1 and Mst2 maintain hepatocyte quiescence and suppress hepatocellular carcinoma development through inactivation of the Yap1 oncogene. *Cancer cell*, 2009;16: 425-438.

73) Zhao B, Ye X, Yu J, et al. TEAD mediates YAP-dependent gene induction and growth control. *Genes Dev*, 2008; 22: 1962-1971.

74) Zhu C, Li L and Zhao B. The regulation and function of YAP transcription co-activator. *Acta biochimica et biophysica Sinica*, 2015;47: 16-28.

75) Skibinski A, Breindel JL, Prat A, et al. The Hippo transducer TAZ interacts with the SWI/SNF complex to regulate breast epithelial lineage commitment. *Cell reports*, 2014; 6: 1059-1072.

76) Kim M, Kim T, Johnson RL and Lim DS. Transcriptional co-repressor function of the hippo pathway transducers YAP and TAZ. *Cell reports*, 2015; 11: 270-282.

77) Valencia-Sama I, Zhao Y, Lai D, Janse van Rensburg HJ, Hao Y and Yang X. Hippo component TAZ functions as a co-repressor and negatively regulates ΔNp63 transcription through TEA domain (TEAD) transcription factor. *The Journal of biological chemistry*, 2015; 290: 16906-16917.

78) Sun T and Diaz FJ. Ovulatory signals alter granulosa cell behavior through YAP1 signaling. *Reproductive Biology and Endocrinology,* 2019a;17: 113.

79) Meignin C, Alvarez-Garcia I, Davis I and Palacios IM.The salvador-warts-hippo pathway is required for epithelial proliferation and axis specification in Drosophila. *Current biology*, 2007; 17: 1871-1878.

80) Sarikaya DP and Extavour CG. The Hippo pathway regulates homeostatic growth of stem cell niche precursors in the Drosophila ovary. *PLoS genetics*, 2015; 11: e1004962.

81) Kawamura K, Cheng Y, Suzuki N, et al. Hippo signaling disruption and Akt stimulation of ovarian follicles for infertility treatment. *Proceedings of the National Academy of Sciences of the United States of America,* 2013; 110: 17474-17479.

82) Cheng Y, Feng Y, Jansson L, et al. Actin polymerization-enhancing drugs promote ovarian follicle growth mediated by the Hippo signaling effector YAP. *FASEB journal,* 2015; 29: 2423-2430.

83) Lv X, He C, Huang C, et al. (2019) Timely expression and activation of YAP1 in granulosa cells is essential for ovarian follicle development. *FASEB journal,* 2019; 33: 10049-10064.

84) Shaul Y. c-Abl: activation and nuclear targets. *Cell death and differentiation*, 2000; 7: 10-16.

85) Wang JY. The capable ABL: what is its biological function? *Molecular and cellular biology*, 2014;34:1188-1197.

86) Kharbanda S, Yuan ZM, Weichselbaum R and Kufe, D. Functional role for the c-Abl protein tyrosine kinase in the cellular response to genotoxic stress. *Biochimica et biophysica acta – Reviews on Cancer*, 1997; 1333: 01-07.

87) Konopka JB and Witte ON. Detection of c-abl tyrosine kinase activity in vitro permits direct comparison of normal and altered abl gene products. *Molecular and cellular biology,* 1985; 5: 3116-3123.

88) Pendergast AM, Muller AJ, Havlik MH, Clark R, McCormick F and Witte ON. Evidence for regulation of the human ABL tyrosine kinase by a cellular inhibitor. *Proceedings of the National Academy of Sciences of the United States of America,* 1991; 88: 5927-5931.

89) Van Etten RA, Jackson P and Baltimore D. The mouse type IV c-abl gene product is a nuclear protein, and activation of transforming ability is associated with cytoplasmic localization. *Cell,* 1989;58: 669-678.

90) Mayer BJ and Baltimore D. Mutagenic analysis of the roles of SH2 and SH3 domains in regulation of the Abl tyrosine kinase. *Molecular and cellular biology*, 1994; 14: 2883-2894.

91) Ren R, Mayer BJ, Cicchetti P and Baltimore D. Identification of a ten-amino acid proline-rich SH3 binding site. *Science*, 1993; 259: 1157-1161.

92) Welch PJ and Wang JY. A C-terminal protein-binding domain in the retinoblastoma protein regulates nuclear c-Abl tyrosine kinase in the cell cycle. *Cell*, 1993; 75: 779-790.

93) Dai Z and Pendergast AM. Abi-2, a novel SH3-containing protein interacts with the c-Abl tyrosine kinase and modulates c-Abl transforming activity. *Genes & development*, 1995; 9: 2569-2582.

94) Shiloh Y. ATM and related protein kinases: safeguarding genome integrity. *Nature reviews*. 2003; 3: 155-168.

95) Baskaran R, Wood LD, Whitaker LL, et al. Ataxia telangiectasia mutant protein activates c-Abl tyrosine kinase in response to ionizing radiation. *Nature*, 1997; 387: 516-519.

96) Shafman T, Khanna KK, Kedar P, et al. Interaction between ATM protein and c-Abl in response to DNA damage. *Nature*, 1997; 387: 520-523.

97) Gong JG, Costanzo A, Yang HQ, et al. The tyrosine kinase c-Abl regulates p73 in apoptotic response to cisplatin-induced DNA damage. *Nature*, 1999; 399: 806-809.

98) Dorsch M and Goff SP. Increased sensitivity to apoptotic stimuli in c-abl-deficient progenitor B-cell lines. *Proc Natl Acad Sci*, 1996; 93: 13131-13136.

99) Shaul Y and Ben-Yehoyada M. Role of c-Abl in the DNA damage stress response. *Cell research*, 2005; 15: 33-35.

100) Yuan ZM, Huang Y, Ishiko T, Kharbanda S, Weichselbaum R and Kufe D. Regulation of DNA damage-induced apoptosis by the c-Abl tyrosine kinase. *Proc Natl Acad Sci*, 1997;94:1437-1440.

101) Ben-Yehoyada M, Ben-Dor, I and Shaul, Y. c-Abl tyrosine kinase selectively regulates p73 nuclear matrix association. *The Journal of biological chemistry*, 2003; 278: 34475-34482.

102) White E and Prives C. DNA damage enables p73. *Nature*, 1999; 399: 734-735, 737.

103) Agami R, Blandino G, Oren M and Shaul Y, Interaction of c-Abl and p73alpha and their collaboration to induce apoptosis. *Nature*, 1999; 399: 809-813.

104) Meltser V, Ben-Yehoyada M, Reuven N and Shaul Y. c-Abl downregulates the slow phase of double-strand break repair. Cell death & disease, 2010; 1: e20.

105) Wang JY. Controlling Abl: auto-inhibition and co-inhibition. *Nature cell biology*, 2004; 6: 3-7.

106) Yuan ZM, Huang Y, Ishiko T, et al. Regulation of Rad51 function by c-Abl in response to DNA damage. *J Biol Chem*, 1998;273: 3799-3802.

107) Kitao H and Yuan ZM. Regulation of ionizing radiation-induced Rad52 nuclear foci formation by c-Abl-mediated phosphorylation. *J Biol Chem*, 2002; 277: 48944-48948.

108) Cheng WH, von Kobbe C, Opresko PL, Fields KM, Ren J, Kufe D and Bohr VA. Werner syndrome protein phosphorylation by abl tyrosine kinase regulates its activity and distribution. *Molecular and cellular biology*, 2003; 23: 6385-6395.

109) Levy D, Adamovich Y, Reuven N and Shaul Y. Yap1 phosphorylation by c-Abl is a critical step in selective activation of proapoptotic genes in response to DNA damage. *Molecular cell*, 2008; 29: 350-361.

110) Levy D, Adamovich Y, Reuven N and Shaul Y. The Yes-associated protein 1 stabilizes p73 by preventing Itch-mediated ubiquitination of p73. *Cell death and differentiation*, 2007; 14: 743-751.

111) Saeed-Zidane M, Linden L, Salilew-Wondim D, et al. Cellular and exosome mediated molecular defense mechanism in bovine granulosa cells exposed to oxidative stress. *PLOS ONE*, 2017; 12: e0187569.

112) Woodring PJ, Hunter T and Wang JY. Regulation of F-actin-dependent processes by the Abl family of tyrosine kinases. *Journal of cell science*, 2003; 116: 2613-2626.

113) Sawyers CL, McLaughlin J, Goga A, Havlik M and Witte O. The nuclear tyrosine kinase c-abl negatively regulates cell growth. *Cell*, 1994; 77: 121-131.

114) Wen ST, Jackson PK and Van Etten RA. The cytostatic function of c-Abl is controlled by multiple nuclear localization signals and requires the p53 and Rb tumor suppressor gene products. *The EMBO journal*, 1996; 15: 1583-1595.

115) Vigneri P and Wang JY. Induction of apoptosis in chronic myelogenous leukemia cells through nuclear entrapment of BCR-ABL tyrosine kinase. *Nature medicine*, 2001; 7: 228-234.

116) Sirvent A, Benistant C and Roche S. Cytoplasmic signalling by the c-Abl tyrosine kinase in normal and cancer cells. *Biology of the cell*, 2008; 100: 617-631.

117) Yildirim E and Yaba A. Determination of c-Abl tyrosine kinase and mTERT catalytic subunit of telomerase expression level during prenatal-postnatal mouse ovary-testis development. *Reproductive biology*, 2020; 20: 555-567.

118) Yaba A, Kayisli UA, Johnson J, Demir R and Demir N. The Abelson tyrosine kinase (c-Abl) expression on the mouse uterus and placenta during gestational period. *Journal of molecular histology*, 2011;42: 91-96.

119) Yaba A, Agus S, Yıldırım E, Erdogan CS and Yılmaz B. Interaction of the mTERT telomerase catalytic subunit with the c-Abl tyrosine kinase in mouse granulosa cells. *Journal of receptor and signal transduction research*, 2020;40: 365-373.

120) Abylkassov R and Xie, Y. Role of Yes-associated protein in cancer: An update. *Oncology letters*, 2016; 12: 2277-2282.

121) Keshet R, Adler J, Ricardo Lax I, et al. c-Abl antagonizes the YAP oncogenic function. *Cell Death & Differentiation*, 2015b; 22: 935-945.

122) Abbassi L, Malki S, Cockburn K, et al. Multiple mechanisms cooperate to constitutively exclude the transcriptional co-activator YAP from the nucleus during murine oogenesis. *Biol Reprod*, 2016. p. 94 - 102.

123) Santos Guasch GL, Beeler JS, Marshall CB, et al. p73 is required for ovarian follicle development and regulates a gene network involved in cell-to-cell adhesion. *iScience*, 2018; 8: 236-249.

124) Devine PJ, Perreault SD and Luderer U. Roles of reactive oxygen species and antioxidants in ovarian toxicity. *Biol Reprod*, 2012; 86-27.

125) Plewes MR, Hou X, Zhang P, et al. Yes-associated protein 1 is required for proliferation and function of bovine granulosa cells in vitro. *Biol Reprod*, 2019; 101: 1001-1017.

126) Sun X, Majumder P, Shioya H, et al. Activation of the cytoplasmic c-Abl tyrosine kinase by reactive oxygen species. *J Biol Chem*, 2000a; 275: 17237-17240.

127) Croteau DL and Bohr VA. Repair of oxidative damage to nuclear and mitochondrial DNA in mammalian cells. *J Biol Chem*, 1997; 272: 25409-25412.

128) Berlett BS and Stadtman ER. Protein oxidation in aging, disease, and oxidative stress. *J Biol Chem*, 1997; 272: 20313-20316.

129) Sun X, Wu F, Datta R, Kharbanda S and Kufe D. Interaction between protein kinase C delta and the c-Abl tyrosine kinase in the cellular response to oxidative stress. *J Biol Chem*, 2000b;275: 7470-7473.

130) Taagepera S, McDonald D, Loeb JE, et al. Nuclear-cytoplasmic shuttling of c-Abl tyrosine kinase. *Proc Natl Acad Sci*, 1998; 95: 7457-7462.

7.APPENDICES

7.1. Ethical Approval

T.C. YEDİTEPE ÜNİVERSİTESİ
Hayvan Deneyleri Yerel Etik Kurulu (HADYEK)

ETİK KURUL KARARI

Protokol No	Toplantı Tarihi	Toplantı Sayısı	Karar No	Proje Yürütücüsü
2020-860	27.08.2020	2020/08	2020/08-7	Doç. Dr. Aylin Yaba Uçar

'Fare granuloza hücrelerinde DNA hasarına cevapta c-Abl ile YAP arasındaki ilişkinin belirlenmesi' isimli proje oy birliğiyle etik açıdan uygun görülmüştür.

Hayvan Türü / Irkı	Toplam Hayvan Sayısı	Hayvanın Cinsiyeti
Fare / BALB/c	16	Dişi

Görevi	Adı Soyadı	Katılım Durumu
Başkan	Prof. Dr. Bayram YILMAZ	
Başkan Vekili	Prof. Dr. Erdem YEŞİLADA	
Üye	Veteriner Hekim Engin SÜMER	
Üye	Prof. Dr. M. Ece GENÇ	
Üye	Prof. Dr. Rukset ATTAR	
Üye	Prof. Dr. Gamze TORUN KÖSE	
Üye	Doç. Dr. Ediz DENİZ	
Üye	Doç. Dr. Aylin YABA UÇAR	
Üye	Doç. Dr. Burcu GEMİCİ BAŞOL	
Üye	Hakan GÖKSEL	
Üye	Ahmet ŞENKARDEŞLER	

T.C. YEDİTEPE ÜNİVERSİTESİ
Hayvan Deneyleri Yerel Etik Kurulu (HADYEK)

ETİK KURUL KARARI

Protokol No	Toplantı Tarihi	Toplantı Sayısı	Karar No	Proje Yürütücüsü
2020-873	30.10.2020	2020/10	2020/10-3	Doç. Dr. Aylin Yaba Uçar

'Fare Granuloza Hücrelerinde DNA Hasarına Cevapta c-Abl ile YAP Arasındaki İlişkinin Belirlenmesi' isimli proje oy birliğiyle etik açıdan uygun görülmüştür.

Hayvan Türü / Irkı	Toplam Hayvan Sayısı	Hayvanın Cinsiyeti
Fare / BALB/C	11	Dişi

Görevi	Adı Soyadı	Katılım Durumu
Başkan	Prof. Dr. Bayram YILMAZ	
Başkan Vekili	Prof. Dr. Erdem YEŞİLADA	
Üye	Dr. Veteriner Hekim Engin SÜMER	
Üye	Prof. Dr. M. Ece GENÇ	
Üye	Prof. Dr. Rukset ATTAR	
Üye	Prof. Dr. Gamze TORUN KÖSE	
Üye	Doç. Dr. Ediz DENİZ	
Üye	Doç. Dr. Aylin YABA UÇAR	
Üye	Doç. Dr. Burcu GEMİCİ BAŞOL	
Üye	Hakan GÖKSEL	
Üye	Ahmet ŞENKARDEŞLER	